THE
PHYSICAL REVIEW
A Journal of Experimental and Theoretical Physics Established by E. L. Nichols in 1893
VOL. 54, NO. 7 OCTOBER 1, 1938 SECOND SERIES

The Absorption of the Shower-Producing Component of Cosmic Radiation in Iron and Lead

JOSIAH CRUDUP
Ryerson Laboratory, University of Chicago, Chicago, Illinois
(Received August 3, 1938)

Measurements of the absorption coefficient of the shower-producing component of primary cosmic radiation give 0.35 cm^{-1} in lead and 0.076 cm^{-1} in iron. The atomic absorption coefficients corresponding to these values are nearly in direct proportion to the squares of the atomic numbers of the absorbing materials. The value 0.35 cm^{-1} for lead agrees rather well with that found by Woodward. A slight minimum was found in the curve of the absorption for lead at a point between 8 and 10 cm, confirming similar findings by Rossi and others. No minimum was found in the absorption curve for iron up to a thickness of 20 cm. For the rays received within a given solid angle, the ratio of the shower rate to the vertical coincidence rate falls from 5.1 percent with no shield to 2.6 percent with 15 cm of lead, and to 3.0 percent with 20 cm of iron.

IT is well recognized that most of the electron showers associated with cosmic rays at sea level are produced by a non-ionizing type of radiation. These non-ionizing shower-producing rays very probably consist of photons, which are in turn excited by primary shower-producing particles that may be electrons. The terms *A*, *B*, and *C* will be applied, respectively, to the primary shower-producing particles, the shower-producing photons, and the shower electrons. The present paper is concerned chiefly with a measurement of the absorption coefficient in iron and lead of rays of type *A*, i.e., the primary shower-producing component of cosmic radiation. A measurement is also made of the relative number of showers and vertical coincidences.

Measurements designed for the same purpose have been performed by Sawyer,[1] Rossi,[2] Woodward,[3] and others. The present experiment has followed Sawyer's procedure of studying showers (*C*-rays) that are produced in a material that differs from the one in which the shower-producing radiation *B* itself is excited. Since with this technique the rays of types *B* and *C* are always produced in the same substance, a direct comparison is obtained of the absorption of the primary shower-producing radiation *A* in various absorbing materials. We have replaced the triangular arrangement of three counters used by Sawyer[1] with the fourfold coincidence arrangement of counters shown in Fig. 1. Thus not only is the number of chance counts reduced, but it also becomes necessary for all of the primary rays to pass through the absorbing materials before producing rays which affect the counters.

EXPERIMENTAL PROCEDURE

With the arrangement of counter tubes shown in Fig. 1 coincidence counts are possible only when showers are produced in the lead scatterer *S*, except for the very rare shower particles which

[1] J. H. Sawyer, Phys. Rev. **50**, 25 (1936).
[2] B. Rossi, Zeits. f. Physik **82**, 151 (1933).
[3] R. H. Woodward, Phys. Rev. **49**, 711 (1936).

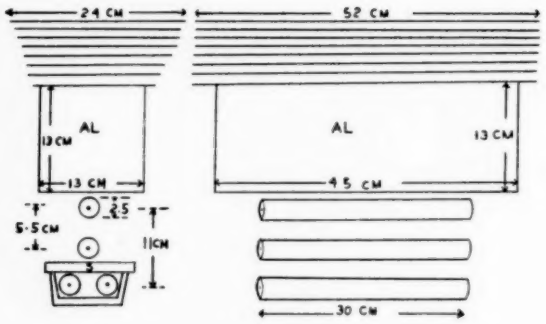

FIG. 1. Arrangement of apparatus in end and side view.

may be able to penetrate 1 cm of lead. Our experiments indicate that the aluminum block placed above the tubes is thick enough to absorb nearly all of the B-type rays entering from above. Thus all of the B-rays which strike the scatterer S are produced in the aluminum block. Above the aluminum block are placed the plates of lead or iron, whose absorption of the A-type of radiation is to be measured. In order to reduce disturbing effects from showers excited in matter in the neighborhood, the apparatus is used under canvass on the roof of Ryerson Laboratory.

The Geiger-Müller tubes are filled with hydrogen to a pressure of 9.6 cm of mercury, and about 0.2 cm of dry air. The center of the plateau of voltage operation is about 1220 volts. Each tube is wrapped in a thin aluminum foil which is grounded. The source of high voltage placed across the counter tubes is a modification of the arrangement given by Street and Johnson.[4] The circuit used with the Geiger-Müller tubes is approximately described by Neher and Harper.[5]

Figure 2 shows in curves A and B the counting rates observed for various thicknesses of iron and lead, respectively. Each datum point represents some thirty hours of readings and the length of the vertical line at each point represents the standard deviation as calculated from the number of counts. Repeated observations at widely separated intervals showed experimental deviations consistent with those to be expected by this statistical calculation. This may be taken as sufficient test of the consistency of the readings.

[4] J. C. Street and T. H. Johnson, J. Frank. Inst. **214**, 155 (1932).
[5] H. V. Neher and W. W. Harper, Phys. Rev. **49**, 940 (1936).

Except for the last two points of curve B, the data may be represented with sufficient accuracy by the empirical expression

$$N = N_0 \epsilon^{-\mu x} + C. \tag{1}$$

The smooth curves in Fig. 2 have been plotted with the values $N_0 = 20$, $C = 10$, $\mu_{Fe} = 0.076$ cm^{-1}, $\mu_{Pb} = 0.35$ cm^{-1}.

INTERPRETATION

If we assume that the primary cosmic rays A are electrons of an absorption coefficient (μ_1), the secondary rays B are photons of an absorption coefficient (μ_2), and the tertiary rays C are shower particles of an absorption coefficient (μ_3), it can be shown that the counting rate N should be given by the following equation.

$$N = \frac{C}{(\mu_3-\mu_1)(\mu_2-\mu_1)} \times \left\{ \epsilon^{-\mu_1 x} - \frac{(\mu_3-\mu_1)}{(\mu_3-\mu_2)} \epsilon^{-\mu_2 x} + \frac{(\mu_2-\mu_1)}{(\mu_3-\mu_2)} \epsilon^{-\mu_3 x} \right\}. \tag{2}$$

The curve shown in Fig. 3 is plotted with the values $\mu_1 = 0.3$ cm^{-1}, $\mu_2 = 0.7$ cm^{-1}, $\mu_3 = 5.0$ cm^{-1} of lead. The shape of the portion AB of this curve is determined primarily by the coefficient μ_3, the portion BC by the coefficient μ_2, and from C to D by the coefficient μ_1. The fact that the data shown in Fig. 2 are on the downward sloping part of the curve thus indicates that the aluminum block is adequate to absorb most of the secondary photons that come from above. This in

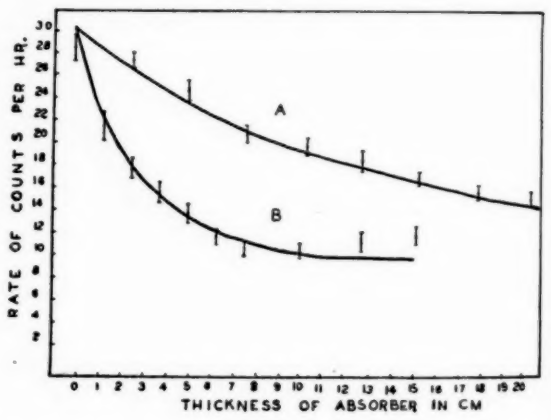

FIG. 2. Counting rates as functions of thickness of iron (curve A) and of lead (curve B).

turn gives assurance that B-type rays reaching the scatterer S are those produced in the aluminum block. Thus we may provisionally identify the absorption coefficient measured by the arrangement of Fig. 1 with the absorption coefficient of the primary shower-producing particles A in iron and lead.

The constant C is due at least in part to the showers produced in the air and in the wood structure placed above the tubes to support the iron and lead. It is noteworthy, however, that the data associated with curve B show a minimum at about 9 cm of lead. This result confirms similar findings by Rossi[6] and others. It is not impossible that the rise beyond 9 cm of lead may represent the excitation of a penetrating cosmic ray by a less penetrating primary ray.[7] In this case the rising datum points at the end of curve B should correspond to the portion of the curve of Fig. 3 lying between B and C. The base line of curve B should then not have the constant value $C=10$, but should rather be sloping upward from the origin. In view of the speculative character of this hypothesis, we preferred to use the simpler assumption represented by Eq. (1). Had the alternative of an upward sloping base line been taken, the value of N_0 would have been increased by roughly fifty percent. The value of μ, however, would not have been greatly altered.

On the basis of the relative absorption in iron and lead we should not expect a similar minimum in curve A until a thickness of 35 to 45 cm of iron is reached. This is in accord with the observed absence of such a minimum in the data for iron, and indicates the importance of using great thicknesses of absorber for measuring this highly penetrating secondary radiation.

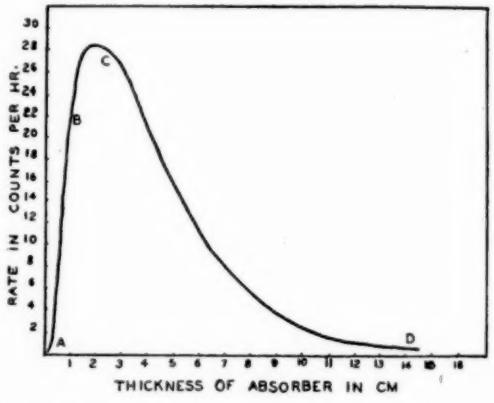

FIG. 3. Theoretical curve, plotted according to Eq. (2), for the variation of counting rate with absorber thickness.

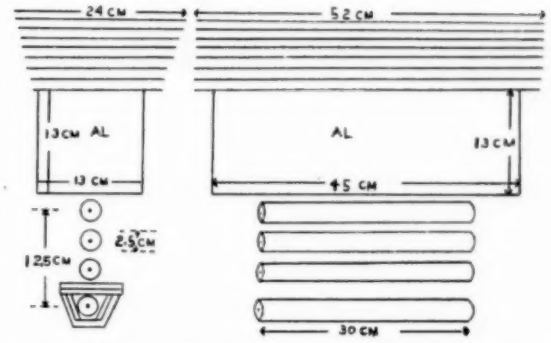

FIG. 4. Arrangement of apparatus to determine ratio of shower-producing rays to the total vertical cone of cosmic rays.

The value of μ required for the empirical formula (1) should thus differ little from the true absorption coefficient of the primary shower-producing ray in iron and lead. The atomic absorption coefficients corresponding to the values of $\mu_{Pb}=0.35$ cm^{-1} and $\mu_{Fe}=0.076$ cm^{-1} are, respectively, 1.05×10^{-23} and 0.08×10^{-23}. These values for lead and iron are approximately in direct proportion to the squares of the atomic numbers of the absorbing materials. This result does not agree with that found by Sawyer.[1] The value for the absorption in lead is in good agreement with the corresponding value of 0.33 cm^{-1} found by Woodward.[3]

THE RELATIVE NUMBER OF SHOWER-PRODUCING RAYS

A rough estimate of the ratio of shower-producing rays to the total vertical cone of cosmic rays was made possible by counting the coincidence rate with four counters in line as shown in Fig. 4. With no absorber above the aluminum block the observed rate of shower coincidence was 11.7 percent as great as that of the observed vertical coincidence. Because, however, of the greater separation of the tubes in vertical arrangement, the solid angle of the vertical cone was less than in the shower arrange-

[6] B. Rossi, *International Conference on Physics* (London, 1934).

[7] Thus, Heitler, Proc. Roy. Soc., June, 1938, suggests that the primary electrons may excite alternatively penetrating barytrons or less penetrating electron pairs through the medium of secondary photons.

ment by a factor of 2.3. Thus for the rays within a given solid angle the shower rate is 5.1 percent as great as the vertical coincidence rate. For the full shield of 15.24 cm of lead the corresponding ratio is reduced to 2.6 percent, and for 20.48 cm of iron to 3.0 percent. These fractions of the primary rays which produce showers are approximately the same as those found by Geiger.[8]

The ratio of the number of recorded showers to the total number produced somewhere along the path of the primary shower-producing rays is unknown. The smaller percentage of the observed showers suggests, however, that the shower-producing component constitutes the smaller part of the primary cosmic radiation.

It gives me great pleasure to acknowledge my indebtedness to Professor A. H. Compton for his constant inspiration and helpful advice throughout this investigation. I wish also to express my sincere appreciation to the General Education Board for the fellowship aid given to me during this time.

[8] H. Geiger, Zeits. f. Physik **97**, 300 (1935).

OCTOBER 1, 1938 PHYSICAL REVIEW VOLUME 54

The Capture of Orbital Electrons by Nuclei

LUIS W. ALVAREZ
Radiation Laboratory, Physics Department, University of California, Berkeley, California
(Received July 26, 1938)

The simple theory of electron capture is outlined and three general methods for its detection are suggested. The first experimental evidence for the process (in activated titanium) is described. A rigorous experimental proof of the hypothesis is given for the case of Ga^{67}. A summary of several isotopes whose properties are best explained on this hypothesis is appended. The properties of Ga^{67} are described in considerable detail, and include the first evidence for internal conversion in artificially radioactive atoms.

INTRODUCTION

THE suggestion that positron emitters might decay by the alternate process of electron capture was first advanced by Yukawa[1] from considerations based on the Fermi theory of beta-ray emission. In this theory, the electrons and positrons are pictured as being created at the moment they are ejected, during neutron-proton transitions. The continuous beta-ray spectrum and the conservation of spin are explained by the simultaneous emission of a neutrino and electron. One may represent the transition involved in electron and positron decay by the following equations:

$$N \rightarrow P + e^- + \nu \quad (1)$$

$$P \rightarrow N + e^+ + \nu. \quad (2)$$

On the basis of Dirac's theory, however, the positron is merely the "hole" left in the continuum of negative energy electrons when one of these electrons is given a positive energy by the addition of at least $2mc^2$. The proton in (2) does not transform into a neutron and positron, but rather captures a negative energy electron, and turns into a neutron, leaving the hole in the negative energy sea, or positron. Eq. (2) may then be written

$$e^- + P \rightarrow N + \nu. \quad (3)$$

The experimental observation that positrons may be annihilated (a positive energy electron falling into the hole), shows that there is no essential difference between electrons in the two energy states. Therefore, there is no *a priori* reason why Eq. (3) demands the use of a negative energy electron. In fact, when the energy difference between parent and daughter nucleus is less than $2mc^2$, it would be impossible for the relation to be satisfied unless a proton could capture an ordinary electron. Since there are many cases of negative beta-ray decay with an

[1] Yukawa and Sakata, Proc. Phys. Math. Soc. Japan **17**, 467 (1935); **18**, 128 (1936).

energy release of less than this value, it is natural to suppose that there would be excited nuclei whose desire to emit positrons could not be allowed on energetic grounds. Yukawa suggested that in these cases, the decay would proceed by the capture of an orbital electron. In addition, he calculated, and others[2, 3, 4, 5] extended the calculations, that even when there was enough energy to create a pair, a certain fraction of the excited nuclei would decay by electron capture. The branching ratio of the two processes was found to depend on the energy available, the spin change involved, and the nuclear charge (density of electrons at the nucleus). Electron capture should become more probable as the energy decreases, and as the spin change, atomic number and half-life increase.

Experimental Methods

Alpha-decay and the two well-established methods of beta-decay are easy to observe, since ionizing radiations are emitted in these processes. Eq. (3) shows that only the undetectable neutrino is given off by the nucleus in this new type of transition, so that more refined experimental methods must be employed if the effect is to be demonstrated.

(1) It is possible in theory at least to count the number of positron-radioactive nuclei formed in a given reaction, and to compare this with the number of positrons emitted in the subsequent decay. Unfortunately, most reactions leading to e^+ emitters are formed in (α, n), (d, n), or (p, n) reactions, which makes the accurate counting of the disintegrations very difficult. In the one case where the number of neutrons has been compared with the number of positrons—in the reaction $C^{12}+d \rightarrow N^{13}+n$; $N^{13} \rightarrow C^{13}+e^+$—a discrepancy was found,[6] which might be interpreted as evidence for electron capture.[7] But the data are not sufficiently precise to make that conclusion necessary. In addition, from theoretical considerations, it is unlikely that N^{13}, which is energetic, light, and involves no spin change, should have a capture branching-ratio large enough to observe by this method.[7a]

(2) If it were possible to count the number of atoms formed when a positron-active substance decayed, this number could be compared with the total number of positrons given off, to give a measure of the branching ratio. This might be applicable if there were any known cases of successive positron activities, i.e., radioactive series, where one could compare the activities of the parent and daughter substances. Since no such cases have as yet been discovered, the alternate, but much more difficult, method of counting the number of stable product nuclei is worth investigation. A radioactive sample with an initial strength of 1 millicurie and a half-life of t days contains $1.6\times10^{12}t$ active atoms, which will give rise to $2.6\times10^{-12}tA$ gram of decay product. (A = atomic weight.) For anything but a noble gas, this is beyond the limit of chemical or spectroscopic detection. It is very fortunate that Na^{22},[8] the longest lived positron-active substance, decays into Ne, the most easily detectable rare gas.[9] Calculation shows that a one day bombardment of Mg in the cyclotron will yield enough Na^{22} to allow the easy measurement of the quantity of Ne produced each month, if no electrons are captured. Theory suggests that 30 times as much Ne will be formed[10] by electron capture as is expected from the positron emission. The small bulk of Na containing the activity can be freed of all gases by prolonged heating in a vacuum, and then the Ne can be allowed to grow in the cold, an ideal case for measurement of small quantities of noble gases by the Paneth method.[11]

(3) In the two previous methods suggested for detecting the capture of electrons, no advantage was taken of the fact that the electron was originally part of the stable electronic system of the parent atom, and that this system is dis-

[2] Mercier, Nature **139**, 797 (1937); Comptes rendus **204**, 1117 (1937).
[3] Hoyle, Nature **140**, 235 (1937); Proc. Camb. Phil. Soc. **33**, 286 (1937).
[4] Møller, Physik. Zeits. d. Sowjetunion **11**, 9 (1937); Phys. Rev. **51**, 84 (1937).
[5] Uhlenbeck and Kuiper, Physica **4**, 601 (1937).
[6] Alvarez, Phys. Rev. **53**, 326 (1937).
[7] Roberts and Heydenburg, Phys. Rev. **53**, 374 (1937).
[7a] *Note added in proof.* Crane and Halpern [Phys. Rev. **54**, 306 (1938)] have recently shown that electron capture plays a negligible role in the decay of N^{13}.
[8] Laslett, Phys. Rev. **52**, 529 (1937).
[9] Günther and Paneth, Zeits. f. physik. Chemie **173**, 401 (1935).
[10] Lamb, Phys. Rev. **50**, 388 (1936).
[11] Professor H. E. White and Mr. H. Weltin are working on this problem at present, in collaboration with the author.

turbed by the loss of one of its component parts. It is well known that x-rays are given off by an atom which has lost one of its inner electrons by photo-ionization, and the same will be true of one which has lost an inner electron to the nucleus. The vacant place in the inner shell will be immediately filled, and a quantum of x-radiation (or an Auger electron) will be emitted in the process. It is this phenomenon which is the basis of the third method of detection. One has again a technical difficulty that the x-rays from the light elements (and no positron emitters are known among the heavy ones[12]) are soft, and difficult to observe in the presence of positrons and gamma-rays. Jacobsen[13] was the first to try this method, in the case of Sc^{43}, but he found no trace of the expected x-rays in a cloud chamber.

Characteristic X-Rays from Active Titanium[14]

Walke[15] has shown that a strong positron activity of 16 days half-life is induced in titanium when it is bombarded with high energy deuterons. The energy of the positrons shows that the transition is not an allowed one (second Sargent curve), and this fact, together with the long life and relatively high atomic number for a positron emitter, suggested that it would be an ideal starting point in a search for the x-rays following electron capture. The isotope responsible for the activity has been identified chemically by Walke as vanadium, so any x-rays would have the wave-length characteristic of the daughter element, titanium. The fact that this wave-length, 2.7A, is just below the "vacuum region" had much to do with the choice. From the arguments given above, Na^{22} would have been a far better choice, but Ne $K\alpha$ has a wave-length of about 14A.

The detection of the soft x-ray quanta presented several difficulties. It was, of course, necessary to eliminate the positrons, and this was easily accomplished with the aid of an electromagnet. Activated Ti has an abnormally high ratio of gamma-rays to positrons, so the problem resolved itself into the detection of a weak component of very soft radiation superposed on a strong, hard one. A counter has an obvious advantage over an electroscope here, but the problem of getting the soft quanta into the counting volume is a serious one. This was solved by constructing the envelope of thin Cellophane, and filling it with argon at atmospheric pressure. This last feature greatly increases its relative sensitivity to 2.7A x-rays, as almost all the quanta are stopped in the gas, while very few gamma-rays are absorbed in the thin walls or gas.

The experimental arrangement is shown in Fig. 1. The Ti sample was placed in a five-sided aluminum box between the poles of an electromagnet, in a field of 2000 oersteds, so that all positrons were kept from reaching the counter. The sample was aged for two weeks, so that all short periods were of negligible intensity. The tube between source and counter was filled with He at atmospheric pressure and capped with Cellophane ends. This reduced the solid angle (counting rate) without discriminating against the soft x-rays. The counter cathode was made of copper foil in the shape of a C, so that x-rays could enter the active volume without passing through too much absorber. The copper foil was only 0.00025 cm thick, to prevent the absorption and counting of gamma-rays. Lead blocks screened the glass tubes which supported the Cellophane wall and copper cathode, for the latter reason also. The anode wire was of 0.0025 cm tungsten wire to keep the counter voltage low—the working potential was about 2000 volts. Alcohol in a side tube made the counter more reliable, and to keep the sensitivity constant, it was found necessary to counteract leaks in the Cellophane system by flowing argon through the counter whenever it was in operation. The background was high, but the counting rate was so great that this caused no inconvenience. Absorbers of thin aluminum foil were arranged on sliding frames so that it was a simple matter to take absorption data.

The experimental procedure consisted in taking 2000 counts at each of seven values of absorber thickness, and in repeating each setting eight times. Each point then had a probable error of less than one percent. The background

[12] Alvarez, Phys. Rev. **53**, 213 (1938).
[13] Jacobsen, Nature **139**, 879 (1937).
[14] Alvarez, Phys. Rev. **52**, 134 (1937).
[15] Walke, Phys. Rev. **51**, 1011 (1937).

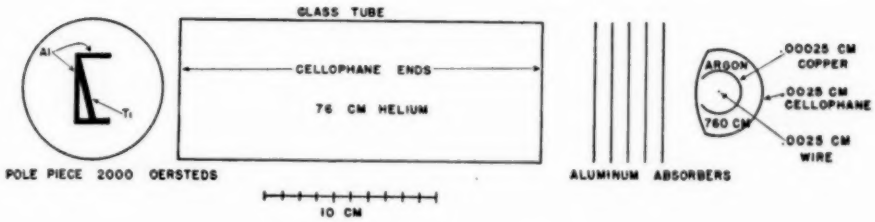

FIG. 1. Experimental arrangement.

count and the linearity of the counting circuit were checked after each series. The counting rate dropped from 21.3 to 15.4 per second as the absorbers were introduced into the beam. The rate remained at the latter value from 0.0025 cm to 0.0075 cm of Al, indicating that the decrease was due to a soft component in addition to the hard gamma-rays.

Figure 2 shows the actual absorption curve, and Fig. 3 is the absorption curve of the soft component. The three lines are drawn through the upper, most accurately known point, with slopes calculated from the measured absorption coefficients in Al of K-radiation from Sc, Ti and V. The agreement of the data with the Ti line is very striking, and indicates that the radiation is homogeneous, and of the expected wavelength, giving support to the electron capture hypothesis.

On the remote chance that this radiation could have been excited by the positrons in passing through the Ti sample, the sample was covered with a thin layer of chromium (actually a 0.00025 cm Ni foil plated on each side with 0.0012 cm of Cr). This foil was thick enough to absorb all the observed Ti $K\alpha$ and if these x-rays were of secondary origin, the positrons should have excited about equal amounts of Cr $K\alpha$ in the Cr foil. Absorption data showed that no soft component was present under these circumstances, so it seemed safe to assume that the x-rays arose from Ti atoms which had been formed by electron capture from the 16-day vanadium period. The assumption as to the period was based on Walke's finding that all but a negligible fraction of the activity in a two-week-old sample of Ti bombarded with deuterons was due to this period. This fact, plus the theory, which suggested that K-radiation should be found in this period made it seem unnecessary to repeat the expensive (because of the argon waste) experiment two weeks later just to check the period.

However, Walke carried this Ti sample to Liverpool shortly after, and Williams and Pickup[16] have followed its activity in a cloud chamber since then. They improved Jacobsen's technique by bending the positrons out of the chamber by a magnetic field, and were thus able to see x-ray photoelectrons much closer to the source, where they are more plentiful. A count of these short tracks against distance verified that they had approximately the correct absorption coefficient to be Ti $K\alpha$. The surprising observation was made that there were about 500 photoelectrons per positron, and that while the positrons decayed with the 16-day period, the number of photoelectrons remained constant for several months, within the statistical error. This indicated that some of the x-rays observed in this laboratory were due to a new, long period in Ti, which had escaped Walke's attention because of its soft radiation. To find what percentage, if any, of the x-rays were due to the 16-day period, the author prepared and sent a fresh sample of Ti to Liverpool, where Williams and Pickup showed that no appreciable fraction was emitted by the 16-day isotope. While this changes the identification of the responsible isotope, the original interpretation that electron capture was probably the cause of the radiation, was still the most plausible guess.

But this interpretation is not the only one which will fit the facts, and if one is to establish the existence of a new phenomenon, there must be no alternative explanations. It is well known that x-rays appear when gamma-rays are internally converted. Here the shell is vacated by an expelled electron, instead of one lost to the

[16] Williams and Pickup, Nature **141**, 199 (1938).

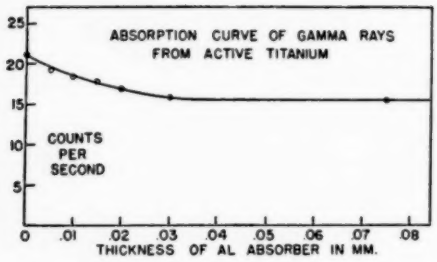

FIG. 2.

nucleus. It is entirely possible that the long-lived x-ray emitting isotope is a metastable state of a stable or radioactive Ti or V isotope. Low lying states of this kind are usually assumed to be responsible for the existence of nuclear isomers, of which this long period would then be an example. It is assumed that the higher level may radiate a gamma-ray to the ground state, and if these states are close, as they must be for a long life to be possible, the soft gamma-rays could be largely internally converted. The soft conversion electrons would not be seen in Williams and Pickup's chamber. While this is not suggested as the probable explanation, it fits all the observed data as well as the electron capture hypothesis. It serves best to emphasize that a more decisive test must be made if electron capture is to be accepted as an established fact.

PROOF OF THE ELECTRON CAPTURE HYPOTHESIS[17]

A glance at the table of isotopes showed that several blank spaces existed on the positron side of the stability band, in the region between Mn and Ge, although this section of the table has been very carefully studied by several workers. It seemed quite probable that some of these missing isotopes might capture electrons, and that they had not been discovered because their soft x-rays had been masked by the strong beta- and gamma-rays of the other periods.

An exploratory investigation was therefore made of the soft quantum radiations emitted by several of these elements after bombardment with deuterons. Of the four elements tried, Fe, Ni, Cu, and Zn, all were found to give off various amounts of soft x-rays. Since the wave-lengths are shorter in this region, it was possible to use an air-filled Lauritsen type electroscope as the detector; the magnet was still necessary to suppress the beta-rays. The absorption curve on the iron radiation showed that about half of gamma-ray ionization was due to a component with an absorption coefficient in Al about equal to that of Cr $K\alpha$. There are several long periods induced in iron, so it did not lend itself easily to investigation. Ni showed about 8 percent K-radiation following the well-known 3.5 hr. period of Cu^{61}. Copper showed about 40 percent x-ray ionization following the 12 hr. Cu^{64}. This is interesting, as it is what one would predict on theory.[5] The activity with the shorter life has a smaller capture branching ratio, and in fact the numbers quoted above fit very well on the theoretical curves. The ratio of these two percentages is a number which does not depend on geometry or the relative sensitivity of the electroscope to various types of radiation, or on atomic number or spin change; so it is well adapted to a comparison with theory. It is encouraging that it fits so well, but it cannot be taken too seriously at present.

Activated zinc was the most interesting of the four elements bombarded, and the rest of this section will be devoted to it. Four of the activities induced in zinc by fast deuterons were found to be accompanied by x-rays with the correct absorption coefficient in Al to be Zn $K\alpha$. Electron periods as well as the positron periods were among these four, so it did not seem possible to

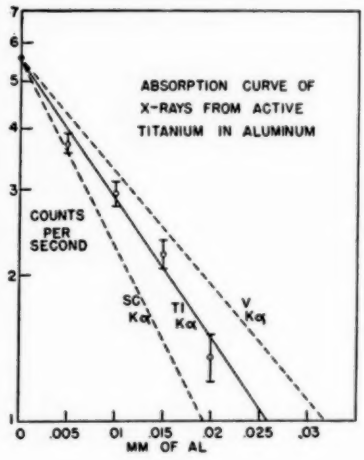

FIG. 3.

[17] Alvarez, Phys. Rev. **53**, 606 (1938).

explain them all as due to electron capture. And if there was an alternate explanation, why could it not explain all the cases?

Most of the work was done on the 83-hour period. This activity has had the following interesting history: It was first found by Livingood,[18] who gave its half-life, without chemistry, as 97 hours. Later, Thornton[19] identified it as a zinc isotope with the same period, and assigned it to Zn^{71}. Next, Du Bridge, Barnes, Buck, and Strain[20] quoted its period as 82 hours, but said it was surprising that although it was prepared from Zn with protons, it was not detected in either copper, zinc, or gallium precipitates. The author gave the half-life as 83 hours, and showed that it was chemically similar to Ga. Strain and Buck[21] have since confirmed this, and Mann,[22] who reported a Ga isotope with a period of about 55 hours, has also shown that his activity is identical with the 83-hour Ga. The isotope has thus been prepared from zinc by deuteron, alpha-particle, and proton bombardment, which pins it down at Ga^{67}.

The Ga^{67} could be separated from the rest of the activities induced in Zn by means of the ether extraction process.[23] This procedure depends upon the fact that $GaCl_3$ is soluble in ether, while the chlorides of the neighboring elements are not. If one then shakes an HCl solution of these metals with ether in a separatory funnel, most of the $GaCl_3$ will be found in the ether layer. The ether may be then evaporated on a metal sheet, leaving an invisible layer of $GaCl_3$ which contains almost all of the original activity. This is probably the simplest way of preparing a pure radioactive sample—no carrier is needed. In the case under discussion, there were no doubt small traces of Ga impurities in the activated Zn, but very recently, Grahame and Seaborg[24] have activated specially prepared, Ga-free Zn and found that the ratio of activity in the ether layer to activity in the aqueous layer is the same for pure radioactive $GaCl_3$ as it is for macroscopic amounts of stable $GaCl_3$.

When a weak, separated sample of Ga^{67} was measured without a magnetic field on a thin walled electroscope, a very soft component was found, which was electronic in nature as shown by the sign of the magnetic deflection. Rough range measurements showed that the energy of these electrons was about 100 kev. This was quite surprising for a period as short as 83 hours. The Sargent relations show that for any given half-life, there is a minimum beta-ray energy, corresponding to an allowed transition of spin change zero. For greater spin changes, the energy released is considerably higher. There are no known beta-ray energies less than that called for by the first Sargent curve, and there is no theoretical reason for expecting them.[25] So it seemed probable that the electrons observed here were conversion electrons instead of primary disintegration particles. No previous example of internal conversion in the artificially radioactive elements has been reported, and it has generally been assumed that it should be very unlikely.

To check this possibility, the absorption curve of these electrons was carefully investigated with a separated sample of Ga^{67}. The data are shown in Fig. 4. It is at once evident that the curve is not exponential, nor a combination of exponentials as one finds for beta-rays, since it is concave toward the origin. Its shape is strong evidence that the electrons responsible have a line structure. The intensity available in the sample was enough to allow its measurement on a high resolution mass spectrograph. Mr. D. C. Kalbfell photographed the electron spectrum in an instrument of his design, and showed that there was indeed a line structure. His plates showed an intense line at 90 kev, and a fainter one at about 99 kev. This is precisely what one would expect if the electrons were due to the internal conversion of a gamma-ray of 100 kev. The K and L absorption edges of zinc are at 1.2 and 12A, respectively, corresponding to energies of 10 and 1 kev. The strong line is then due to K-conversion of the gamma-ray, and the weak one to L-conversion. Dr. E. M. Lyman examined the specimen in his high

[18] Livingood, Phys. Rev. **50**, 425 (1936).
[19] Thornton, Phys. Rev. **53**, 326 (1938).
[20] Du Bridge, Barnes, Buck, and Strain, Phys. Rev. **53**, 447 (1938).
[21] Strain and Buck, Phys. Rev. **53**, 943 (1938).
[22] Mann, Phys. Rev. **53**, 212 (1938).
[23] Noyes and Bray, *Qualitative Analysis for the Rare Elements* (Macmillan Company).
[24] Grahame and Seaborg, Phys. Rev. **54**, 240 (1938).
[25] See later section on Hg^{197}.

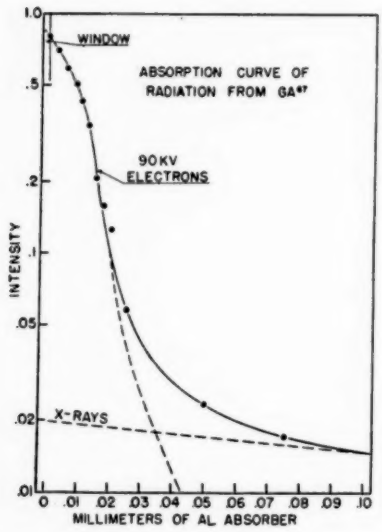

FIG. 4.

resolution beta-ray spectrograph equipped with a Geiger counter, and obtained the spectrum shown in Fig. 5.[26] This electron group is interesting in that it is the purest radioactive line source known.

Attention was next directed to the x-rays. Although it would have been possible to determine the atomic number of the element whose characteristic radiation was emitted from active Ti, by careful absorption measurements in Al, this is not true of the radiation from Ga. The absorption coefficient of the K-radiation from Sc, Ti, and V is a very sensitive function of Z, as shown in Fig. 3, but it is a slowly varying function in the neighborhood of Zn. One must therefore resort to a more refined method to identify the wave-length of the Ga x-rays. There is enough intensity available to diffract the rays in a bent crystal spectrograph,[27] and this method was the first tried. If this were the only possibility, it is certain that results could have been obtained without too much difficulty. But the attempt was abandoned in favor of the simpler method described below.

It is well known that if one plots absorption coefficient in a given element against wave-length, sharp discontinuities appear at certain wave-lengths which are known as "critical absorption limits," and which correspond to the binding energies of the K, L, etc. shells of the absorbing atom. If one now plots the same type of curves for the two neighboring elements, he finds that the curves are very similar, except that the discontinuities have shifted slightly to either side.

If one could find two neighboring elements which absorbed the Ga x-rays very differently, it would show that the wave-length of this radiation lay between the two critical limits. Experiments showed that Ni and Cu foils exhibited this property. The data are plotted in Fig. 6. The Ni and Cu absorption limits are at 1.48 and 1.38A, respectively, so most of the radiation is between these limits. Zn $K\alpha$ is the only strong line satisfying these conditions, so one may conclude that it is responsible for most of the effect. Zn $K\beta$ should accompany it, and since it has a shorter wave-length than either of the two absorption edges, it is strongly absorbed in both Ni and Cu. It is seen that the copper curve resolves into two components corresponding to $K\alpha$ and $K\beta$ of zinc, and the ratio of the intensities of the two lines is approximately correctly given by the intercepts of the resolved components on the vertical axis. That the absorption in Ni is not as great as one would expect from the tabulated absorption coefficients is due to the imperfection of the geometrical conditions. Ni $K\alpha$ is excited as fluorescence radiation when Zn $K\alpha$ is absorbed in Ni foil, and some of these x-rays are detected in the chamber, to give too high a reading. When the geometry was made still poorer, the apparent absorption coefficient fell further, showing that this explanation of

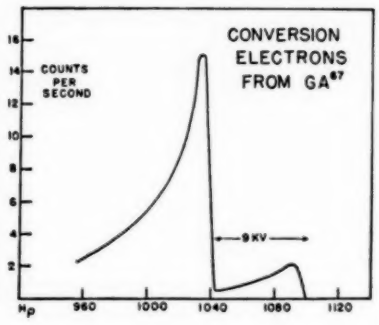

FIG. 5.

[26] I wish to thank Dr. Lyman and Mr. Kalbfell for examining the active Zn in their spectrographs.

[27] Du Mond and Kirkpatrick, Rev. Sci. Inst. **1**, 88 (1930); Cauchois, J. de Physique **3**, 320 (1932).

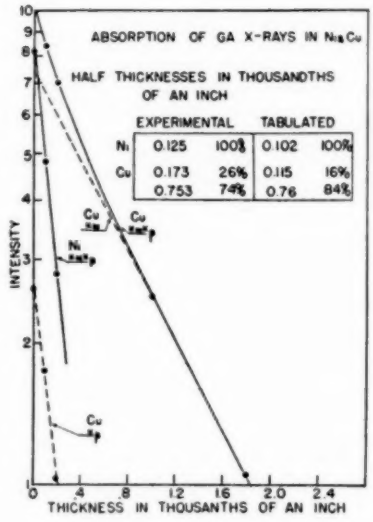
ABSORPTION OF GA X-RAYS IN Ni & Cu
HALF THICKNESSES IN THOUSANDTHS OF AN INCH
EXPERIMENTAL
TABULATED
Ni 0.125 100% 0.102 100%
Cu 0.173 26% 0.115 16%
0.753 74% 0.76 84%
INTENSITY
THICKNESS IN THOUSANTHS OF AN INCH

FIG. 6.

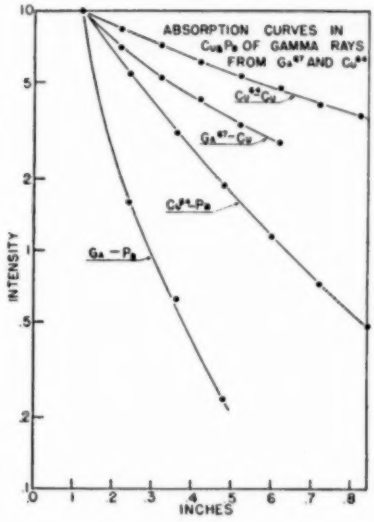

FIG. 7.

the discrepancy was correct. The evidence is therefore conclusive that the soft component of the undeflectable radiation is composed of zinc characteristic x-rays, and that therefore, the daughter substance is an isotope of zinc.

The gamma-ray spectrum was next investigated by two methods. Absorption data in copper and lead showed that there was a component in the neighborhood of 250 kev. It was particularly important to establish whether or not any annihilation radiation accompanied the decay. The absorption curve in lead was compared with one taken on Cu^{64} with identical geometry. The latter emits only annihilation radiation.[28] From the two curves (Fig. 7) one can see that if any of this type of gamma-rays is given off from Ga^{67}, it is a very small fraction indeed. Confirmatory evidence was obtained in a cloud chamber, where no positrons could be observed. No trace of the unconverted fraction of the 100 kev line was detectable in the absorption data, so a more sensitive method based on transition effects was used. The gamma-ray effects in an electroscope are due to Compton and photoelectrons ejected in the material between the source and the sensitive region of the chamber. As one piles lead over the source, the gamma-ray ionization at first increases, and then decreases. For lighter absorbers, the maximum will not be as high, and the rate of decrease will, of course, be smaller. These initial rises are due to the production of electrons in the absorber (in heavier elements the equilibrium ratio of electrons to gamma-rays is higher). If one places enough lead over the source to bring the ionization current up to near its maximum value, and then absorbs out the electrons from the lead with aluminum sheets, the ionization current will fall to the low value for equilibrium in Al. The amount of Al necessary to accomplish this lowering is equal to the range of the electrons, and therefore is a measure of the energy of the gamma-ray which projected them from the lead.

This method was applied to the annihilation radiation from Cu^{64}, and gave a value near 500 kev. When Ga^{67} was substituted, the transition curve showed a large group of electrons from a gamma-ray at about 250 kev, in agreement with the absorption data. A careful search with very thin absorbers showed another group due to the unconverted 100 kev line. (See Fig. 8.) Thus the line is not totally internally converted, as had at first been suspected. An examination of the transition curve near the 500 kev portion showed no trace of a drop, so it is quite certain that positrons play no important part in this activity.

Summing up the evidence, we see that a radioactive Ga isotope has changed into a zinc isotope, and during the process, no positrons have been emitted. (The gamma-ray evidence

[28] Van Voorhis, Phys. Rev. **50**, 895 (1936).

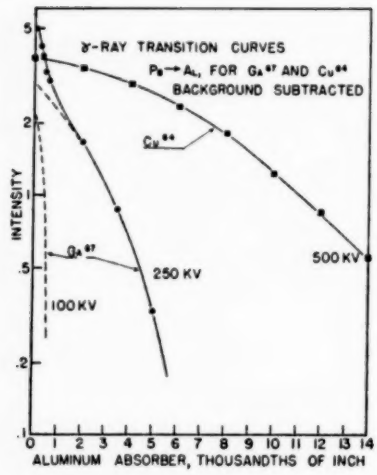

FIG. 8.

eliminates the possibility that the positrons might have been too soft to be detected.) To investigate the small chance that protons were emitted during the disintegration, a sample was examined in a linear amplifier, and also placed inside the electroscope chamber. No evidence was found for protons, and there are in addition good theoretical reasons for believing that extremely slow protons could not emerge in such numbers with a half-life as short as 83 hours. It must then be concluded that the transition from Ga to Zn has not been accompanied by the emission of any known particle of single positive charge. (The possibility that a heavy electron is responsible for the transition is ruled out on energetic grounds. There is not enough energy available for the transition to Zn^{67} and, if it went to Zn^{66}, the latter would be left too highly excited.)

We are therefore forced to the conclusion that the Ga^{67} nucleus has captured a negative electron from its orbital system, and been transformed into stable Zn^{67}.

OTHER DATA BEARING ON ELECTRON CAPTURE

Ta^{180}

The second artificially radioactive body shown to emit characteristic x-rays was Ta^{180}, reported by Oldenberg.[29] He irradiated tantalum with fast neutrons from the Li+D reaction, and separated an active form of tantalum by chemical methods. Since this period could not be induced by slower neutrons, it was assumed to be formed by neutron loss, and therefore assigned to the isotope with atomic weight one less than the only known stable isotope of Ta, Ta^{181}. The beta-rays from this isotope were all negative, as determined by a trochoid analyzer. The gamma-rays had an absorption coefficient in Al equal to that of Hf K-radiation. No magnetic field was necessary, as the first Al absorber cut out all the electrons. The curve could then be followed for several half-thicknesses of Al, with the aid of a Geiger counter. Oldenberg interpreted the x-rays as due to electron capture, giving Hf^{180}. Since W^{180} was not known, he suggested that the beta-rays were conversion electrons from an internally converted gamma-ray from an excited level of Hf^{180} to ground.

Sizoo[30] has shown on simple theoretical considerations that if the middle one of three neighboring isobars is radioactive, and emits negative electrons, it is almost certain to transform some of the time by electron capture. (If it could not do this, i.e., if the isotope with smallest Z had greater mass, the latter would transform by negative electron emission to the middle one, and would therefore not be observed as stable.) On the chance that the negative electrons observed here were disintegration betas —that this case were an example of Sizoo branching—the author asked Professor A. J. Dempster to reexamine his mass spectra of W to see if there was any evidence for W^{180}. The old plates showed faint lines, and new plates confirmed the existence of this isotope.[31] Thus Oldenberg's activity is probably the first example of electron emission-electron capture branching.

K^{40}

Weizsäcker[32] has made the suggestion that the natural radioactivity of potassium may be a branching reaction of the Sizoo type. In addition to the well-known electron decay to Ca^{40}, he postulates electron capture to A^{40}. This would explain several anomalies in the abundance of argon. The position of argon in the periodic table is not given by its sequence in the list of

[29] Oldenberg, Phys. Rev. **53**, 35 (1938).

[30] Sizoo, Physica **4**, 467 (1937).
[31] Dempster, Phys. Rev. **52**, 1074 (1937).
[32] Weizsäcker, Physik. Zeits. **38**, 623 (1937).

atomic weights. This situation would be corrected if the percentage abundance of A^{40} were smaller. The abundance of argon in the atmosphere is about one percent, which is vastly greater than any of the other rare gases. This might be termed circumstantial evidence, but it does fit well with theoretical ideas about electron capture.

Zn^{65}

Barnes and Valley,[33] and Livingood and Seaborg,[34] have reported an 8-month zinc period which emits positrons, and which has an abnormally high ratio of gamma-rays to positrons. This is no doubt the longest of the four periods in zinc mentioned above, which emit x-rays. Absorption measurements on the x-rays in Ni and Cu were made at that time, which showed that the radiation was characteristic of copper.[35] This is what one would expect from Zn^{65} if it captured electrons. It seems relatively safe to assume that the two zinc activities are identical and to assume, as Barnes and Valley, and Livingood and Seaborg did, that this is the first case of positron emission-electron capture branching.

Hg^{197}

Heyn[36] has reported a period of about 43 minutes induced in mercury by very fast neutrons. No details of the radiations emitted were noted by him, but he made the reasonable suggestion that the reaction was of the $n-2n$ type. McMillan, Kamen and Ruben,[37] in their survey of the neutron induced activities in the heavy metals, investigated this activity in some detail. They showed that the period was due to mercury, and that the electrons were all negative. They noted that the beta-ray energy was too low for even the first Sargent curve, and in private conversations, they suggested that the electrons might be conversion electrons from a gamma-ray after electron capture. An absorption curve of the gamma-rays showed a "possible complex structure with energies in the range 70–250 kev." On this basis, the assignment would have been to Hg^{197}. But these authors preferred the idea that the electrons were disintegration betas, and so assigned the activity to Hg^{203}.

An obvious difficulty with this assignment is the failure to observe the period with slow neutrons. Slow neutron capture is always energetically possible, and could not have escaped detection with such a short period. This would lead one to assign the period to Hg^{197}, since Hg^{196} is present only to 0.1 percent. The electrons then would not be primaries, which would eliminate the only point on a "negative Sargent curve." Since no positrons were observed, and since the gamma-ray spectrum does not extend to 500 kev, this is probably a case of electron capture.

Ag^{106}

Pool, Cork and Thornton[38] discovered an interesting case of isomerism in Ag^{106}. The 24-minute period emits positrons, while the one of 8-days half-life is electron active. Pool[39] has investigated the radiations from the isotope, and concluded that the 8-day period also captures electrons. If this explanation were correct, one would expect to find about three quanta of Pd K x-rays, and one Auger electron for every four gamma-rays. Pool's gamma-ray spectrum shows no electrons in this energy range, but they would have been a little difficult to measure. To check this point, a search for Pd $K\alpha$ was made in this laboratory. The source of radio-silver was covered with paraffin to absorb the beta-rays, and was thin enough to have negligible self-absorption for the x-rays. The gamma-ray ionization was measured in an electroscope filled with CH_3Br.[40] This type of instrument is much more sensitive to Pd x-rays than to gamma-rays, so almost all of the observed ionization should have been due to the former, if electron capture were taking place. Aluminum absorbers had very little effect on the ionization current, so it must be concluded that electron capture does not play an important part in the decay.

[33] Barnes and Valley, Phys. Rev. **53**, 946 (1938).
[34] Livingood and Seaborg, Phys. Rev. **54**, 239 (1938).
[35] The shortest of these four periods in unseparated, activated zinc was a new electron emitting isotope with a half-life of 15 minutes. The x-rays are definitely Zn K-radiation, and since this period is unknown, it might be due to Ga^{65} capturing electrons.
[36] Heyn, Nature **139**, 842 (1937).
[37] McMillan, Kamen and Ruben, Phys. Rev. **52**, 375 (1937).
[38] Pool, Cork and Thornton, Phys. Rev. **52**, 380 (1937).
[39] Pool, Phys. Rev. **53**, 116 (1938).
[40] I am indebted to Mr. Philip Abelson for the use of this instrument.

Cd^{107} or Cd^{109}

Ridenour, Delsasso, White, and Sherr[41] have found a 6.7-hour proton-induced activity in silver, which they ascribe either to Cd^{107} or Cd^{109}. The radiations emitted by this isotope are a soft electron group, a strong x-ray with the correct Al absorption coefficient, and a very weak gamma-ray. They conclude that the whole situation in this radioelement is similar to the case of Ga^{67}.

Be^7

Roberts, Heydenburg, and Locher[42] have very recently observed an interesting example of electron capture in Be^7. This new radioactive isotope may be formed in either of the following two reactions:

$$Li^6+D\rightarrow Be^7+n,$$

or

$$B^{10}+D\rightarrow Be^7+He^4.$$

This isotope is the only one known which emits nothing but gamma-rays; their energy is about 425 kev. The neutron yield in the reaction leading to Be^7 from Li is ten times the radioactive gamma-ray yield, which is a large enough discrepancy to mean something. The interpretation given by these authors is that in 90 percent of the disintegrations, the neutrino carries away all the available energy, leaving the Li^7 nucleus in the ground state. In 10 percent of the cases, which are those observed, the Li^7 is left in the well-known level at 440 kev, from which it radiates to the ground state.

Mn^{54}

Livingood and Seaborg[43] have found a long lived manganese isotope which may be prepared in three different reactions, and thus assigned to Mn^{54}. The radiations from this isotope are a strong x-ray absorbed in Al as Cr $K\alpha$, a gamma-ray of about 1 Mev, and a very weak negative electron group which is probably of secondary origin. These data are best interpreted as evidence for electron capture. The gamma-rays are internally converted to a very small extent, if at all.

The author wishes to acknowledge several valuable discussions of these problems with Professors E. O. Lawrence and J. R. Oppenheimer. The work has been materially aided by grants to the laboratory from the Research Corporation and the Chemical Foundation. The experiments were facilitated by assistance from the W.P.A.

Appendix

Additional data on Ga^{67}

Since this paper is primarily concerned with electron capture, only those data about Ga^{67} which bore directly on the problem were included in the section above. This appendix will complete the discussion of Ga^{67}, merely as an interesting case of artificial radioactivity. It was established earlier that the following radiations were emitted by this isotope: a line spectrum of electrons, the characteristic x-rays of zinc, a gamma-ray of about 250 kev and one at about 100 kev. In order to obtain a more complete picture of the processes involved, it is necessary to have some idea of the relative intensities of the various radiations.

An absorption curve in aluminum, of the total radiation from a thin, separated sample of Ga^{67}, showed that the ionization current due to the electrons was about 40 times that due to the x-rays. The chamber had a depth of 6 cm; from the absorption coefficient, one can calculate that 6 percent of the x-rays were absorbed in the active volume of the electroscope. The electrons have a range of about 10 cm in air, so about half of their energy was expended in the chamber. Each electron has ten times as much energy as an x-ray quantum. The relative intensity of x-rays and electrons is then

$$10/(40\times 0.06\times 2)\leqq 2.$$

The fluorescent yield for Zn is 0.5, so the ratio of K electron excitations to conversion electrons is about 4.

The intensity of the gamma-rays may be estimated in the following manner: since the gamma-ray ionization was obtained with aluminum absorbers over the sample, it is necessary to calculate the equilibrium ratio of electrons to quanta in aluminum. The mass absorption coefficient of the gamma-rays is 0.11 cm^2/g, and the range of the electrons is 0.045 g/cm^2, so 0.005 of the gamma-ray energy will be converted into electronic form in the effective upper layer of the aluminum. The range of the electrons in air is $0.045/0.001=45$ cm, but only 6 cm of this range is effective in the chamber. The ratio of x-ray ionization to gamma-ray ionization was observed to be 3.5, so the relative intensity of these two types of radiation is then

$$\frac{3.5\times 0.005\times 6\times 250}{0.06\times 45\times 9}\leqq 1.$$

The relative intensities of K-excitations, gamma-rays, and electrons are therefore approximately 4 : 2 : 1. These

[41] Ridenour, Delsasso, White, and Sherr, Phys. Rev. **53**, 770 (1938).
[42] Roberts, Heydenburg, and Locher, Phys. Rev. **53**, 1016 (1938).
[43] Livingood and Seaborg, Phys. Rev. **54**, 391 (1938).

values suggest that there are two excited states in the Zn^{67} nucleus—one at 350 kev, and the other either at 100, or 250 kev above ground. Every case of electron capture leaves the Zn^{67} in the upper state, from which it cascades to ground in two steps. One of the transitions gives rise to the 250 kev gamma-ray, and the other is responsible for the internally converted radiation at 100 kev. The internal conversion coefficient is fairly high, since the transition curves show the 100 kev line to be weaker than the one at higher energy. The relative intensities of electrons and x-rays confirm this. If the line were totally internally converted, the K-excitation would be twice as great as the electron emission, since the K shell would be emptied by capture and conversion in each transition. The observed ratio is 4, which indicates that the conversion coefficient is about 40 percent. All the intensities are consistent with the scheme outlined above.

The question then arises:—how is it possible to have such a large internal conversion factor in an element as light as zinc? It has been quite generally thought by theoretical physicists that internal conversion would play a negligible part in artificial radioactivity, since the equations predict a Z^3 dependence. (Total conversion in a 0–0 transition would be possible, however.) When it first became apparent that Zn^{67} had an anomalously high internal conversion coefficient, Dancoff and Morrison[44] reexamined the theory, and found that in the energy range near 100 kev for zinc, the factor could be quite high. The 40 percent observed (internal conversion coeff. ~0.7) would mean the gamma-rays were due to a quadripole transition. No detailed calculations of this nature had been made previously for light nuclei, as it had seemed certain from an inspection of the formulae that there were no terms entering which could make the ratio appreciable. All details of the picture, both experimental and theoretical, are now self-consistent.

It might be interesting to look for coincidences between the two x-rays ejected almost simultaneously in 1/8 of the disintegrations. (40 percent × (fluorescent yield)^2 = 1/8.) An apparatus for this experiment has been constructed, but has not as yet been used. The x-ray spectrum might yield interesting information about the relative lifetimes of x-ray and gamma-ray states. If the K shell were doubly excited, the wave-length of the characteristic radiation would be slightly changed, and this could be detected on a bent crystal spectrograph. No such case of a doubly excited K shell is known.

[44] Dancoff and Morrison, Phys. Rev. **54**, 149 (1938).

OCTOBER 1, 1938 PHYSICAL REVIEW VOLUME 54

Vibrational Analysis for a New CuCl Band System Excited by Active Nitrogen

SIDNEY BLOOMENTHAL
Ryerson Physical Laboratory, University of Chicago, Chicago, Illinois

(Received August 12, 1938)

The CuCl band spectra in the near ultraviolet, first observed by Strutt and Fowler who used active nitrogen excitation, were photographed and classified. The wave number of any band head in this system may be calculated from the formula

$$\nu = 25{,}282 + [383(v' + \tfrac{1}{2}) - 2(v' + \tfrac{1}{2})^2] - [415(v'' + \tfrac{1}{2}) - (v'' + \tfrac{1}{2})^2].$$

This band system has a common lower state with five other systems in the visible, observed in absorption and analyzed by Ritschl.

INDEPENDENTLY of Harnack,[1] who photographed the spectrum of copper in a chlorine gas flame, Strutt (now Lord Rayleigh) and Fowler,[2] working with copper chloride in active nitrogen, observed a set of bands in the near ultraviolet, which Kien[3] had not observed at an earlier date in the flame. Eder and Valenta show some of the bands in their Atlas.[4] Using a tungsten lamp as source, Ritschl[5] photographed the absorption spectra of all the copper halides and made a fairly thorough analysis of the CuCl spectrum into five systems, but he failed to record or classify any of the CuCl bands below 4050A previously observed in emission, save one, the 7 2 band of the E system. The possibility of the presence of a sixth system was mentioned previously in a paper by Mulliken,[6] who excited

[1] A. Harnack, Zeits. f. Wiss. Phot. **10**, 281 (1912).
[2] R. J. Strutt and A. Fowler, Proc. Roy. Soc. **A86**, 105 (1912).
[3] P. Kien, Zeits. f. Wiss. Phot. **6**, 337 (1908).
[4] Eder and Valenta, *Atlas Typischen Spektren* (Wien, 1928).
[5] R. Ritschl, Zeits. f. Physik **42**, 172 (1927).
[6] R. S. Mulliken, Phys. Rev. **26**, 1 (1925).

all the copper halide spectra by means of active nitrogen, and gave the first analysis for Cu I.

In the process of testing a new tube for exciting spectra from solid materials by bombardment with a jet of active nitrogen produced in a side tube fitted with large graphite electrodes, (Fig. 1) the author photographed the near ultraviolet band spectra emitted by CuCl with a dispersion sufficient for resolution into sequences (16.8 to 24.6A per mm), but not great enough for a clear demonstration of the isotope effect. With large graphite electrodes, considerably more power can be introduced into the nitrogen discharge than previously with tungsten wire electrodes. The use of a jet for introducing active nitrogen, glowing with a bright yellow hue, into the reaction chamber, causes the formation of a concentrated blue glow above the hot Cu_2Cl_2, which was projected upon the slit of the spectrograph by means of a quartz lens. A large quartz window for the reaction chamber was supplied by Mr. F. Pearson, Jr., through the kindness of

TABLE I. CuCl *F band spectra.*

v'	v''	I	λ (A)	ν (cm^{-1})	$O-C$	EDER AND VALENTA	HARNACK	STRUTT AND FOWLER
3	0	0	3789.3	26,383	−8		3788	3785
3	1	1	3848.8	25,975	−3			
2	0	1	3842.1	26,929	0		3839	3835
3	2	1	3909.9	25,569	+2			
2	1	1	3903.8	25,609	+2			
1	0	2	3898.3	25,645	0		3896	3885
3	3	1	3973.5	25,160	+2			
2	2	1	3968.0	25,195	−1			
1	1	1	3961.9	25,233	+1			
0	0	2	3956.9	25,265	−1	3962	3955	3945
2	3	1	4032.9	24,789	+2			
1	2	2	4027.4	24,823	+2			
0	1	3	4022.7	24,852	−1	4007	4020	4010
3	5	1	4106.0	24,348	+1			
2	4	2	4100.6	24,380	0			
1	3	3	4095.1	24,413	+1			
0	2	2	4090.3	24,441	−1	4063	4089	4080
3	6	2	4175.9	23,940	−3			
2	5	2	4169.9	23,975	0			
1	4	4	4165.1	24,005	0			
0	3	3	4159.7	24,033	0	4125	4159	4150

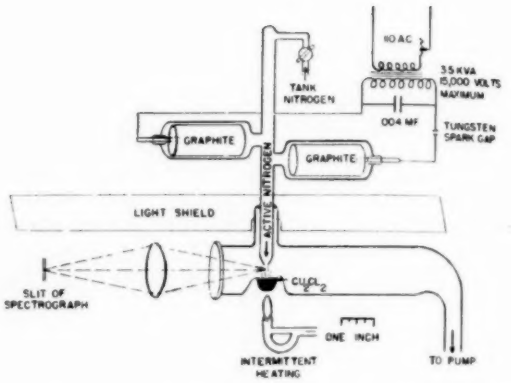

FIG. 1. Experimental arrangement for exciting the CuCl spectrum by means of active nitrogen.

Dean H. G. Gale of this institution. The exposure time was one hour, the plates were Eastman 40.

During a brief visit to Ryerson Laboratory in June of this year, Professor F. A. Jenkins mentioned that he had photographed the absorption spectrum of CuCl recently at Berkeley, and found some new bands in the ultraviolet. He had not published his analysis however, and the following classification of the measured band heads is given for the sake of comparison with his present findings.

Table I contains the wave-length data for this and previous investigations, together with a vibrational quantum analysis, which was effected through the resolution of previously known band groups into sequences. The formula

$$\nu = 25{,}282 + [383(v'+\tfrac{1}{2}) - 2(v'+\tfrac{1}{2})^2] - [415(v''+\tfrac{1}{2}) - (v''+\tfrac{1}{2})^2]$$

fits the data within the accuracy of measurement. The new band system appears to have a common lower state with the five systems of bands for CuCl analyzed by Ritschl from absorption measurements. The intensity of the new system appears to be appreciably less than that of the visible bands of CuCl observed in emission.

Thanks are due Professor R. S. Mulliken and Dean H. G. Gale of the University of Chicago for encouraging this investigation.

Čerenkov Radiation

GEORGE B. COLLINS AND VICTOR G. REILING
Department of Physics, University of Notre Dame, Notre Dame, Indiana
(Received July 29, 1938)

Electrons of two million volts energy from an electrostatic generator were used to investigate the properties of the asymmetric radiation discovered by Čerenkov. This radiation is produced when electrons traverse a material medium with a velocity greater than the velocity of light in that medium. It was found for several solids and liquids that the direction of the emission of the radiation is accurately expressed by the relation, $\cos\theta = 1/\beta n$, and that the intensity maximum is quite sharp. The nature of the radiation from all solids and liquids investigated was found to be continuous and identical in appearance. The radiation apparently extends with increasing intensity from the infra-red to the ultraviolet absorption limit of the medium in which it is produced. Rough quantitative measurements of its intensity indicate that one 1.9 million volt electron in being brought to rest in water produces 40 quanta in a wave-length range 4000A to 6700A. These results are in good agreement with the classical explanation of the phenomenon given by Frank and Tamm.

INTRODUCTION

ČERENKOV[1] in 1934 reported the existence of a visible radiation from pure liquids and solids when electrons traverse the medium with a velocity greater than that of light in the medium. The radiation was observed to be unusual in several ways, and its characteristics were such as to indicate that the physical processes responsible for its production were not any of the usual ones associated with atomic or molecular changes. It seems to result rather from a cooperative phenomena between the incoming electrons and an assemblage of atoms. In his original investigation Čerenkov showed that the radiation was not fluorescent, and that it was polarized with the electric vector parallel to the direction of the electron beam. Later work by Čerenkov[2] showed that the radiation had the unusual property of being emitted asymmetrically and that its intensity depended only on the refractive index of the medium.

Frank and Tamm[3] have given a theoretical explanation of this phenomenon which is entirely classical, but which is in agreement with the qualitative observations of Čerenkov. A striking feature of this theory is that it describes a new process for the production of radiation.

In his experiments Čerenkov used both β-rays and Compton electrons produced by gamma-rays from radioactive substances. These are, of course, not "monochromatic" sources of electrons, and furthermore they produce only a very feeble radiation which made it difficult to obtain results of a quantitative nature. In the investigation reported here the high speed electrons were obtained from an electrostatic generator and accelerating tube. This equipment produces a well-collimated homogeneous beam of electrons of about 10 microamperes at potentials up to 2.0 million volts. With this, fairly strong sources of radiation could be obtained which allowed a considerable extension of the work of Čerenkov.

THEORY

In the theoretical investigation of this phenomenon Frank and Tamm treated the radiation as due to an electron passing through a medium of refractive index n with a variable velocity v. Their work consisted in a purely classical derivation of the relation between the current density of the moving electron and the electrical and magnetic field strengths of the emitted radiation. The solution of the resulting differential equation, for $\beta n < 1$, results in a damped radiation whose intensity decreases exponentially with distance, so that the radiation is not observable. The situation is similar to the penetration of light into the second medium in the case of total reflection. The solution for $\beta n > 1$ gives spherical waves which are continually being emitted by the moving electrons and constructive interference (see Fig. 1) between these rays gives rise

[1] P. A. Čerenkov, C. R. Acad. Sci. USSR **8**, 451 (1934).
[2] P. A. Čerenkov, C. R. Acad. Sci. USSR **14**, No. 3 (1937); Phys. Rev. **52**, 378 (1937).
[3] I. Frank and Ig. Tamm, C. R. Acad. Sci. USSR **14**, No. 3 (1937).

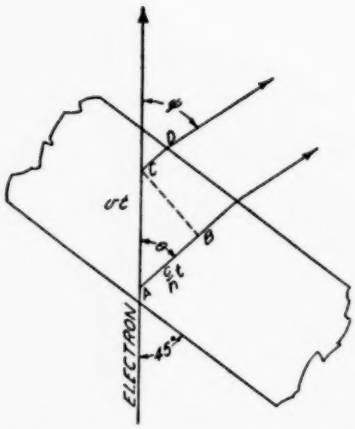

FIG. 1. Diagram showing interference between rays produced by a moving electron in a medium which leads to the relation, $\cos\theta = 1/\beta n$.

to an observable radiation.

Equation (1) was obtained by these authors and expresses

$$W = \frac{e^2 l}{c^2} \int_{(\beta n > 1)} \omega d\omega \left(1 - \frac{1}{\beta^2 n^2}\right) \qquad (1)$$

the total energy W radiated by the electron as a function of the length of path l, the velocity ratio β, the frequency of the emitted light ω, and the refractive index n.

It should be noted that this result is independent of all physical properties of the medium with the exception of the refractive index. The theory also shows that the radiation should be continuous, that it should extend from the infrared to the ultraviolet absorption limits of the medium in which it is produced, and that its intensity should vary inversely with the cube of the wave-length.

It is to be understood that the electron in its passage through the medium gradually loses nearly all its energy through ionization and excitation processes, and that the resulting acceleration is responsible for the Čerenkov radiation. The process may be compared to the classical explanation of the continuous x-ray spectrum. It differs in that the acceleration which the electron suffers is in comparison much smaller, and the energy lost by the electron which does not appear as radiation is in comparison much larger. A calculation of the total energy lost by a fast electron ($\beta \sim 1$) through radiation as given by (1) was shown by Frank and Tamm to be only several kilovolts, a negligible amount compared to losses by other causes.

The theory also implies that the radiation emitted by the electron along its path is coherent and its asymmetrical character is due to interference of the light produced at points along the electron's path. This conclusion leads directly to Eq. (2)

$$\cos\theta = 1/\beta n, \qquad (2)$$

where θ is the direction of emission of the asymmetrical radiation measured with reference to the direction of the electron beam, and n and β have their usual significance. The derivation of this relation may be seen by referring to Fig. 1. For any two light rays, AB and CD, to be in phase after leaving the medium, the light ray produced first must travel a distance $AB = ct/n$ while the electron travels the distance $AC = vt$. Equating these in terms of the angle of emission θ yields $vt\cos\theta = ct/n$ which reduces immediately to Eq. (2). This relation holds for all the rays produced in the medium no matter what their separation may be. The verification of this relation, which follows, is then essentially a proof of the fact that the radiation produced by an electron is coherent.

EXPERIMENTAL

In general the aim of this investigation was to obtain additional experimental information about this radiation, and to compare the results with

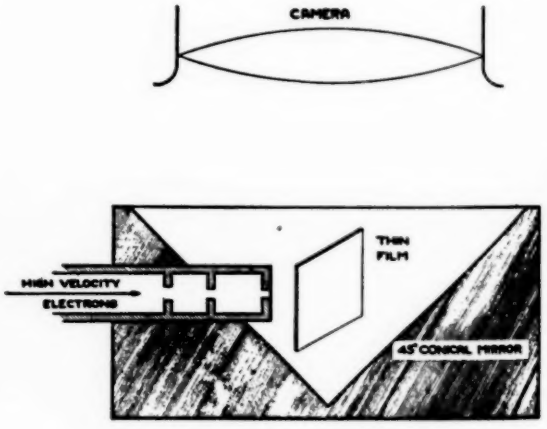

FIG. 2. Diagram of apparatus to show angular distribution of Čerenkov radiation.

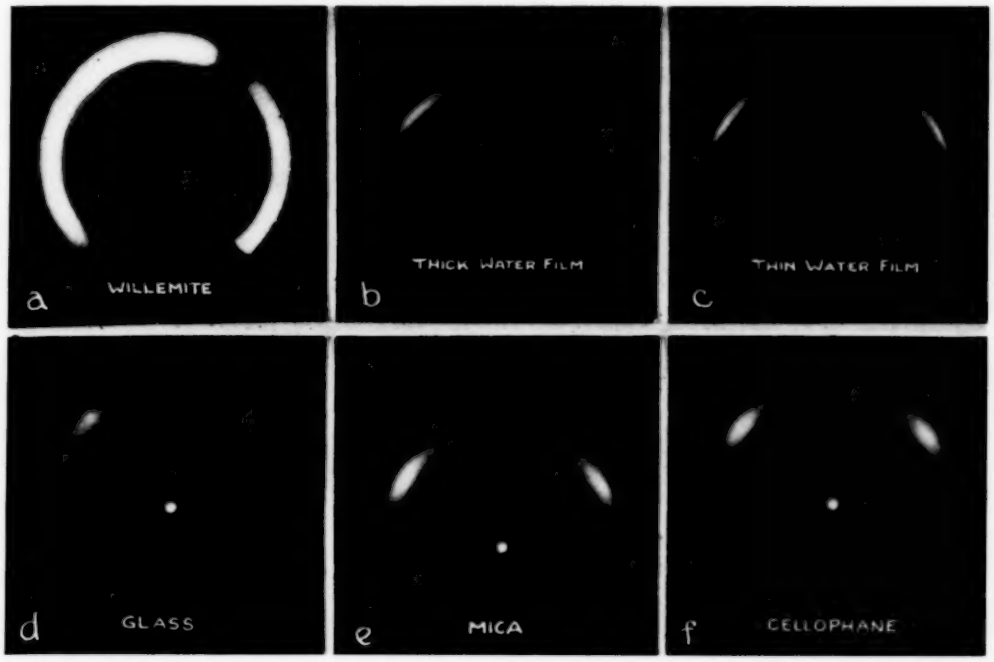

FIG. 3. Photographs of the radiation after reflection from a conical mirror showing the angular distribution of intensity. (*a*) powdered willemite; (*b*) 0.1 cm film of water; (*c*) 0.03 cm film of water; (*d*) 0.006 cm glass; (*e*) 0.002 cm mica; (*f*) 0.002 cm Cellophane. Lines indicate angles calculated from Eq. (2).

the theory of Frank and Tamm. The work was therefore divided into three parts whose purposes were the following: (1) to investigate quantitatively the direction of emission of the radiation from several solids and liquids and to compare these results with the values obtained from Eq. (2); (2) to determine the spectroscopic character of the radiation; (3) to determine in absolute units the intensity of the radiation and compare these results with the theoretical predictions of Eq. (1).

I. Direction of emission of the radiation

The apparatus used to investigate the direction of emission and asymmetrical character of the radiation is given in Fig. 2. Thin films of the substances under investigation were placed in the center of the conical mirror in the path of the electron beam which had been collimated by three 0.5 mm circular aperatures and the radiation produced in the film was then reflected by the conical mirror and photographed with a conventional camera. This optical system is such that if radiation is emitted in all directions from the film a circular ring is obtained on the photographic plate. The system was tested for optical uniformity by photographing the radiation induced in a fluorescent substance, which should show a uniform angular distribution of intensity. For this purpose a small rectangular fluorescent screen of willemite was placed at the center of the conical mirror and bombarded with electrons. Fig. 3a resulted and shows a uniform intensity distribution, as expected, except for the gaps in the ring which are due to the shadows cast by the film holder and electron beam windows.

With this arrangement the asymmetrical character of the Čerenkov radiation from several solids and liquids was investigated. The liquid films were produced by flowing the liquid over a copper plate in which was drilled a 2 mm hole. Surface tension maintained a fairly uniform film over the hole whose thickness was altered by varying the thickness of the copper plate. Figs. 3b and 3c show the directions of emission of the Čerenkov radiation from films of water 0.1 cm and 0.03 cm thick, which were set normal to the electron beam. Both show a decided tendency towards asymmetry, and it is to be noted that the sharpness of the intensity maxima increases

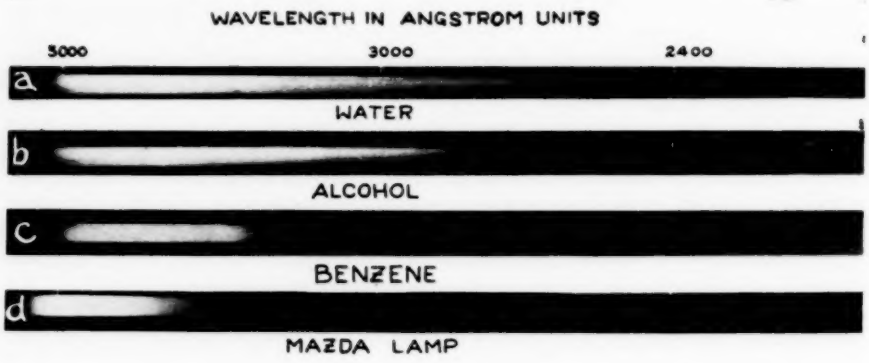

FIG. 4. Spectra of Čerenkov radiation produced in liquids by high velocity electrons. 1 mm slit, exposures 10 minutes.

with decreasing film thickness. Thus one is led to believe that the breadth of the intensity maxima is due to a considerable extent to scattering of the electron beam in the film. No definite conclusion as to the limiting sharpness of the intensity maxima is possible, as a reduction in the thickness of the film always resulted in an increased sharpness, to the point where the films became too thin to give sufficient intensity. From this it is concluded, however, that the intensity maxima from a perfectly collimated beam of electrons probably would result in very sharp intensity maxima.

Quantitative measurements of the angle of emission of the radiation were made only with solids because the liquid films used did not have optical surfaces sufficiently good to give reliable results. Sheets of glass, mica, and Cellophane were investigated. For these substances it was found necessary to set the sheet at a large angle to the electron beam so that the Čerenkov radiation produced inside the sheet would not be totally reflected at the surface.

Figures 3d, 3e, and 3f were obtained by setting the sheet of the material under investigation at an angle of 45° to the incident electron beam (Fig. 1) and, with a current of about 1 microampere, exposing the plate for 10 seconds. The sheet was then rotated to an angle of 45° on the other side of the electron beam and the exposure repeated on the same plate. The lines on each figure mark the position of the calculated maxima as given by Eq. (2), after correction was made for refraction at the surface of the sheet. The relationship used to obtain the theoretical value of the angle of emission outside the medium for sheets set at 45° to the electron beam was $\psi=45°+\sin^{-1} n\cdot\sin(\theta-45°)$ where ψ is the angle of emission outside the medium and θ is the angle of emission inside the medium as given by the relation $\cos\theta=1/\beta n$. The comparison between the observed and calculated angles may be found in Table I. The agreement is quite good and what discrepancy there is can be explained by a slight unavoidable bending of the thin sheets used.

II. Spectroscopic character of the radiation

The Čerenkov radiation was bluish white in color and was identical in appearance for all the solids and liquids investigated. With thick samples of liquid the intensity was sufficient to obtain spectrograms with moderate dispersion. The source of the radiation was a very thin walled quartz bulb, 0.5 cm in diameter, containing the liquid, which was supported in the electron beam. The spectra of this radiation from several liquids were photographed with a quartz spectrograph having a dispersion of 30A/mm at 3500A. A rather wide slit was used as it was found desirable to reduce the exposure

TABLE I. *A comparison of the observed and computed angles of emission of the Čerenkov radiation from sheets of various substances set at 45° to the electron beam.*

MEDIUM	THICKNESS	n	OBS. ANGLE	COMPUTED ANGLE
Mica	0.002 cm	1.59	53° 30′	52° 10′
Glass	0.006 cm	1.47	45° 15′	46° 30′
Cellophane	0.002 cm	1.54	50° 0′	49° 22′

time to a few minutes. Figs. 4a, 4b, and 4c are reproductions of the spectra of the radiation obtained from water, alcohol and benzene. Fig. 4d is the spectrum of a tungsten lamp taken with the same instrument and slit for the purpose of comparison. In every case the spectrum was found to be continuous and to extend from the long wave limit of sensitivity of the plate approximately to the ultraviolet absorption limit of the medium in which it was produced. It is to be noticed also that the intensity of the Čerenkov radiation at short wave-lengths is relatively stronger than the radiation from the tungsten lamp. The radiation was also inspected visually with a glass spectroscope (dispersion about 45A/mm). Even with a very narrow slit, no indication of structure was observed. This result seems to confirm that the radiation is continuous as stated in the theory of Frank and Tamm. It seems also likely that the radiation extends throughout the region where the condition $\beta n > 1$ holds.

III. Intensity of the radiation

As an additional test of the validity of Eq. (2) a determination of the absolute intensity of the radiation was made. The method consisted essentially in focusing a part of the radiation from a 0.5 cm bulb of water, produced by 1.9 Mev electrons upon a photoelectric cell (RCA 868) whose absolute sensitivity curve in microamperes per watt was provided by the manufacturers. In order to convert the photoelectric current obtained into watts emitted by the source per microampere of beam-current several assumptions of an approximate nature were necessary. The most serious was one concerning the angular distribution of the radiation emitted by the bulb. Reasonable assumptions, however, led to the conclusions that 9×10^{-4} watt of radiation between 4000A and 6700A resulted from each microampere of 1.9 Mev electrons. Expressed in another form each electron of this energy produced 40 photons between 4000 and 6700A in being stopped by the liquid. The value of W obtained from Eq. (2) upon introducing appropriate values for the limits of ω, and the range of electrons in water, is 22×10^{-4} watt per microampere which is twice the experimental value. This result indicates an agreement as far as order of magnitude is concerned and the discrepancy is perhaps not significant in view of the uncertainties in the assumptions that were necessary.

While investigating the Čerenkov radiation it was suggested that there might be some connection between this radiation and one investigated by Cohn[4] and others.[5] Cohn observed under certain conditions a visible radiation emanating from the anodes of x-ray tubes. This radiation was reported as bluish-white, evidently similar in color to the Čerenkov radiation, but differing from it in that it was unpolarized. To establish the fact that the Čerenkov radiation and that observed by Cohn were distinct phenomena, metal foils, about 0.001 cm thick, of platinum, silver, copper, and aluminum were irradiated with electrons of 1.95 Mev energy. All metals exhibited a feeble radiation which was bluish-white in character, including silver which has a refractive index less than unity throughout the visible region. The radiation, therefore, cannot result from the Frank-Tamm process which requires that $\beta n > 1$, and this together with the fact that the radiation from metals is not polarized shows that the two phenomena are distinct.

In conclusion it may be stated that the experimental results reported here are in complete agreement with the classical explanation as developed by Frank and Tamm. It would be expected, however, that at very short wave-lengths a determination of the intensity would result in a deviation from the classical theory in much the same way that the classical theory of Rayleigh-Jeans fails at short wave-lengths.

The authors are indebted to Dr. E. Guth for many helpful suggestions and discussions while the work was in progress.

[4] Willi M. Cohn, Zeits. f. Physik **72**, 302 (1931).
[5] J. E. Lilienfeld, Physik. Zeits. **20**, 280 (1919).

The S–H Frequency of the Mercaptans

DUDLEY WILLIAMS
University of Florida, Gainesville, Florida

(Received August 5, 1938)

The spectra of one aromatic and two aliphatic mercaptans have been studied in the region between 2.75μ and 4.25μ. In addition to the bands near 3.3μ arising from the carbon-hydrogen linkage, absorption maxima were observed at 3.85μ in benzyl mercaptan, at 3.83μ in *n*-propyl mercaptan, and at 3.80μ in *n*-butyl mercaptan. These bands are attributed to a vibration of the S−H group. The data obtained in the present study are compared with the existing Raman data and with the infra-red bands arising from the O−H group.

NUMEROUS studies of the spectra of organic compounds have shown that the vibrational frequencies of certain groups are approximately the same in all compounds. For example, the C−H and O−H groups give rise to bands near 3.3μ and 3.0μ, respectively. It has been of interest to determine the position of the band arising from the S−H groups in the mercaptans. Bell[1] measured the transmission of iso-amyl, *n*-butyl, and *n*-propyl mercaptan in the region between 1μ and 12μ and compared the spectra of these compounds with those of the corresponding sulphides. This author reported that the absorption of the mercaptans in the short wave-length region is similar to that of the amines, which he had investigated previously.[2] However, Ellis[3] was inclined to believe that the S−H group was responsible for a small absorption band near 3.8μ in the transmission curves published by Bell.[1] Ellis studied the spectra of the mercaptans in the region from 0.59μ to 2.8μ in the hope of observing harmonics of the 3.8μ band. A band observed at 1.99μ–2.00μ was identified as the first harmonic of the S−H frequency. The deviation from a simple multiple relationship is obvious. Since the 3.8μ band in Bell's curves is poorly resolved and its presence is indicated by only one or two points, it appeared desirable to make a more intensive study of the mercaptan absorption near 3.8μ. Accordingly, the transmission of benzyl, *n*-propyl, and *n*-butyl mercaptan has been determined in the region 2.75μ to 4.25μ. A rocksalt prism spectrometer with an amplifier was used in obtaining the present data.

The results are shown in Fig. 1. In each curve two bands appear. The bands at shorter wave-

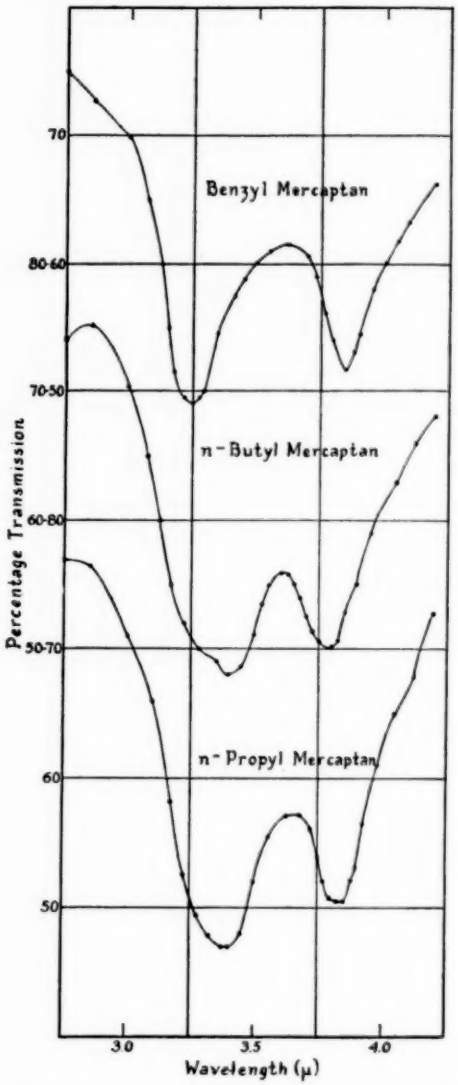

FIG. 1. The transmission of three mercaptans. Region: 2.75μ to 4.25μ. Cell thickness: 0.05 mm.

[1] F. K. Bell, Berichte **60**, 1749 (1927).
[2] F. K. Bell, J. Am. Chem. Soc. **49**, 1837 (1927).
[3] J. W. Ellis, J. Am. Chem. Soc. **50**, 2113 (1928).

lengths arise from C−H vibrations and have maxima at 3.25μ in the aromatic mercaptan and near 3.4μ in the aliphatic compounds. The bands observed at longer wave-lengths are attributed to the S−H vibration. The positions of the minima are 3.85μ in benzyl mercaptan, 3.80μ in butyl mercaptan, and 3.83μ in *n*-propyl mercaptan. The S−H bands are apparently clearly resolved, but the exact positions of the observed minima are possibly affected slightly by the proximity of the intense C−H bands. The relative intensity of the C−H and S−H bands is different from that observed by Bell.[1] However, the total absorption is in approximate agreement with Bell's results, if differences in cell thickness are taken into consideration.

The differences between the infra-red bands of the mercaptans and those of the alcohols are striking. The O−H bands of the liquid alcohols are broad, while the S−H bands of the liquid mercaptans are sharp, resembling in shape the O−H bands observed in alcohol vapor. Errera[4] has suggested that the broadening and shift of the alcohol bands in the gas-to-liquid transition indicate a strong association between the O−H groups of neighboring molecules. If this interpretation is correct, the sharpness of the S−H band probably indicates the absence of a similar type of association in the mercaptans, a result in accord with chemical data. There is also a marked difference in the absorption coefficient. (See Table I.)

TABLE I. *Comparison of results with Raman data. The relative extinction coefficient in the last column is the ratio of the* SH *extinction coefficient to that of the corresponding* OH *compound.*

COMPOUND	S−H FREQUENCY (cm^{-1}) INFRA-RED	RAMAN*	RELATIVE EXTINCTION COEFFICIENT
Benzyl Mercaptan	2600	—	—
n-Butyl Mercaptan	2630	2574	0.08†
n-Propyl Mercaptan	2610	2575	0.12†

* Raman data: Venkateswaran (reference 5).
† Alcohol data: W. Weniger, Phys. Rev. **31**, 388 (1910).

A comparison of the present infra-red data with the Raman is rather interesting. The S−H vibration is strongly Raman-active[5] but produces a relatively weak infra-red band. The O−H vibration giving rise to intense infra-red absorption is so weakly Raman-active that an O−H line has been observed in only one alcohol (methyl).[6]

The writer wishes to express his appreciation to the American Association for the Advancement of Science for a grant making this study possible.

[4] J. Errera and P. Mollett, Comptes rendus **204**, 259 (1937).

[5] S. Venkateswaran, Ind. J. Phys. **5**, 219 (1930).

[6] K. W. F. Kohlrausch, *Der Smekal-Raman Effekt* (J. Springer, Berlin, 1931), p. 309. (Summary of Raman Work on alcohols.)

The Velocity of Sound in Liquid Helium

J. C. FINDLAY, A. PITT, H. GRAYSON SMITH AND J. O. WILHELM
McLennan Laboratory, University of Toronto, Ontario, Canada

(Received July 8, 1938)

The velocity of sound in liquid helium under its vapor pressure has been determined by an ultrasonic method over a temperature range from 4.22°K to 1.76°K. From the measurements obtained, the compressibility of the liquid helium has been computed. At temperatures not too close to the λ-point, the values are in fair agreement with those estimated from thermodynamical considerations, but the expected discontinuity at the λ-transition has not been observed.

INTRODUCTION

AS a part of a general program of obtaining as much information as possible about the physical properties of liquid helium, the velocity of sound has been measured in liquid He I and He II. This provides an experimental determination of the compressibilities of these liquids under their vapor pressures, and of the possible change in compressibility at the λ-transition.

According to the relations developed by Ehrenfest[1] for a so-called phase change of the second order, there should be a discontinuous change in compressibility at the λ-point, and therefore a change in the velocity of sound. Von Laue[2] has raised objections to Ehrenfest's treatment of this type of transition, but Rutgers and Wouthuysen[3] have shown that in a transition which extends over a small but finite range of temperature without a discontinuous absorption of latent heat, Ehrenfest's relations should still be valid. From these relations, the slope of the λ-line on a pressure temperature diagram should be given by

$$(dp/dT)_\lambda = -\Delta\alpha/\Delta K_T, \qquad (1)$$

where $\Delta\alpha$ is the change in the coefficient of expansion, and ΔK_T the change in the isothermal compressibility, in going from He II to He I. However, the measurements to be described in the present paper show that there is very little change, if any, in the velocity of sound at the λ-point.

[1] P. Ehrenfest, Proc. Kon. Akad. van Weten. Amsterdam **36**, 153 (1933). (Leiden Comm. Suppl. 75b.)
[2] M. von Laue, Physik. Zeits. **35**, 945 (1934).
[3] A. J. Rutgers and S. A. Wouthuysen, Physica **4**, 515 (1937).

EXPERIMENTAL METHOD

The method of measuring the velocity of sound in liquids by means of ultrasonic waves has been extended to condensed gases by Pitt and Jackson,[4] who obtained values in liquid oxygen and liquid hydrogen, but were unable to obtain detectable standing waves in liquid helium, with its high compressibility and small density. After the method had been modified so that it was sufficiently sensitive to give measurements in gases, it was found satisfactory for the liquid helium.

The apparatus, shown in Fig. 1, consisted of a quartz crystal B, sputtered on both sides with

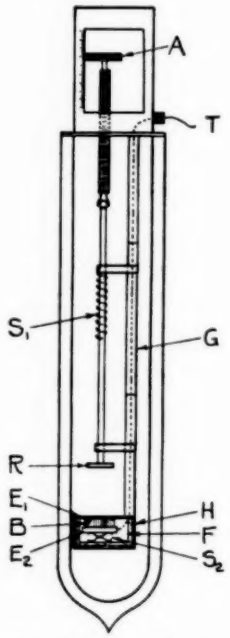

FIG. 1. Arrangement of ultrasonic crystal and reflector.

[4] A. Pitt and W. J. Jackson, Can. J. Research **12**, 686 (1935).

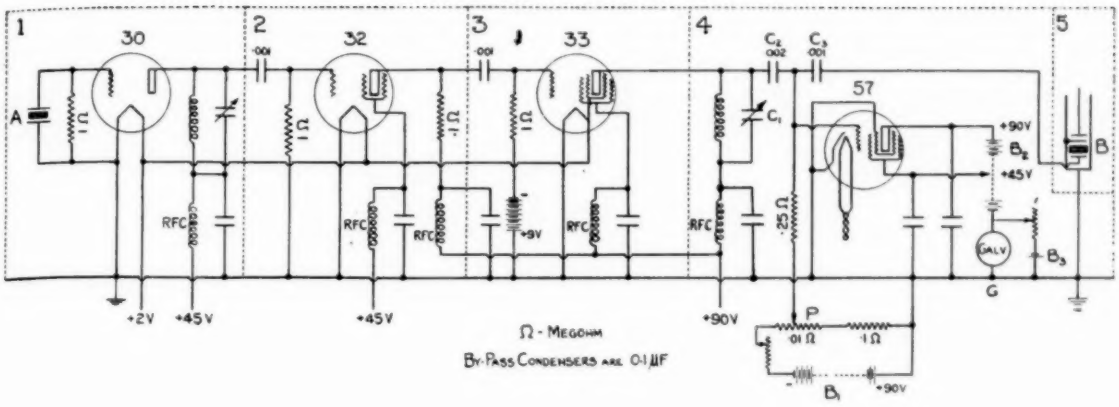

FIG. 2. Crystal-controlled ultrasonic generator circuit.

aluminum, which was held by means of a spring S_2 between a brass ring E_1 and a disk E_2. With this arrangement, the crystal was clamped at its edges. The crystal, in a fiber shell F and a metal sheath, was supported by a German silver tube G, which served as the grounded lead from E_1, and also as a shield for the lead T from E_2. A reflector R was mounted at one end of a thin German silver tube, the other end of which was held by means of the spring S_1 against a ball and socket joint at the end of a micrometer screw A.

The crystal which generated the ultrasonic waves was driven at a very constant frequency by means of a generator whose frequency was controlled by a second crystal. In Fig. 2, A represents the controlling crystal, whose signal is amplified and imposed on B, the crystal in the liquid. The amplitude of vibration of B is indicated by the galvanometer G, connected in the plate circuit of a 57 detector tube. As the reflector was moved through intervals of one-half wave-length, sharp maxima were observed in the galvanometer deflection, which were due to the setting up of standing waves in the liquid column. A much more vigorous response was obtained by driving the sonic crystal at a frequency close to its natural resonance.

The micrometer screw was calibrated by means of a highly accurate comparator. The driving frequency, the second harmonic of the frequency of crystal A (Fig. 2), was determined by the method of obtaining audio-beats with the carrier waves of various broadcasting stations. The fundamental was determined to be 669 kc, the harmonic 1337.9 kc. Preparatory work was done in ether, benzene, liquid oxygen, and helium gas. A few results of these preliminary tests are shown in Table I, together with values obtained by other experimenters for comparison.

TABLE I. *Preliminary results which show the reliability of the apparatus and method.*

SUBSTANCE	FREQUENCY KC/SEC.	TEMPERATURE °C	VELOCITY M/SEC.	COMPARATIVE VALUE
Ether	669	22.3	984	
	1338	21.4	1010	
	669	13.0	1045	1024[1]
Liquid Oxygen	1338	−182.9	908	912[2]
				903[3]
Helium Gas	1338	−182.9	540	559[4]
	1338	−268.9	104	102[5]

[1] At 15°C (I. C. T.). Independent measurements in ether are not consistent because of the variability of its composition.
[2] Pitt and Jackson, reference 4 in text.
[3] Debye-Sears method; R. Bär, Nature **135**, 153 (1935).
[4] W. H. Keesom and A. van Itterbeek, Kon. Akad. van Weten. Amsterdam **33**, 440 (1930). (Leiden Comm. 209a.)
[5] W. H. Keesom and A. van Itterbeek, Kon. Akad. van Weten. Amsterdam **34**, 204 (1931). (Leiden Comm. 213b.)

MEASUREMENTS IN LIQUID HELIUM

When determining the wave-length in liquid helium at various temperatures, readings of the micrometer screw were taken at every fifth maximum of the galvanometer deflection over a range of 25 to 100 half wave-lengths. The wave-length for the frequency used—1338 kc—was of the order of 0.16 mm. The velocities calculated from these measurements are shown plotted against temperature in Fig. 3, and values derived from the original smoothed graph are given in Table II.

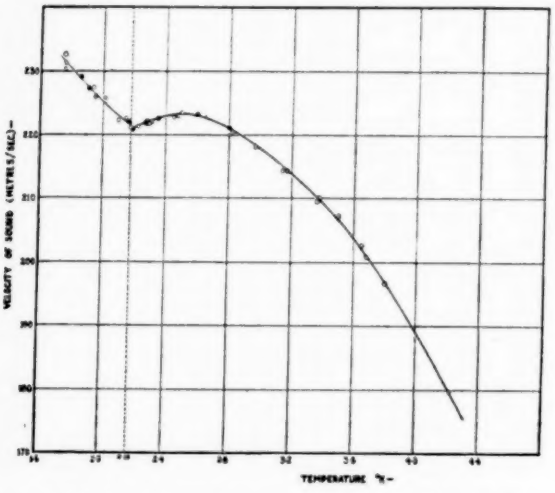

FIG. 3. Velocity of sound (meters per sec.) in liquid helium.

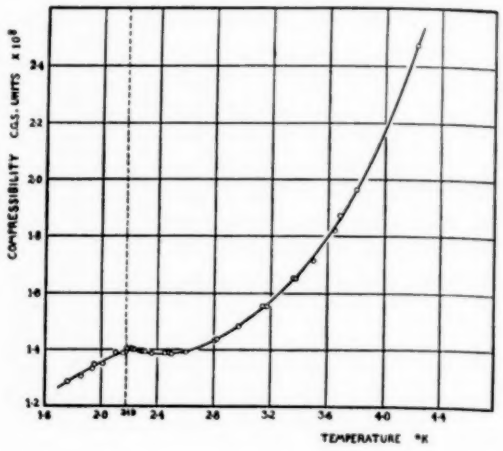

FIG. 4. Adiabatic compressibility of liquid helium, deduced from velocity measurements.

As a check on the measurements at different temperatures, the reflector was set at a fixed distance from the crystal while the temperature was altered. The galvanometer fluctuations then gave the change in the number of half-waves between the reflector and the crystal. From this the change in velocity was calculated and found to agree very well with the values obtained by moving the reflector at constant temperature. As the λ-point was crossed, the galvanometer movement was erratic, and attempts to determine by this method whether there was a change in velocity at the λ-point were unsuccessful.

The temperature was controlled by the vapor pressure of the helium, which was maintained constant within 1 mm of mercury. Fluctuations of temperature would not cause errors in the measurement of wave-length greater than 0.03 percent in He I or 0.2 percent in He II. If allowance is made for the possible error in measuring the displacement of the reflector, the results should be correct within 0.2 percent in He I and 0.4 percent in He II. The graph shows that practically all the results are within this limit of error.

TABLE II. *The velocity of sound and the compressibility of* He I *and* He II *at various temperatures.*

TEMPERATURE °K	VELOCITY M/SEC.	COMPRESSIBILITY C.G.S. UNITS
He I		
4.22	179.8	2.474×10^{-8}
4.0	189.2	2.170
3.6	206.5	1.722
2.5	223.3	1.382
2.20	221.2	1.402
He II		
2.18	221.7	1.392
2.0	225.3	1.355
1.76	231.4	1.285

COMPRESSIBILITY OF LIQUID HELIUM

The measured values of the velocity are about 12 percent lower than the values predicted from the formula

$$W=1/(K\rho)^{\frac{1}{2}}.$$

However, the adiabatic compressibility at low pressures can only be estimated roughly from the published data on pressure, density, and specific heat. There seems to be no reason to suppose that, in He I at least, the usual formula for the velocity of sound does not hold. Values for the adiabatic compressibility have therefore been deduced from the measured velocities. These are shown plotted against temperature in Fig. 4, and values taken from the graph are given in Table II.

The estimated value for the change in expansion coefficient at the λ-point, $\Delta\alpha$, is 0.0499, while the value for $(dp/dT)_\lambda$ is -82×10^6 c.g.s. units per degree.[5] Hence from relation (1), the change ΔK_T in the isothermal compressibility should be -6.2×10^{-10} c.g.s. unit, which represents a decrease of 5 percent in the estimated values. Since the calculated value of γ is about

[5] Values derived from experimental results of W. H. Keesom and Miss A. P. Keesom, Proc. Kon. Akad. van Weten. Amsterdam **36**, 482 and 612 (1933), (Leiden Comm. 224*d*, *e*); Physica **1**, 128 (1933), (Leiden Comm. Suppl. 76*b*.)

1.005 for both He I and He II near the λ-point, the relative change in the adiabatic compressibility should be very nearly the same as that in the isothermal value. This should cause an increase in the velocity of sound of about 2.5 percent. However it will be seen from Fig. 3 that the change at the λ-point, if any, is not more than 0.5 percent. It will be seen, further, that the measured velocity is a maximum in He I at 2.5°K. Such a maximum is not predicted by calculations based on the published data for liquid helium, and there may be some significance in the fact that the increase from the value in He II at the λ-point to the maximum in He I is approximately equal to the increase predicted by Ehrenfest's relations.

Wave Form

As the reflector was moved, there appeared in addition to the main maxima of the galvanometer deflection, smaller secondary peaks. These peaks maintained the same positions relative to the primary maxima as the reflector was moved, and were the same for all liquids used, with the exception of liquid He II. Hence they could not be attributed to different velocity or frequency components. It is thought that they are due to some discontinuity in the activity of the crystal. In liquid helium, there was a distinct change in the form of these secondary peaks on passing from He I to He II. However, their form remained constant throughout the motion of the reflector in both liquids, and hence the measurements of the wave-length should not be affected. This change in wave form may be related in some way to the peculiar physical properties of He II.

In conclusion, the authors wish to thank Dr. E. F. Burton for his kindly interest and guidance in this research.

OCTOBER 1, 1938 PHYSICAL REVIEW VOLUME 54

The Inelastic Scattering of Slow Electrons From a Silver Single Crystal

John C. Turnbull* and H. E. Farnsworth
Brown University, Providence, Rhode Island

(Received July 26, 1938)

The energy distribution of electrons inelastically scattered from a (111) face of a silver single crystal has been studied by the method of magnetic deflection. At about 45° incidence primary electrons are regularly reflected into the analyzer, and diffraction beams are observed at primary energies of 7.7, 23.2, and 83.2 ev. The structure in the energy distribution shows two discrete loss peaks at 3.9 and 7.3 ev, respectively, in general agreement with that found by Rudberg for polycrystalline silver. However, the relative intensities of the two discrete loss peaks depend on both the primary voltage and the target angle in the neighborhood of the diffraction beams, while Rudberg has found that for polycrystalline targets the peaks are independent of these variables. The energy distribution curves are also distorted by an extra inelastic scattering which accompanies the elastic scattering of the diffraction beams, and which extends down to an energy loss of 10 to 15 ev. Thus, maxima are observed in the curves giving the amount of inelastic scattering as a function of the primary energy for the constant values of energy loss. The maxima occur at secondary energies equal to the critical voltages of the diffraction beams. This indicates the existence of a double process consisting of inelastic scattering of the incident electrons followed by diffraction of the scattered electrons by the crystal lattice.

Introduction

PREVIOUS measurements[1] of the energy distribution of electrons scattered from an outgassed metal target in high vacuum have shown that certain discrete energy loss peaks are superposed on the general background of inelastic scattering. For polycrystalline silver there are two such peaks at 3.9 and 7.8 ev

* Part of a dissertation presented for the degree of Doctor of Philosophy at Brown University.

[1] Rudberg, Phys. Rev. **50**, 138 (1936); **45**, 764 (1934); Proc. Roy. Soc. **A127**, 111 (1930); K. Svenska Vet. Akad. Handl. **7**, 1 (1929). Haworth, Phys. Rev. **48**, 88 (1935); **37**, 93 (1931); **42**, 906 (1932).

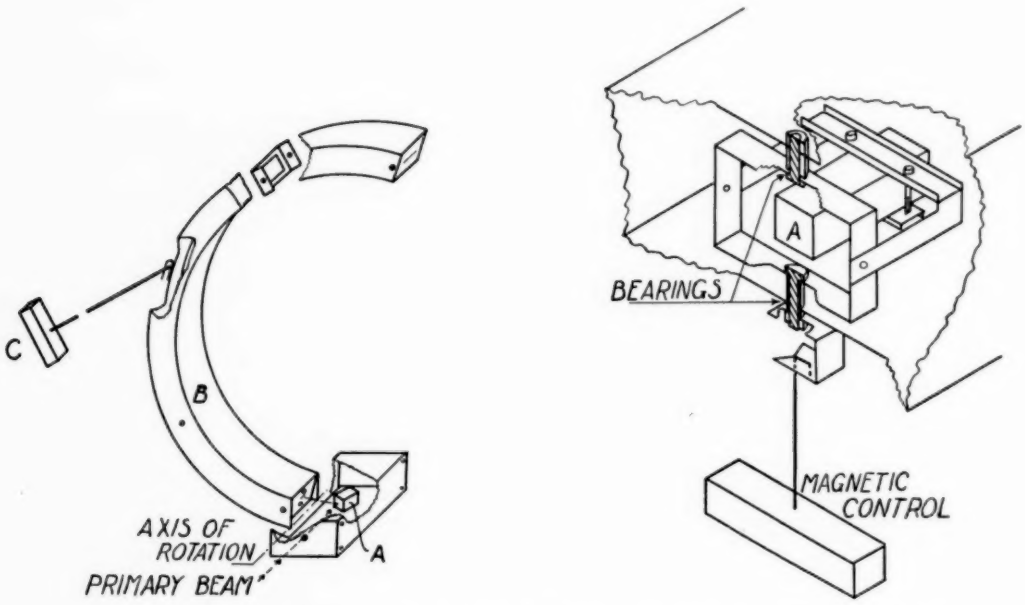

FIG. 1. Diagram of apparatus showing (a) (left) magnetic analyzer, (b) (right) detail of crystal mounting.

energy-loss. The intensities of these discrete loss peaks were found to be independent of the energy of the incident electrons and also of the angle of incidence.

The present experiments show that for a single crystal of silver the intensities of the discrete loss peaks are a function of both the energy of the incident electrons and the angle of incidence. Such a variation might be expected in the neighborhood of the intense diffraction beams which issue from the single crystal surface. A recent theoretical treatment by Slater[2] shows that inelastic scattering of the incident electrons should modify a diffraction beam by lowering and broadening the theoretical maximum. Agreement with the experimental maximum is obtained when considerable inelastic scattering is assumed. Consequently, the presence of a diffraction beam may be expected to modify the inelastic scattering. Davisson and Germer[3] observed a change in the background inelastic scattering in the neighborhood of a diffraction beam. In the present paper a more detailed study of this has been made, in addition to an investigation of the effect of a diffraction beam on the discrete loss peaks.

[2] Slater, Phys. Rev. **51**, 840 (1937).
[3] Davisson and Germer, Phys. Rev. **30**, 705 (1927).

APPARATUS AND PROCEDURE

The apparatus and procedure are similar to Rudberg's.[1] Most of the metallic parts are made of molybdenum. As shown in Fig. 1a the primary electrons move parallel to the magnetic analyzing field, and the analyzer B gives the distribution in energy of the secondary electrons leaving a 2 mm spot on the surface of the target A in a direction perpendicular to the magnetic field. The analyzer contains stops which limit the spread in angle of the collected electrons so that sharp diffraction beams are obtained. Consequently the slit widths must be large enough to give measurable collector currents, thus producing a relatively low resolving power ($\Delta V = 0.027 V$) as compared with $\Delta V = 0.012 V$ obtained by Rudberg and $\Delta V = 0.006 V$ obtained by Haworth.

The crystal is one which was formerly used by H. E. Farnsworth in experiments on diffraction of low speed electrons. Its target face is cut, ground and etched parallel to the (111) planes.[4] The crystal is turned by a magnetic control about a vertical axis (Fig. 1b) which lies in this face and which is perpendicular to the axis of the electron gun and to the initial direction of motion of the electrons going through the analyzer. The

[4] Farnsworth, Phys. Rev. **49**, 602 (1936).

target angle is measured between the normal to the crystal face and the axis of the gun. A second magnetic control C rotates the analyzer through a small angle about an axis parallel to its slits, thus slightly moving the spot on the crystal face from which secondary electrons are collected. In this way the normal to the crystal face may be brought accurately into the plane in which the primary and secondary electrons under consideration move by maximizing the elastic scattering when the other variables are adjusted for a diffraction beam. The output of the gun is constant during the experiment, and in order to permit the above adjustment (of the normal) the primary beam diverges from a hole in the end of the gun so that primary electrons strike the entire face of the crystal. The target and analyzer are at the same potential, and the distribution in energy is obtained by varying the magnetizing current of the Helmholtz coils (radius 7 inches) producing the magnetic field. This current, which passes through a standard resistance, and the primary voltage are obtained with a type K potentiometer. The current to the collector of the analyzer (10^{-13} to 10^{-14} ampere) is measured as a direct deflection by the single tube FP-54 balanced amplifier circuit. The target is outgassed at a dull red heat by bombardment of the mounting on the back side. The system is pumped continuously, and during the final stages of the outgassing pressures of about 5×10^{-8} mm were recorded. At this time a curve could be repeated for several hours after outgassing the target. The pumping system consists of two Apiezon oil vapor pumps backed by a Cenco Hyvac pump. The condensing traps between the experimental tube and vapor pumps, and between the Hyvac pump and vapor pumps are cooled with CO_2 snow in acetone.

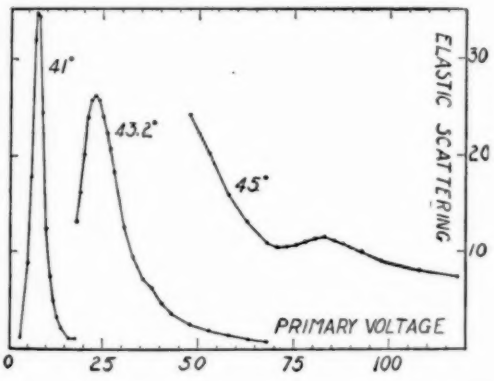

FIG. 2. Elastic scattering as a function of the primary voltage. The values of target angle for regular reflection on the (111) planes are indicated.

RESULTS AND DISCUSSION

The elastic scattering

The energy distribution curve of the secondary electrons has a sharp peak due to electrons reflected from the crystal. The height of this peak is taken as a measure of the elastic scattering. Fig. 2 gives the elastic scattering as a function of the primary energy, which is corrected for contact potential difference. There are maxima at 7.7, 23.2, and 83.2 ev which represent diffraction beams from the (111) planes. The target angle (indicated beside each curve) is set for maximum collector current with the primary energy adjusted on the maximum in the voltage curves. The angle for the 83.2-volt beam is assumed to be 45°. The angle of the 23.2-volt beam is then 43.2°, and of the 7.7-volt beam 41°. Inaccurate alignment could account for only about one-half of the observed variation of 4° in the critical angle. This variation is probably real since Farnsworth[5] has observed a similar

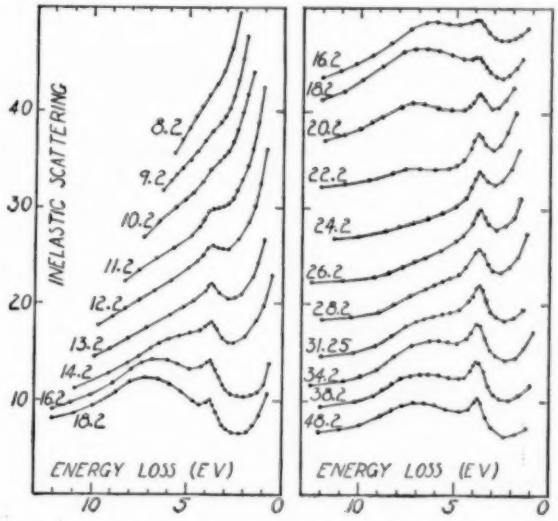

FIG. 3. Distribution curves for the primary voltages given on the curves. The target angle was set at 41° for (a) left), and at 43.2° for (b) (right). The curves are normalized so that the intensity of scattering is 10 at the peak at about 3.7 ev energy loss. Beginning with the lowest curves, the ordinate zeros are at 0, 4, 8, 12, etc., units.

[5] Farnsworth, Phys. Rev. **40**, 684 (1932).

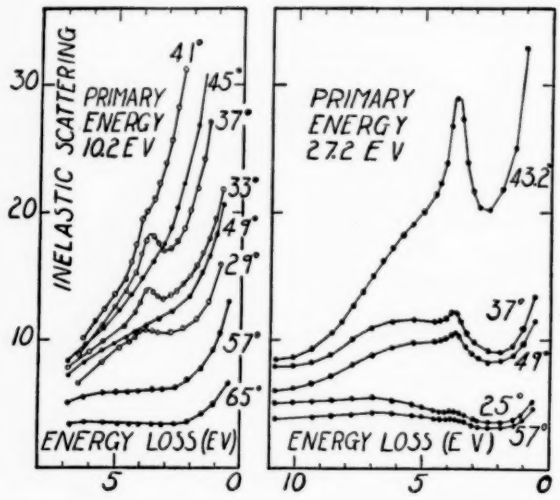

FIG. 4. Distribution curves as a function of the target angle, for values of primary voltages near two diffraction beams.

change in the angle for regular reflection from a silver crystal. Possibly this variation is connected with the nonsymmetrical colatitude curves found by Farnsworth[4] which indicate the existence of beams other than those corresponding to Bragg reflection. The intensities of the beams increase to constant values as the outgassing proceeds. The data given in Fig. 2 were taken immediately after outgassing and were repeated within 10 percent over a period of a month. The beams are not due to a lattice of gas atoms since Farnsworth[5] has found that the gas beams from a silver crystal are weak and disappear rapidly when the target is outgassed.

The discrete loss peaks

The curves in Fig. 3 show distributions in energy losses for various primary voltages. The target angle is set at the critical value for the nearest diffraction beam, 41° for Fig. 3a and 43.2° for Fig. 3b. Except for the lowest values of primary energy, the energy distribution curves have two maxima in addition to the peak due to the elastically scattered electrons which is not shown in the figures. In Fig. 3a, the peak at about 3.7 ev energy loss first appears at a primary voltage of 10.2 volts and increases in intensity relative to the background scattering as the primary voltage is increased. The observed energy loss for this peak increases from about 3.7 ev at 10 ev primary energy to the value given by Rudberg (3.9 ev) at primary energies above 50 ev. In the neighborhood of the second diffraction beam (Fig. 3b) the relative intensity of the first energy loss peak is nearly constant. The second peak at about 7.3 ev energy loss first appears at a primary voltage of 14.2 volts. It disappears (Fig. 3b) at a primary voltage of about 23, but reappears rapidly as the primary voltage is increased above this value. Corresponding results in the neighborhood of the third diffraction beam indicate that, when the primary voltage is varied, the intensities of the discrete loss peaks change by about the same relative amount as the elastic scattering.

Figure 4 gives the distribution in energy losses as a function of the target angle, in the neighborhood of the diffraction beams at 7.7 and 23.2 ev, respectively. Fig. 4a, taken for a primary voltage of 10.2, shows that the development of the first discrete loss peak at about 3.7 ev energy loss depends strongly on the target angle. This peak is strongest at an angle of about 37°. The angle for its maximum development increases as the primary voltage increases, and approaches the critical angle for diffraction at about 20 ev primary energy. At 7.2 ev primary energy these angles differ by about 10°, so that the change in the first angle (about 10°) is much larger than the change in the critical angle (about 2°) in this range of primary voltage. In Fig. 4b, taken for a primary voltage of 27.2, the intensity of the first peak increases to a maximum at a target angle of 43.2°, which is also the critical angle of the diffraction beam. The development of the peak is nearly symmetrical about this value of target angle. The intensity of the second peak is also greatest at the critical angle, but the relative intensities of the two peaks vary with the target angle. The results observed about the third diffraction beam are similar to those in Fig. 4b except that the discrete loss peaks retain about the same relative intensities as the target angle is varied.

Background scattering with energy loss

If one neglects the structure in the curves of Figs. 3 and 4, it becomes evident that the inelastic scattering for energy loss up to 10 or 15 ev is large when the elastic scattering is large. In Fig. 4a, for example, the curve for 41° rises

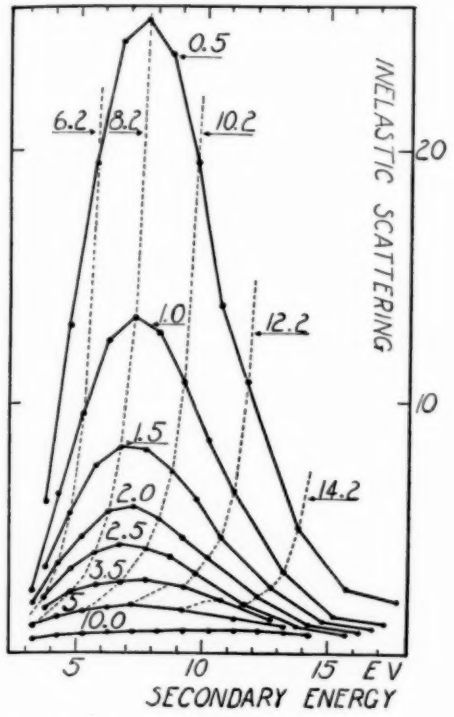

FIG. 5. Inelastic scattering about the diffraction beam at 7.7 ev. The dotted lines are parts of the distribution curves, on which the primary voltages are indicated. The full lines give the inelastic scattering for constant values of energy loss, which are also given on the curves.

faster at low values of energy-loss than the curve for 57°. The same behavior can be seen in Fig. 3 as the primary voltage is varied. Thus, there is an extra amount of inelastic scattering for small values of energy-loss, which accompanies the large elastic scattering of the diffraction beams, and which increases as the energy-loss is decreased.

The dependence of this extra inelastic scattering on the secondary electron energy is given in Figs. 5 and 6. Fig. 5 is taken at the critical angle (41°) and for energies near the diffraction beam at 7.7 ev. The dotted lines are parts of the distribution curves. The inelastic scattering for constant values of energy-loss is given as a function of the energy of the secondary electrons by the solid curves, which are obtained from the dotted curves. The maxima in these curves lie within one ev of the critical energy of the first diffraction peak (7.7 ev). The maxima become broader and disappear as the energy-loss is increased. The curves of Fig. 6, taken directly about the second diffraction beam at 23.2 volts, are entirely similar to those of Fig. 5. The small bump in the elastic scattering at 40 ev (Fig. 2) appears in some of these curves at a secondary energy of 40 ev. The results for the third diffraction peak are also like those of Fig. 5. This behavior of the inelastic scattering is not due to scattering within the analyzer, which would produce maxima at constant values of *primary* energy. There is, however, a possible source of error. The primary current density at the spot on the crystal from which the analyzer collects electrons depends on the analyzing field because of magnetic focusing, even though the output of the gun is constant. This would be expected to decrease the scattering for small secondary energy, and thus displace the maxima towards higher values of energy. The magnetic focusing, however, depends on the potentials of the elements of the electron gun, and, since the maxima are unchanged when these potentials are varied, it is thought that the effect of the magnetic focusing is negligible.

Discussion of results

Davisson and Germer,[3] who first observed the extra inelastic scattering by the retarding potential method, suggested that the extra elec-

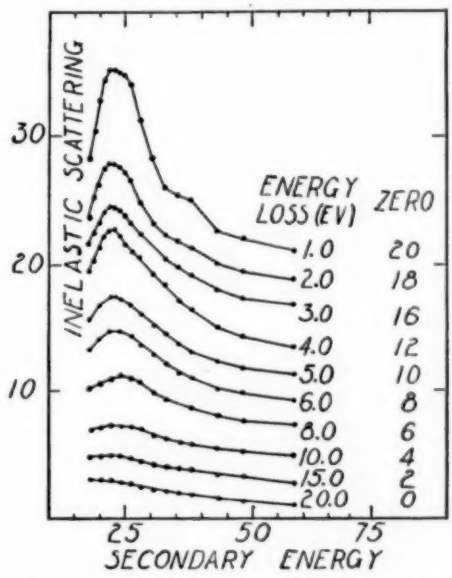

FIG. 6. Inelastic scattering for constant values of energy loss, about the diffraction beam at 23.2 ev. Successive curves are shifted vertically; the zeros and energy losses are given on the curves.

trons were due to a double process consisting of diffraction of the incident electrons followed by energy loss of the reflected electrons as they leave the crystal. Rudberg and Slater[6] have shown that for single collisions the probability of scattering on a crystal should be approximately proportional to some inverse power of ΔK, where ΔK is the change in momentum for the collision. The inelastic scattering thus decreases as the energy loss increases and, for a given energy loss, is a maximum in the original direction of the primary beam. Hence the contribution of the above double process should be a maximum when the elastic scattering is largest. The observed angle for maximum inelastic scattering does in general coincide with the critical angle for diffraction. But, since the maxima in Figs. 5 and 6 occur at constant values of secondary energy, the above double process is inadequate. These experimental results indicate the existence of another double process in which the primary electrons are first inelastically scattered without appreciable change in their original direction of motion, and then reflected from the (111) planes. Thus the reflection of the inelastically scattered electrons should be a maximum at the critical angle, and at a secondary energy equal to the critical energy for diffraction. This is just what is observed.

If the above double process also applies to the electrons responsible for the discrete loss peaks, we should expect that (1) the inelastically scattered electrons would be diffracted in the same direction as that of the elastically scattered electrons, and (2) the secondary energy, i.e., the energy after collision, should be the one which governs the diffraction of these electrons rather than the energy of the incident electrons before collision. As seen from Fig. 4, condition (1) is satisfied by the first discrete loss peak except for the deviation at very low primary energies. Condition (2) requires that the intensities of the discrete loss peaks should be a maximum when the secondary energy equals that for a diffraction beam of elastically scattered electrons, i.e., when the primary energy is that for a diffraction beam plus the energy loss corresponding to the discrete loss peak. Similar reasoning should apply to the minimum intensities as a function of primary voltage. Referring to Fig. 3b, we note that the second discrete loss peak disappears at about 24 volts. By subtracting the energy loss of 7 for this peak we obtain 17 volts which checks well with the minimum at about 17 volts in the curve of Fig. 2. However, there appears to be no minimum in the intensity of the first discrete loss peak at about 21 ev primary energy where it would be expected. The primary voltages for which the discrete loss peaks attain maximum values are less certain, but, as mentioned previously, they do appear to be in the neighborhood of the voltages for diffraction beams of the elastically scattered electrons. However, further experiments are required to determine whether or not a detailed correlation exists. Plans are being made in this laboratory to construct an electrostatic analyzer with which it will be possible to extend the present observations to the neighborhood of many more diffraction beams, particularly for the case of normal incidence.

[6] Rudberg and Slater, Phys. Rev. **50**, 150 (1936).

On the Electrical Breakdown of the Alkali Halides

R. J. SEEGER AND E. TELLER
George Washington University, Washington, D. C.

(Received August 10, 1938)

A theoretical justification is given for the mechanism proposed by von Hippel to account for the electrical breakdown of the alkali halides. Values of the breakdown field calculated on the basis of the theory are found to compare favorably with those obtained experimentally. A critical comparison is made with another explanation of the breakdown proposed by Fröhlich.

INTRODUCTION

THE experimental investigations of von Hippel[1] concerning the electrical breakdown of the alkali halides have shown marked regularities. One of these is the fact that the breakdown decreases with the atomic weight of both the anion and the cation (from 4.9×10^5 volts per cm for RbI to 31×10^5 volts per cm for LiF). He has proposed the following mechanism to account for the breakdown. The few free electrons, which are always accidentally present in such a crystal, on the one hand, are accelerated by the field; and, on the other hand, are slowed down by collisions with the ions of the lattice. It is assumed that every time an electron of appropriate speed collides with an ion there will be a considerable probability of excitation of a vibration of the lattice. Neither very slow, nor very fast electrons will be slowed down appreciably; the former because they lack sufficient energy to excite a quantum of vibrational energy, the latter because they lack sufficient time to do so. If the external field becomes strong enough to produce a net acceleration even for electrons of medium speed, which are retarded most strongly by the lattice vibrations, then each of these will be accelerated until it has sufficient energy to produce a second free electron by collision with a halogen ion. Thus there will be built up an avalanche of electrons; a breakdown will occur.

Von Hippel finds that this picture gives satisfactory agreement with his experimental material if it is assumed that the electrons which lose most energy excite one optical, or "reststrahl," vibration as they cross 0.5 to 0.9 of a lattice cell. Such a mean free path for free electrons is in marked contrast with the value of several hundred lattice distances which is found in the theory of metals. Calculations by Fröhlich,[2] however, show that the mean free path in these crystals is of the very order of magnitude given by von Hippel. For some speeds, indeed, it appears to be even shorter.

The difference in behavior between free electrons in insulators and those in metals is due primarily to the fact that in metals their number is comparable with the number of atoms in the lattice. This fact has several consequences that all work in the same direction. (1) The interaction of an electron in a metal with all the ions except the few neighboring ones is negligible because of the shielding effect of the other free electrons. (2) The free electrons in a metal, obeying the Fermi-Dirac statistics, occupy all different orbits so that the highest orbit has a kinetic energy far greater than the thermal energy $3kT/2$, and all the lower orbits are completely occupied. Since the kinetic energy of an electron changes little upon collision with the lattice, only the electrons on the surface of the Fermi-Dirac distribution can make transitions by such collisions, and then only to a limited number of free final states. (3) The great kinetic energy and high speeds of the metallic electrons result in less likelihood of a transfer of energy to an ion.

Fröhlich proposes that the breakdown occurs when all the electrons which have sufficient energy to produce additional free electrons by collisions (i.e., energy equal to the ionization potential) can be accelerated by the field. Clearly this process does not give rise to an electronic avalanche, inasmuch as the breakdown field is not great enough to accelerate the new free

[1] A. von Hippel, J. App. Phys. **8**, 815 (1937).

[2] H. Fröhlich, Proc. Roy. Soc. **A160**, 230 (1937).

electrons, nor even the original electrons that have lost energy by this ionization. From his view it is only by thermal excitation that the electrons will attain sufficiently high energy for such further acceleration, a process which is too improbable to account for the breakdown phenomenon.

In the numerical work of Fröhlich there appears an assumption that the force of interaction between a free electron and a lattice ion is of the form e^2/r^2, where e is the elementary charge on each of them and r is the distance between them. This has to be modified, however, in accordance with the dielectrical and optical properties of alkali halide crystals. Accordingly the force is smaller than e^2/r^2, and consequently the mean free path greater than that obtained by Fröhlich. If this modification is made, the breakdown field turns out to be sufficiently strong to accelerate all free electrons affected, i.e., even those which have energies only slightly greater than the quantum of lattice-vibrational energy, and which, therefore, lose most energy in collisions with the vibrating ions. Hence, what follows in this paper may be considered as a theoretical justification of the breakdown mechanism proposed by von Hippel.

Energy Loss in a Lattice Field

The slowing down of electrons in a lattice field has been treated by Fröhlich with the help of Born's quantum mechanical perturbation theory. We prefer to discuss the problem in a way analogous to Bohr's calculation[3] of the energy loss of alpha-particles as they pass through a gas. This method has the advantage of showing the physical process more clearly. Moreover, the application of Born's approximation in this problem cannot be considered more rigorous, as we shall discuss later. Both methods, it is true, yield similar results.

Let the force between a free electron and an ion be given by

$$\epsilon e^2/r^2, \tag{1}$$

where ϵ is a dimensionless constant which accounts for the fact that an ion displaced in a dielectric medium will act, in effect, with a modified electric charge. Leaving ϵ to be determined in the following section, we integrate this force over the time of the electron's passage near the ion. Thus we obtain for the total momentum (P_b) transferred to the ion during this time

$$P_b = 2\epsilon e^2/vb,$$

where v is the speed of the electron (assumed to be constant) and b is the distance of nearest approach of the electron to the ion. The kinetic energy (W_b) which any one ion receives in this encounter will then be

$$W_b = P_b^2/2M,$$

where M may be either M_+, the mass of the positive ion or M_-, the mass of the negative ion. Taking the sum of the above expression for both ions, we may write the result in terms of the reduced mass μ, where $1/\mu = 1/M_+ + 1/M_-$. Thus

$$W_b = 2\epsilon^2 e^4/\mu b^2 v^2.$$

Within the limits of b and $b+\Delta b$ the number of ions receiving energy when the electron has gone unit distance is

$$\pi b \Delta b/a^3,$$

where a is the distance between two neighboring ions. (This simple expression can be used instead of a summation over the lattice points because of the predominant influence of the distant ions.) Hence, the average energy ($\Delta W_b/\Delta s$) lost by an electron along unit path in a lattice of the NaCl type, for ions between b and $b+\Delta b$, is

$$\frac{\Delta W_b}{\Delta s} = \frac{\pi b \Delta b}{a^3} \cdot \frac{2\epsilon^2 e^4}{\mu b^2 v^2}.$$

Integrating this expression over all the ions in the lattice, we obtain for the space rate of energy loss of the electron

$$\frac{dW}{ds} = \int \frac{2\pi\epsilon^2 e^4}{\mu a^3 v^2} \cdot \frac{db}{b}.$$

This integral diverges if taken over all the values of the variable b. The physical limitations, however, do not justify integration over the range of values as b approaches either zero or infinity. Up to this point our calculation has been carried out on the assumption that the ions behave as if they were free. This is a good

[3] N. Bohr, Phil. Mag. **24**, 10 (1913).

approximation only if the time of the electron's passage is short as compared with the period of vibration of the ions in the lattice, specifically if

$$2b/v \ll 1/\omega,$$

where ω is given by $2\pi\nu$, and ν is the frequency of the lattice vibration. The normal modes of vibration of such a lattice are of two kinds, *viz.*, the acoustic ones in which ions of opposite charges vibrate with small phase-differences and the optical ones in which they vibrate with large phase-differences. The electron, repelling the negative ions and attracting the positive ions, will excite primarily the optical vibrations. Because of the importance of distant ions in the process described, those vibrations will contribute most to the slowing down of the electron that have ions of the same charge vibrating nearly in phase. These vibrations have frequencies close to the so-called "reststrahl" frequency so that we may choose the value of this as the approximate frequency of the lattice vibration. Now if the time of passage becomes longer than the period of this vibration, the lattice can follow the motion of the electron in an adiabatic way so that the resulting energy-loss is zero. From these considerations we take as the upper limit of our integral the value of b given by

$$b_{\text{upper}} = v/2\omega.$$

The lower values of b are limited by our use of the particle concept of classical theory. This cannot be applied without quantum modification for distances smaller than λ, i.e., the wave-length of the particle divided by 2π. Hence, we choose

$$b_{\text{lower}} = \lambda.$$

(This choice corresponds in Born's approximation to the fact that an electron wave cannot excite a lattice vibration which has a wave-length short compared to its own wave-length.) Introducing these limits into the integral, we obtain

$$\left(\frac{dW}{ds}\right)_c = \frac{2\pi\epsilon^2 e^4}{\mu a^3 v^2} \cdot \ln\left(\frac{\frac{1}{2}mv^2}{h\nu}\right). \qquad (2a)$$

We note that the space rate of loss of energy is zero when the kinetic energy of the electron is equal to the quantum of *reststrahl* vibration.

Formula (2a) agrees with a similar one given by Fröhlich (Cf. No. 17 in reference 2) except for the logarithmic factor. Fröhlich's expression can also be obtained by the use of Bohr's method, however, if the lower limit of b is chosen as $2^{4/3}\pi a$ instead of λ. Now for high speed electrons $2^{4/3}\pi a$ is greater than λ so that this limit is justifiable. But for slow electrons, which are important in our theory, $2^{4/3}\pi a$ is less than λ so that the expression (2a) is the better approximation. Modifying Fröhlich's calculations so as to include electrons of low energy, we obtain the following quantum formula

$$\left(\frac{dW}{ds}\right)_q = \frac{\pi\epsilon^2 e^4}{\mu a^3 v^2} \cdot \ln\left(\frac{p^2 - mh\nu + (p^4 - 2mh\nu)^{\frac{1}{2}}}{p^2 - mh\nu - (p^4 - 2mh\nu)^{\frac{1}{2}}}\right), \qquad (2b)$$

where p represents the momentum of the electron. Expression (2b) agrees with the classical one (2a) when p^2 is large compared with $mh\nu$ (except for an additive term, i.e., ln 4). The applicability of Born's approximation used in obtaining (2b), however, is questionable in this problem.

Born's approximation can be employed only if less than one transition occurs, on the average, during the longer one of the following two times: the period of the lattice vibration, or the time during which an electron moves a distance equal to its own wave-length. In our problem the first of these is the longer time. Yet, according to Fröhlich's work, several quanta are emitted during this time. Thus Born's method is not valid here.

In the case of metals, although the transition probability is much smaller, there is also doubt as to the validity of this same perturbation theory being applied. Peterson and Nordheim[4] have shown that if coupling between the electronic motions and the lattice vibrations becomes strong, it is more correct to start with an electronic wave function that represents the motion of the electron in the lattice distorted by the vibration. This treatment leads to results similar to those obtained by the use of Born's

[4] E. L. Peterson and L. W. Nordheim, Phys. Rev. **51**, 355 (1937).

approximation. In Bohr's classical method, however, the lattice vibrations need not be quantized; hence, there is no difference between it and the procedure of Peterson and Nordheim.

In our present problem even the time required for an electron to move through the distance of its wave-length will be shorter than the time for the occurrence of one transition. In the use of Bohr's correspondence principle the speed of the electron, then, cannot be considered constant because of the retarding influence of the lattice. Fortunately, only those electronic speeds are important in determining an electrical breakdown for which there is a balance between the acceleration due to the external field and the retardation due to the ionic lattice. For these reasons we believe that the results obtained by the correspondence method give a fairly accurate picture of the actual behavior of the electrons. Indeed, the agreement with the results of Fröhlich help to justify the use of Born's approximation.

Modified Ionic Charge

In a real crystal the energy density due to an electric displacement D is given by

$$D^2/8\pi\kappa,$$

where κ is the dielectric constant. Let us imagine, however, a fictitious crystal in which the ions are fixed. The energy density in this case would be

$$D^2/8\pi\kappa',$$

where κ' is the dielectric constant under this condition. (κ' can be obtained by extrapolation of the square of the refractive index n to infinite wave-length with the omission, however, of the infra-red terms in the dispersion formula.) Now the difference between the energy density of the real crystal and that of the fictitious crystal, namely,

$$D^2/8\pi\kappa'-D^2/8\pi\kappa$$

is just the energy density due to the displacement of the ions. It can be obtained also by considering directly the energy of vibration of two neighboring ions in terms of their force of interaction F. We obtain the value

$$F^2/8\pi^2\mu\nu^2.$$

Multiplying this by $1/2a^3$, which is the number of such dipoles in unit volume, we have for the energy density due to ionic displacements

$$F^2/16\pi^2\mu\nu^2a^3.$$

Equating the two expressions for the energy density, we find

$$F=\left[2\pi\mu\nu^2a^3\left(\frac{1}{\kappa'}-\frac{1}{\kappa}\right)\right]^{\frac{1}{2}}D.$$

The interaction of an electron with an ion results in an electric displacement equal to e/r^2. Therefore, we may now identify our expression for the force of interaction with our assumption (1). Thus we obtain

$$\epsilon=\frac{1}{e}\left[2\pi\mu\nu^2a^3\left(\frac{1}{\kappa'}-\frac{1}{\kappa}\right)\right]^{\frac{1}{2}}. \tag{3}$$

Breakdown Field

Electrical breakdown will occur if the electric field causes a net acceleration of all free electrons, even though their speed is such that the space rate of their energy loss is a maximum. If this condition is fulfilled, an avalanche is produced. We choose the following equation, therefore, for the determination of the breakdown field (E_B):

$$E_B=(dW/ds)_{\max}. \tag{4}$$

In order to find $(dW/ds)_{\max}$ we rewrite Eqs. (2a) and (2b), respectively, as

$$\left(\frac{dW}{ds}\right)_c=\frac{\pi m\epsilon^2e^4}{h\nu\mu a^3}\left(\frac{1}{x}\ln x\right), \tag{5a}$$

where x represents $mv^2/2h\nu$; and

$$\left(\frac{dW}{ds}\right)_q=\frac{\pi m\epsilon^2e^4}{h\nu\mu a^3}\left[\frac{1}{y}\ln\frac{y-1+(y^2-2y)^{\frac{1}{2}}}{y-1-(y^2-2y)^{\frac{1}{2}}}\right], \tag{5b}$$

where y represents $mv^2/h\nu$. Now $(dW/ds)_c$ becomes a maximum when x is equal to 2.7; hence, $(1/x)\cdot\ln x$ has a maximum value of 0.37. On the other hand, $(dW/ds)_q$ becomes a maximum when y is equal to 3.4; hence,

$$\frac{1}{y}\cdot\ln\frac{y-1+(y^2-2y)^{\frac{1}{2}}}{y-1-(y^2-2y)^{\frac{1}{2}}}$$

has a maximum value of 0.91. Substituting these

TABLE I. *Comparison of calculated values of breakdown field with experimental values. Ratio of effective to ordinary mass of the electron which produces agreement between theory and experiment.*

CRYSTAL	h (10^{-2} VOLT)	κ	n	E_{Bq} (Calc)* (10^6 VOLT/CM)	E_B (Exp)[1] (10^6 VOLT/CM)	m/m_0
LiF	7.2	10.0	1.39	26	31	1.2
NaF	3.3	6.0	1.32	12	24	2.0
NaCl	2.4	5.9	1.48	6.1	15	2.5
NaBr	1.8	6.39	1.63	3.5	8.1	2.3
KCl	1.9	4.7	1.48	6.0	10.0	1.7
KBr	1.5	4.87	1.41	3.9	7.0	1.8
KI	1.3	5.58	1.55	3.2	5.7	1.8
RbCl	1.7	4.8	1.49	3.6	8.3	2.3
RbBr	1.15	5.0	1.55	2.2	6.3	2.9
RbI	1.05	5.2	1.69	1.5	4.9	3.3

* These calculated values have not been corrected for preferential directions as was done by Fröhlich. Such a correction seems to us to be inadvisable at present, as long as the theory for breakdown in different directions has not yet been discussed.

values, respectively, in (5a) and in (5b), we have

$$\left(\frac{dW}{ds}\right)_{c-\max}=\frac{0.37\pi me^2\epsilon^4}{h\nu\mu a^3} \tag{6a}$$

and

$$\left(\frac{dW}{ds}\right)_{q-\max}=\frac{0.91m^2e^4}{h\nu\mu a^3}. \tag{6b}$$

Now substituting these expressions and (3) in our condition (4), we obtain for the breakdown field

$$E_{Bc}=\frac{0.74\pi^2me\nu}{h}\left(\frac{1}{\kappa'}-\frac{1}{\kappa}\right) \tag{7a}$$

by the use of the classical picture, and

$$E_{Bq}=\frac{1.82\pi^2me\nu}{h}\left(\frac{1}{\kappa'}-\frac{1}{\kappa}\right) \tag{7b}$$

by the use of the quantum mechanics.

In order to compare these formulae with the experimental values of von Hippel we need to know ν, κ, κ', and m. We have used the values of ν listed by von Hippel. For κ we have taken an average of the values given in Landolt-Bornstein's *Tabellen* (1936). For κ' we computed the square of the index of refraction for wave-lengths just beyond the infra-red region, thus eliminating the effect of the infra-red lattice vibrations. The mass of the electron (m), however, presents a problem. For one cannot use the real mass; one must insert the so-called "effective mass,"[5] which describes the motion of an electron in a periodic field. This mass, in general, will be greater than the ordinary mass (m_0) of the electron because of the smaller speed with which an electron of a given energy is propagated through the potential barrier of a periodic field. Because the calculation of the "effective mass" is complex, we have preferred to compute the breakdown field for m_0 and then to determine the ratio m/m_0 necessary for absolute agreement between the theoretical value and the experimental one in each case. In Table I we list only the quantum mechanical values E_{Bq} (7b), which are approximately twice the classical ones E_{Bc} (7a).

[5] F. Bloch, Zeits. f. Physik **52**, 555 (1928).

ANALYSIS OF RESULTS

The values obtained for m/m_0 are in a range not unreasonable for alkali halide crystals. We believe, however, that the theoretical values are not very accurate and that the theory ought to be revised in several respects. For example, the breakdown field may be actually lower than the one calculated and the ratio m/m_0, consequently, higher. For, even though all the electrons cannot be accelerated by the field, electrons of sufficiently high speeds may be produced by thermal fluctuations. In this way any small field could produce a breakdown in a long enough time unless a mechanism for reabsorption into the lattice were designed. Nevertheless, our result would probably not be modified much. For the breakdown field calculated by us would have to be corrected only by a quantity varying logarithmically with the time necessary for the electron to be reabsorbed. In connection with this process, however, the dependence of the breakdown field upon temperature might be explained. Another important effect which is probably related to the behavior of electrons at high speeds is the breakdown in preferential directions that has been found by von Hippel. In spite of the incompleteness of the theory presented here we believe that it does indicate the properties of the crystal upon which the magnitude of the breakdown field depends.

The authors wish to express their thanks to Professor Arthur von Hippel and to Professor James Franck for their helpful discussions on the subject of this paper.

Carrier Mobility Spectra of Liquids Electrified by Bubbling

SEVILLE CHAPMAN
Department of Physics, University of California, Berkeley, California
(Received July 5, 1938)

The mobility spectra produced by bubbling water and various aqueous solutions of salt, acid, base, sugar, and soap have been investigated with an Erikson mobility tube under conditions of high resolving power. Curves of current against mobility show that for water there are five distinct negative groups of carriers having mobilities 1.80, 0.95, 0.45, 0.32, and 0.20 cm/sec. per volt/cm. There are two definite positive groups at mobilities 1.0 and 0.40 (varying between 0.44 and 0.34). Few carriers are produced with mobilities less than 0.1. Depending on the size of the bubbling capillary, the ratio of the total amount of positive electrification to negative varies from one to three (small capillary) to one to one hundred (12 mm tubing). Addition of salts to water favors production of slow carriers at the expense of fast ones; the curves degenerate to continuous distributions of mobilities from mobilities roughly 0.5 to 0.01. Medium concentrations (10^{-3} molal) produce more total electrification than distilled water, high concentrations (1 molal) less. With the addition of sugar to water, several groups of carriers appear whose mobilities lie between 0.1 and 0.001. There are large numbers of carriers in these groups, so that the total amount of electrification increases to about 12 times that for water. The use of air blasts of high humidity favors production of slow carriers, and gives heterogeneous spreads of mobilities. From new experiments on spraying water and salt solutions, some weak groups previously unobserved have been detected. Comparisons have been made between curves of bubbling and curves of spraying.

THE electrification of liquid droplets produced by spraying, bubbling, and similar methods is well known.[1–4] These phenomena depend upon the surface condition of the liquid, the presence of an electrical double layer within the surface being the important factor.[1] In a previous article by the author[4] on the mobility spectra of the charged carriers produced by spraying water and aqueous solutions, one curve was included in which the carriers were produced by bubbling. It was noted that the groups of carriers of unique mobility were somewhat more sharply defined in the case of bubbling than in the case of spraying. Accordingly, it seemed desirable to extend the data to the case of bubbling. This paper is a report of that work.

Apparatus and Procedure

The Erikson mobility tube used for making measurement is essentially the same as that already described.[4] The bubbles are generated by a piece of thin-wall glass tubing drawn down to a capillary of 0.7 mm inside diameter. At a pressure of 19 cm of Hg, the air passed through the capillary at the rate of 77 cm³/sec. The droplets generated by the bubbling blast are blown into the Erikson tube by the bubbling blast assisted by a dry auxiliary blast of 150 cm³/sec. The main blast in the tube blows the carriers down the tube while an electric field draws the charged carriers across the tube.

Two new sizes of electrodes have been provided, one effectively 2.5×41 mm, the other 15×41 mm. The smaller electrode has improved the resolving power by roughly 50 percent over that of the old electrode, which was effectively 6×41 mm. The larger electrode has been used at distances far down the tube where intensities are weak.

The design of the bubbler, which is of glass except for a small sealed-in platinum electrode, like *D*, Fig. 1, reference 4, has been improved so that the outlet of the bubbler fits snugly over the inlet *I* (Fig. 1, reference 4). The auxiliary blast is now led through the chamber *M*, directly to the top of the bubbler. Glass wool and cotton filters (like *F*) have been placed on all three blasts ahead of the pressure regulators *AAA*.

The volume of the main air-blast has been measured in three ways, yielding: 2900 cm³/sec. by extrapolation of readings taken by a gas meter, a value that should be too high, if anything; 3200±50 cm³/sec. by a velometer; 3000 cm³/sec. from measurement by an orifice under

[1] Lenard, Ann. d. Physik **47**, 463 (1915).
[2] Bühl, Kolloid Zeits. **59**, 346 (1932). A review.
[3] Chapman, Physics **5**, 150 (1934).
[4] Chapman, Phys. Rev. **52**, 184 (1937).

conditions of Reynolds number somewhat too low for the formula for volume to be strictly accurate. In previous work[4] the value of 2900 cm³/sec. was used. In this paper the average of the three values is taken.

The mobility of the ions is given by the equation

$$k = Qd/wlV, \qquad (1)$$

where k is the mobility of the carriers in cm/sec. per volt/cm (all mobilities mentioned in this paper are expressed in this unit); Q is the volume of air in cm³/sec. traveling down the tube (i.e., the sum of the volumes of the main blast, the 150 cm³/sec. auxiliary blast, and the 77 cm³/sec. bubbling blast); d is the average distance the ions travel across the tube; w is the width of the tube; l is the distance downstream to the collecting electrode; and V is the voltage difference between the plates.

The data were taken by fixing Q and l, and varying V. For mobilities faster than 0.12 cm/sec. per volt/cm, the 2.5 mm electrode was used; l was 2.5 cm, and Q was 3260 cm³/sec. For mobilities between 0.5 and 0.016, l was ordinarily fixed at 10 cm and the volume of the main blast was reduced until Q became 1630 cm³/sec. For mobilities between 0.06 and 0.004, l was 20 cm and Q was 815 cm³/sec. Slower mobilities were handled by suitable changes in l and Q. The 15 mm electrode was used at $l \geq 10$ cm if intensities were weak. Thus the complete curves consisted of three overlapping portions. From the overlapping sections coefficients by which to multiply the ordinates could be determined, so that the curves could be drawn as continuous.

In the spraying experiments (see p. 188, reference 4), all the air in the spray chamber was at least 99 percent saturated. Because of the nature of spraying, and also because of the high humidity in the chamber, many neutral particles or large slow carriers were led into the Erikson tube. Thus it was found that moving the electrode downstream resulted in disappearance of fast carriers probably by attachment to these large particles.

In the case of bubbling, relatively few slow carriers or large neutral particles are produced. Because the dry (35 percent humid) auxiliary blast is connected directly to the top of the bubbler, the air at the outlet of the bubbler is found to be less than 65 percent humid. Evaporation can occur so that with water very few large carriers are observed. Likewise there are probably few large neutral particles. Thus moving the electrode downstream results merely in reduced intensity and a small loss of resolving power, probably due to diffusion and residual turbulences in the air-blast. The values of the mobilities, and the relative intensities, are unaffected.

Experimental Results

The experimental results are given in Figs. 1–15, and in Tables I and II. The curves indicate current to the electrometer (representing number of charged particles, since they are believed to be singly charged[4]) as a function of the mobility of the particles, determined from Eq. (1). The ordinates of all curves are given in the same arbitrary units.

The abscissae of all curves are plotted on a logarithmic scale. It will now be shown that with this scale the *area* under the curve represents the *total charge* produced in unit time.

If y is plotted as a function of x, then $\int_a^b y dx$ equals the total area under the curve from a to b. In our case we are plotting the charge (per unit time) to the electrometer q, as a function of voltage V. We may choose to take the ordinates y as proportional to q. But if we wish to make $\int y dx$ equal to the total charge, we must *not* take the abscissae x, proportional to V, as is shown from the following reasoning.

Because of the finite width of the electrode, the carriers incident on it will always have a certain spread of mobilities. For an electrode at a fixed downstream distance l, from the inlet of the tube, the downstream width of the electrode δl, will of course be a certain fixed fraction of l. Hence, as seen from Eq. (1), the spread of mobilities of the carriers incident on the electrode will be this same fixed fraction of the mean mobility, i.e., $(k_2 - k_1)/k = \delta l/l$. Likewise, for all mobilities, the *same* fractional increase of voltage $\delta V/V$ will cause carriers to sweep from the downstream edge of the electrode to the upstream edge. Thus the reading q of the electrometer, samples the charge of the carriers in constant *fractional* increments. On the other hand, the

ordinate of any curve samples the area under that curve by constant *additive* increments—that is, the area of a curve,

$$\int y dx = \operatorname{Lim}_{\delta x \to 0} \sum y_i \delta x_i,$$

where δx_i are constant increments. Thus in our curves of q as a function of V, we must take increments of abscissae δx, proportional to fractional increments of voltage $\delta V/V$. Hence in the limit (when we draw a smooth curve instead of a series of rectangular steps side by side), we must have $dx = \text{const.}\ dV/V$. On integrating, $x = \text{Const.}\ (\log V)$, and thus we see that if we wish the area under the curve to represent the total charge produced in unit time, we must plot abscissae on a logarithmic scale.

The total amounts of positive and negative electrification have also been determined by turning off the main downstream blast and collecting all the charge on the 15 mm electrode directly opposite the inlet to the Erikson tube. These values for totals check those obtained from areas of curves. The totals, good to about five or ten percent, are given in Tables I and II.

Distilled water

Figure 1 shows the curve for ordinary fresh distilled water. The significant feature of the curve is the very definite grouping of the charge into carriers of unique mobility. Since the inlet and electrode are of finite size, a group of unique mobility is represented not by a sharp spectral line, but by a narrow band whose half-width (width at half the maximum ordinate) is 10 percent; i.e., (voltage width)/(median voltage) = 10 percent. The age of these carriers is about ½ second, so that a spread of mobilities of at least an additional 10 percent is to be expected.[5, 6] Since the actual half-width of group I is 22 percent, it may be considered to be a group unique in characteristics. Its mobility is -1.8 ± 0.1 cm/sec. per volt/cm.[7] This value is not necessarily absolute, since an air-blast method is not capable of yielding accurate absolute values, although the relative values obtained by it may be good to one or two percent. Mobilities of the other groups are: II^- 0.95, $IIIa^-$ 0.45, $IIIb^-$ 0.32, IV^- 0.20; II^+ 1.0, III^+ 0.40 (varying between 0.44 and 0.34). Other curves definitely prove the existence of the unresolved and apparently doubtful $IIIa^-$. The total amount of negative electrification compared to the total positive is in the proportion -4.0 to $+1.0$. (See Table I.)

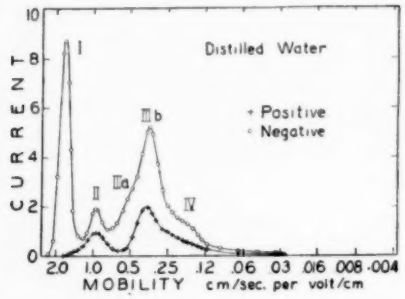

FIG. 1. Mobility spectrum produced by bubbling distilled water.

Salts

Figure 2 shows the curve for 1×10^{-5} molal potassium chloride. (The broken curve represents a portion of the negative curve for 4×10^{-5} molal, each break in the curve being an experimental point.) Groups II^- and II^+ are weaker than for distilled water; $IIIa^-$, IV^- and IV^+ are considerably enhanced.

Figure 3 is for 1×10^{-4} molal potassium chloride. The I and II groups are weakened further, the III groups are being lost in the tails of IV. The carriers slower than 0.12 are becoming more prominent, and the total amount of both positive and negative electrification is increasing.

In Fig. 4 for 1×10^{-3} molal potassium chloride, almost all the structure of the curves has been lost, and there remains only a broad spread of mobilities with a maximum ordinate of about 5 at mobility 0.06.

With a 10^{-2} molal solution (not illustrated), the maximum of the broad smear shifts to a mobility of about 0.03, but remains at about the same height. The positive and negative totals are equal. A solution of 0.1 molal shifts the maximum to mobility 0.016, with ordinate of about 3, so that the total amount of electrification is now being reduced by further increase of concentration. No carriers have a mobility greater than

[5] Zeleny, Phys. Rev. **38**, 969 (1931).
[6] Loeb and Bradbury, Phys. Rev. **38**, 1716 (1931).
[7] In an abstract, Chapman, Phys. Rev. **53**, 211 (1938), because of a typographical error, this value was given as 1.07.

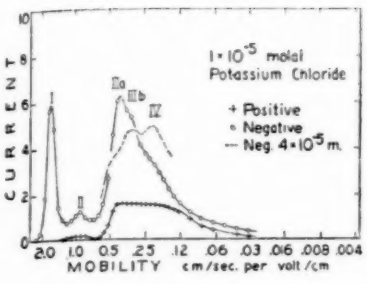

FIG. 2.

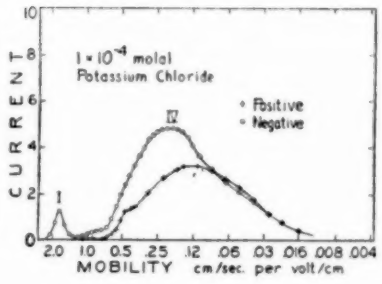

FIG. 3.

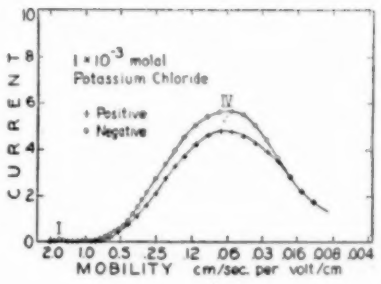

FIG. 4.

FIGS. 2–4. Mobility spectra produced by bubbling solutions of potassium chloride of various concentrations.

0.25. With one molal solution the maximum shifts to mobility about 0.008, and the totals are still further reduced. With 4 molal the trends continue.

The characteristics in the $MgSO_4$ series and also in the $AlCl_3$ series are found to be about the same as those just discussed for the KCl series. The only significant difference is that the total amount of positive electrification is proportionally greater with $AlCl_3$. (See Table I.)

Acid and base

The curves for NaOH are very similar to those of KCl, except for the fact that with NaOH the II^+ peaks are more rapidly reduced with increasing concentration. The curves for HCl and HNO_3 are different from those of KCl, particularly with regard to the II^- and II^+ peaks. The II^- peaks are weaker than for the corresponding concentration of KCl, and the II^+ peaks are strongly enhanced. This fact is brought out by Fig. 5 for 1×10^{-4} molal HNO_3. The structure of the curves persists even to a strength of 1×10^{-3} molal.

Sugar

Figures 6–9 show some of the results for sucrose. (Note the change in ordinate scale at high concentration.) The striking features of the curves are the number of distinct mobilities that are present in the negative curves, and the complete absence of fast positives. Even for 1×10^{-5} molal, II^+ is practically nonexistent, and III^+ is weak. In the negative curves it is difficult to be sure whether the slower (less well resolved and doubtless somewhat heterogeneous) groups shift gradually to lower mobilities, or whether with increasing concentration there are new groups appearing that smear the previously existing ones into their sides in such a way as to cause an apparent gradual shift of the maximum. The "reappearance" of a group at -0.06 in Fig. 9 tends to point to the latter conclusion, although probably both phenomena occur.

The total amounts of electrification increase with increasing concentrations (see Table I) until the amount of sugar in the solution is about ten percent by weight. Further increase of concentration changes the viscosity of the solution so that the decrease in the total amount of electrification can probably be ascribed to reduction of effectiveness of the bubbling mechanism.

Violence of bubbling

The regular capillary tube used to generate the bubbling was one that passed 77 cm^3 of air per second. The apparent violence of the bubbling could be considerably increased by using a capillary that passed 200 cm^3/sec. The negative curve marked "violent" in Fig. 10 was made with the 200 cm^3/sec. capillary. The chief point of interest is that the totals have been increased by a factor of about five (see Table I), and that there is a relative increase in the number of particles of mobility less than 0.12. The positive curve is not shown, but the changes in it resulting from the use of the 200 cm^3/sec. capillary instead of the 77 cm^3/sec. capillary are similar to those of the negative curve. The total amounts of negative and positive electrification have been changed from $-4/+1$ with the usual 77 cm^3/sec. capillary to $-18/+6$ (ratio 3 to 1) with the 200 cm^3/sec. capillary.

By using a tube of 12 mm inside diameter to produce the bubbles (still using 77 cm^3/sec. of air), the bubbling appeared to be very gentle and

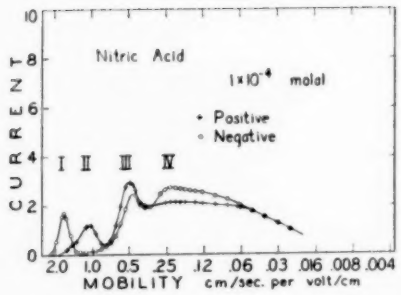

FIG. 5. Mobility spectrum produced by bubbling 1×10^{-4} molal nitric acid.

uniform. The curve marked "gentle" in Fig. 10 was made with the 12 mm tube. Although the amount of negative charge was reduced to about $\frac{1}{6}$ of the usual value (Fig. 1), the ratio of negative to positive was certainly greater than one hundred to one. No positive electrification could be detected.

Effect of age

As mentioned under "Apparatus and Procedure," no change in the distilled water curves was noted when the measurement was made far downstream. Likewise, doubling the age of the particles before they entered the Erikson tube produced no significant change other than about a 25 percent loss of the faster particles due to longer time for diffusion.

Humidity and temperature effects

Humid air.—Under normal conditions of operation, the relative humidity of the various air blasts was about 35 percent or less, and their temperature was the same as that of the room (i.e., about 23°C). Usually the equilibrium temperature in the bubbler was about 6°C below room temperature.

A certain amount of control over the humidity in the bubbler could be obtained by turning off the dry (35 percent humid) auxiliary blast. Thus the air in the bubbler had all been bubbled so that its humidity was over 95 percent. As a result of this operation, the number of carriers of both signs of mobilities less than 0.25 was roughly doubled. As can be seen from Fig. 1, there are few carriers in this range so that doubling their number did not greatly affect the total amount of charge. In fact, the loss in the number of carriers of mobilities greater than 0.25 (particularly in groups I^- and $IIIa^-$) was more than sufficient to compensate for the increased number of slow carriers, so that the total amounts of charge were reduced by about 10 percent (see Table I).

TABLE I. *Total amounts of negative and positive charge produced by bubbling the solutions indicated. The same units are used throughout Tables I and II.*

Distilled Water (Fig. 1)	−4.0	+1.0	Sucrose 0.8 molal	−25	+25
			Sucrose 2 molal	−5.5	+6.5
KCl 1×10^{-5} molal (Fig. 2)	−4.7	+1.7			
KCl 1×10^{-4} molal (Fig. 3)	−5.3	+3.1	Water, violent, 200 cc/sec., auxiliary off	−25	+7.0
KCl 1×10^{-3} molal (Fig. 4)	−7.5	+7.2	Water, violent, 200 cc/sec., auxiliary on (Fig. 10)	−18	+5.5
KCl 0.01 molal	−7.7	+7.7	Water, normal, 77 cc/sec., auxiliary off	−3.5	+0.95
KCl 0.1 molal	−5.0	+5.0	Water, gentle, 12 mm tube, auxiliary on (Fig. 10)	−0.7	+0.00
KCl 1 molal	−2.2	+2.2			
KCl 4 molal	−1.5	+1.5	Water, 99 percent humidity in aux., bubbling temp. at equilibrium 6°C below room temp.	−6.0	+1.7
$AlCl_3$ 3×10^{-5} molal	−6.5	+3.5	Water, 99 percent humidity in aux., bubbling at room temp. (Fig. 11)	−8.2	+2.6
$AlCl_3$ 3×10^{-3} molal	−8.0	+12	Water, supersaturated in aux. (Fig. 12)	−10	+3.5
$AlCl_3$ 0.03 molal	−6.0	+8.0			
$AlCl_3$ 0.3 molal	−4.0	+4.0	Hot water 55°C, dry aux. (Fig. 13)	−9.0	+1.2
			Hot water 80°C, dry aux.	−11	+0.6
NaOH 1×10^{-5} molal	−4.4	+1.4			
NaOH 1×10^{-4} molal	−6.3	+3.0	Sodium Stearate 3×10^{-6} molal	−4.5	+1.3
HNO_3 1×10^{-5} molal	−3.9	+1.4	Sodium Stearate 1×10^{-5} molal	−7.0	+1.8
HNO_3 1×10^{-4} molal (Fig. 5)	−3.2	+3.1	Sodium Stearate 1×10^{-4} molal	−8.0	+4.5
HNO_3 1×10^{-3} molal	−3.4	+3.4	Sodium Stearate 1×10^{-3} molal	−12	+12
Sucrose 3×10^{-6} molal (Fig. 6)	−5.4	+1.7			
Sucrose 3×10^{-5} molal	−7.5	+2.7			
Sucrose 3×10^{-4} molal (Fig. 7)	−11.7	+6.8			
Sucrose 3×10^{-3} molal (Fig. 8)	−18	+14			
Sucrose 0.03 molal	−28	+21			
Sucrose 0.3 molal (Fig. 9)	−35	+31			

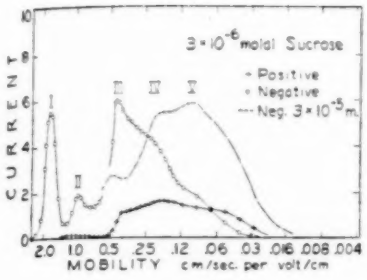

FIG. 6

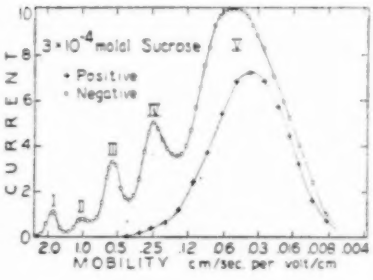

FIG. 7

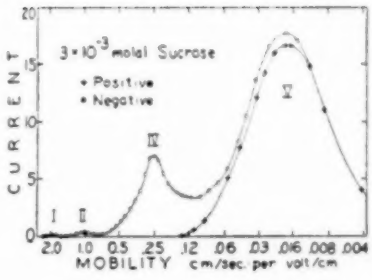

FIG. 8

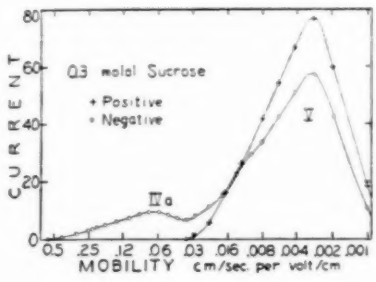

FIG. 9.

FIGS. 6–9. Mobility spectra produced by bubbling solutions of sucrose of various concentrations.

By bubbling the air to the auxiliary through hot water and filtering out all the electrification, a supply of strictly 100 percent humid air was obtained. By mixing this moist air with a certain amount of dry air, a fair control over the humidity was obtained. No noticeable changes in the curves occurred unless the humidity was over 90 percent. The humidity of the auxiliary was the controlling factor in the humidity experiments. Humidifying the other two blasts had little effect.

Figure 11 shows a distilled water curve made with bubble temperature 24.5°C, the room temperature 24.6°C, and the temperature of both the wet and dry bulb thermometers of the auxiliary 24.0°C. The humidity in the auxiliary was probably a trifle under 100 percent, since there was no condensation of moisture on a dry surface. It is seen that group I^- is weaker than in Fig. 1, II^- is smeared out, $IIIa^-$ virtually missing, $IIIb^-$ strong, IV^- strong, and that there are considerable numbers of carriers of mobility less than 0.12. II^+ has shifted to a lower mobility, as has III^+. There are also considerable numbers of slow positive carriers. The total amounts of both positive and negative electrification have nearly doubled. It is likely that some of this increase has come from carriers that evaporated slowly (and hence were of low mobility), so that they did not diffuse to the walls of the bubbler as they did in the normal dry-air experiments.

Moist air.—By using only moist air, so that condensation was actually occurring in the *auxiliary* blast, the curves in Fig. 12 were obtained. Remarks made in "Apparatus and Procedure" about the maintenance of the shape of curves when the electrode is moved downstream do not apply to this humidity experiment. In plotting the curves in Fig. 12, the ordinates have already been multiplied by the usual dry-air coefficients necessary to obtain overlapping curves (as mentioned in "Apparatus and Procedure").

The reason the curves in Fig. 12 do not overlap is that evaporation of the carriers has been occurring in the dry (35 percent humid) main blast of the Erikson tube. The carriers in curves *AA* have been in the dry blast for 0.013 second; those in *BB*, 0.11 second; and those in *CC*, 0.44 second. It is seen that the longer the time the carriers spend in the dry blast, the greater the number of fast carriers, and the fewer the number of slow ones. Because of condensation on the insulation, it was impossible to obtain results when moist air was used in the main blast.

Temperature.—With dry (35 percent humid) air used in all blasts, if the water in the bubbler is heated, there is an increase in negative electrification due to the reduction of viscosity of the water changing the bubbling mechanism. The change of mechanism is made evident by the fivefold increase in the amount of water splattered out of the bubbler. With increase in temperature, the total amount of positive electrification first increases slightly, and then decreases. (For examples, see Table I.) Group II^- is

enhanced by heating, and IIIa$^-$ is nearly eliminated. Groups II$^+$, III$^+$, and IIIb$^-$ move toward lower mobilities. Fig. 13 shows a typical curve from this set.

Soap

Solutions of sodium stearate of various strengths were investigated in order to test the effect of the lowering of surface tension. Surprisingly enough, the changes produced were relatively slight. Group II$^-$ was trebled in magnitude in weak solutions (10^{-5} mole per liter). Stronger solutions (10^{-3} molal) virtually eliminated the I and II groups, although not so effectively as salt. The total amount of electrification from the strongest solution that could be investigated (3×10^{-3} molal) showed about twice as much electrification as salt of the same concentration. In half-width, the slowest stearate group resembled the slowest sugar group, rather than the broad maximum of salt.

Normal ions

By placing a radioactive source in the inlet, "normal ions" could be led into the Erikson tube. The negative ion peak came at mobility 1.66 with half-width of 34 percent. The positive group came at 1.15, half-width 46 percent. Introducing 99 percent humid air gave $k^-=1.64$, half-width 23 percent, and $k^+=1.11$, half-width 38 percent. In each case there was a disappearance of some of the faster carriers in the group, resulting in a slight decrease in mobility of the peak. Immediately afterward, bubbling peaks were made with dry (35 percent humid) air, yielding: I$^-=1.80$, half-width 21 percent; II$^-=0.95$; II$^+=1.0$. Spraying peaks were then observed; negative 1.67, half-width 41 percent; and positive about 1.52 and 0.95 (see next section).

Spraying

An attempt was made to correlate the groups previously observed[4] by spraying, with the present bubbling groups. The improved resolving power of the 2.5 mm electrode brought out a few previously undetected weak groups. Figs. 14–15 show curves obtained by spraying distilled water and some KCl solutions. The groups observed are of mobilities -1.67, approximately -0.85, -0.44, -0.28, a broad maximum about -0.06 with a gradual tailing off down to -0.002; $+1.52$, $+0.95$, $+0.70$, $+0.49$, $+0.28$, and a broad maximum at about $+0.06$. The curves for sprayed KCl solutions show which of the groups shift into the peaks previously observed with spraying. For the negative carriers there is a one to one correspondence between the sprayed groups and the bubbled groups; the mobilities in the case of spraying are only slightly less than in

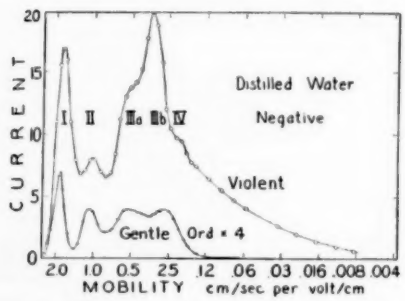

FIG. 10. Mobility spectra for negative carriers produced by violent and gentle bubbling (see text). The ordinates of the "gentle" curve have been multiplied by 4.

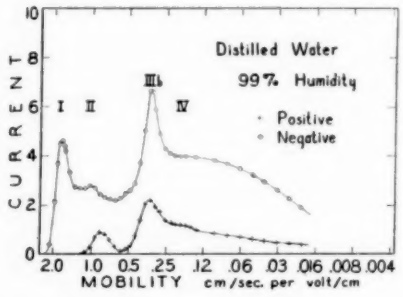

FIG. 11. Mobility spectrum of distilled water produced by bubbling in the presence of approximately 99 percent humid air (see text).

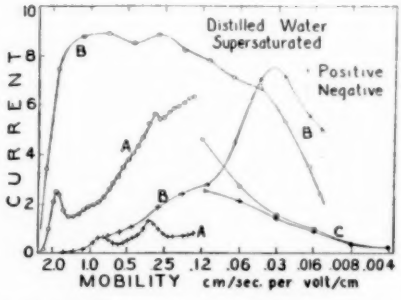

FIG. 12. Mobility spectrum of distilled water produced by bubbling in the presence of supersaturated air (see text). Curves AA made at $l=2.5$ cm, $Q=3260$ cm^3/sec. with 2.5 mm electrode. Curves BB, $l=10$, $Q=1630$, 15 mm electrode. Curves CC, $l=20$, $Q=815$, 15 mm electrode.

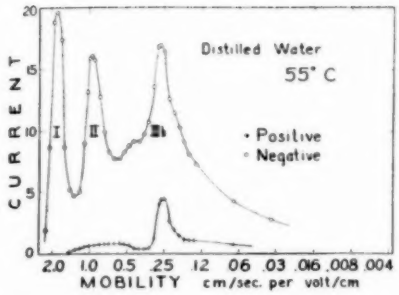

FIG. 13. Mobility spectrum produced by bubbling distilled water at 55°C.

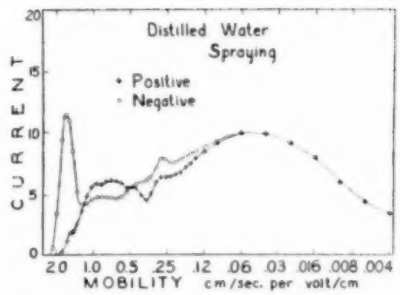

FIG. 14. Mobility spectrum produced by spraying distilled water.

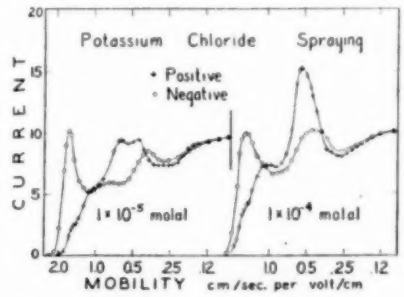

FIG. 15. Mobility spectra produced by spraying solutions of potassium chloride.

the case of bubbling. The equality of corresponding mobilities is quite marked with the bubbling curves made under conditions of high humidity (when conditions more nearly resemble the humid spray atmosphere). For the positive carriers, there are apparently no bubbling analogues to the groups +1.52, +0.70, and probably +0.49; yet in the bubbling curves, the positive groups are not so sharp as the negative groups, and it is quite possible that traces of these positive groups do exist. For instance, the high mobility side of the II^+ peak is particularly gradual in dropping off to zero. It is almost certain that a weak group could be found in this region if the intensities were five times as great. Such a positive mobility of 1.52 corresponds very nearly to that of the "normal" positive ion in absolutely *dry* air. New measurements on the amounts of total electrification produced by spraying salt solutions of concentrations up to 1 molal are given in Table II. These results confirm previous conclusions regarding the decrease of total amounts of electrification with increasing concentration in solutions more concentrated than 10^{-4} molal.[4]

TABLE II. *Total amounts of negative and positive charge produced by spraying.*

Distilled water (Fig. 14)	−38	+38
KCl 1×10^{-5} molal (Fig. 15)	−40	+40
KCl 1×10^{-4} molal (Fig. 15)	−42	+43
KCl 0.01 molal	−11	+11
KCl 1 molal	−2	+2

In conclusion, the writer wishes to thank Professor L. B. Loeb, under whose direction the experiments were carried out, for his continual interest and invaluable suggestions concerning all phases of the work.

Interpretation of Carrier Mobility Spectra of Liquids Electrified by Bubbling and Spraying

SEVILLE CHAPMAN
Department of Physics, University of California, Berkeley, California
(Received July 5, 1938)

The homogeneous group of negative carriers of mobility 1.8 cm/sec. per volt/cm, produced by bubbling distilled water, consists of a normal negative ion in moist air. The positive and negative groups at mobilities +1.0 and −0.95 appear to be due to carriers containing an extra H^+ and OH^- ion, respectively. It is likely that the other distilled water groups are formed partly by the breaking of the thin bubble film in uniform fashion, and partly by the evaporation of larger carriers. The presence of electrolytic ions in the bubble film seems to cause irregular rupture, and thus a wide distribution of mobilities. With increasing concentration in solutions more concentrated than 10^{-3} mole per liter, the reduced vapor pressure of the carriers containing solute causes the main maximum to shift gradually to lower mobilities (i.e., larger drop sizes). Presence of sucrose in the bubble film appears to provide "nuclei" so that a greater number of droplets are formed than is the case with distilled water. Thus more total charge and more types of carriers are produced. When distilled water is bubbled more violently than usual, the bubble films are more extensively torn into thick fragments by the air blast, so that the positive charges (which on Lenard's theory are in the under layer of the electrical double layer) are more frequently torn off. Hence the proportion of positive charge produced relative to the negative is greater. The less turbulent breaking of the bubble film in the case of gentle bubbling seldom exposes positive charges, so that no positive carriers are produced. The use of supersaturated air in the bubbling blasts inhibits evaporation so that only a wide distribution of carriers of all sizes is observed.

IN the preceding paper the author has reported the results of an investigation of the electrification of droplets produced by bubbling water and various aqueous solutions. It is the purpose of this paper to interpret these results on bubbling, and to correlate them with some results previously observed on spraying.[1] Although all the conclusions are interrelated, the paper is divided into sections. In general, each one primarily relates to the interpretation of a particular set of experiments, or to the nature of a particular group of carriers.

Existence of Carrier Groups

The striking peaks in the curves of the preceding article showing current as a function of mobility indicate the existence of homogeneous groups of carriers of nearly unique mobilities. The formation of these groups (some of which are labelled with Roman numerals in the figures) is conditioned by the mechanism of breaking of the bubble film. It is known from high speed motion picture studies of the formation of drops from tips[2] that, in general, primary drops of a certain size are formed along with a number of smaller secondaries. It is thought likely that when the thin bubble film breaks a similar type of droplet formation occurs, except that in this case the droplets are much smaller. The charged droplets thus formed account for the existence of the various groups discussed in greater detail below.

According to the electrical double layer theory of liquid surfaces first proposed by Lenard,[3] the electrical nature of molecular forces causes a stratification of charge at the liquid surface. The *negative* charge at the outer surface of water (corresponding to one electron for about 10^5 H_2O molecules in the surface region) is composed partly of polarization charge, and partly of electrons which have migrated to the surface.

Under ordinary conditions the breaking up of a polarized medium produces no separation of charge. The structure of the molecules in water, however, is such as to permit it to form an extended electropolar complex.[4] It is not impossible that a mechanical tearing apart of such a surface of polar molecules as H_2O in H_2O, in which there are strong linkage forces (hydrogen

[1] Chapman, Phys. Rev. **52**, 184 (1937).
[2] Edgerton *et al.*, J. Phys. Chem. **41**, 1017 (1937). Hauser *et al.*, J. Phys. Chem. **40**, 973 (1936).
[3] Lenard, Ann. d. Physik **47**, 463 (1915).
[4] Bernal and Fowler, J. Chem. Phys. **1**, 515 (1933).

bonds) between adjacent molecules, can occasionally[5] produce a separation of charge either by breaking off electrons (see discussion of group I, below) or by actually splitting up the molecular complex giving rise to groups containing H^+ or OH^- (see discussion on group II, below). Positive electrolytic ions, if present, will migrate into the outer negatively charged component of the double layer, while the negative *ions* will be found further down in the liquid.[3] Thus one would expect that the smallest charged droplets might contain electrons; larger droplets, H^+ or OH^-; and still larger droplets, single electrolytic ions. Droplets of radii greater than about 10^{-6} cm might contain electrolytic ions of both signs in about equal quantities.

All the ion groups observed have doubtless evaporated to equilibrium sizes determined by their age, charge, surface tension, vapor pressure, and the conditions of humidity. These observed groups are characteristic then, not so much of the surface layer, but of the configurations (about an electrically charged nucleus) that are stable under the existing conditions.

Group I

The figures (of the preceding article) show that by bubbling solutions weaker than 10^{-4} mole per liter, there is produced a very prominent group of negatively charged carriers (labelled group I), having a mobility of 1.8 cm/sec. per volt/cm. [All mobilities in this paper are expressed in this unit.] The corresponding positive group I is very weak and is generally lost in the tail of the adjacent group II^+, although it may be distinctly seen in Figs. 14 and 15 for spraying. Since the mobility of group I^- is identical with that of the normal negative ion in moist air, it has been concluded[1] that the carriers of this group consist of single electrons attached to at least one and probably not more than three water molecules.

Since the outer component of the double layer is negative,[3] the chance of creating a *small* drop containing an excess of positive charge is very slight. Thus the fact that the positive group I is very weak shows that the carriers in the group I must have come from the *smallest* droplets originating at the surface (radii less than 10^{-7} cm). These droplets, subsequent to their creation, must then have evaporated down to the configuration of a stable normal negative ion in pure, moist air.

[5] It can be estimated from the magnitude of the currents observed that only a very small fraction (perhaps 10^{-4}) of the droplets with radii less than 5×10^{-7} cm are charged.

Normal Ions in Moist Air

In conjunction with the group I carriers, it is desirable to discuss the ions ordinarily observed in air. For conditions of high purity and very dry air, the accepted values of mobility are[6] 2.21 for the negative ions, and 1.60 for the positive ions. Since the air used in the present experiments always contained some water vapor, one would expect the values of mobilities to be less than these, and indeed, the observed mobilities of group I were -1.8 and $+1.5$, values which are consistent with those obtained by other workers for normal ions in pure, moist air.[7]

In attempting to test the apparatus on "normal ions" from a radioactive source, such intense ionization from polonium was used in order to give convenient currents, that the air was contaminated by ionization products such as nitric oxides. The ions formed in the presence of these impurities gave broader peaks and lower mobilities than the pure bubbler produced ions from water.[8]

Group II

The effects of acids, bases, and salts on the bubbling curves are essentially similar to one another with but one exception: Although salt is approximately equally effective in reducing the amount of charge associated with both the II^- and the II^+ groups, acids and bases are strongly selective in their action on these II groups. With dilute acid the II^+ peak is strongly enhanced, while the II^- peak is suppressed. With dilute base, the opposite effect occurs. These facts suggest that the II^+ group probably contains an H^+ ion and the II^- group contains an OH^- ion. As shown from their mobilities, the

[6] Bradbury, Phys. Rev. **40**, 508 (1932).

[7] Tyndall and Grindley, Proc. Roy. Soc. **A110**, 341 (1926), **A110**, 358 (1926); Mahoney, Phys. Rev. **33**, 217 (1929); Erikson, Phys. Rev. **33**, 403 (1929); Zeleny, Phys. Rev. **34**, 310 (1929).

[8] For discussions on mobility spectra of normal ions, see Loeb and Bradbury, Phys. Rev. **38**, 1716 (1931); Varney, Phys. Rev. **42**, 547 (1932).

II^- group is slightly larger in size than the II^+ group. This can be ascribed to secondary valence linkage (the hydrogen bond) favoring a smaller size in the case of the carrier containing H^+ than in the case of the carrier containing OH^-. These group II carriers originate in droplets that come from thicker portions of the bubble film than do the droplets that account for the group I carriers. It is in the thicker portions of the film that ions are to be expected.[3]

Size of Carriers

For radii less than 6×10^{-8} cm, theory is incapable of giving the *actual* radius of the carrier from its mobility. The reason for this is that the mobility depends on the mean free path of the carrier, and it is impossible to distinguish the effect of polarization forces in changing the mean free path, from the forces affecting cluster formation. Despite the effectiveness of Langevin's theory[9] (as modified by Hassé) for large radii (see next paragraph) and its effectiveness in accounting for the mobility in the case of monatomic ions, the probable inapplicability of the normal value of the dielectric constant at distances of about 3×10^{-8} cm makes this theory indeterminate in the case of carriers of radii less than about 6×10^{-8} cm.

For larger radii the dielectric forces of attraction become inappreciable and Langevin's equation reduces to the form of a solid elastic equation:

$$k=76\times10^{-16}/s^2, \qquad (1)$$

where k is the mobility of the carrier in cm/sec. per volt/cm, and s is the sum of the radii in cm of the carrier and of a molecule of the gas in which the measurement is made (in this case air at atmospheric pressure and 20°C). In this paper the sizes of large carriers have been based on Eq. (1).

Other Groups

The IIIa, IIIb, and IV groups observed in bubbling distilled water are stable configurations of molecules, probably formed partly by the breaking of the thick portions of the bubble film in a uniform manner as discussed in the section "Existence of Carrier Groups," and partly by the evaporation of carriers that were large when created. [See also the section on "Humidity Effects," below.] If the diameter of a water molecule is assumed to be 3×10^{-8} cm, Eq. (1) gives the diameters of the droplets comprising the IIIa, IIIb, and IV groups as 8, 9–10, and 12 molecules, respectively. Of these groups, IIIb is definitely the most stable, for experiments on variation of humidity show that for high humidity (see Fig. 11 of the preceding article) $IIIa^-$ is nearly lost, and IV is greatly enhanced, as might be expected if $IIIa^-$ were formed by evaporation of a layer of molecules from $IIIb^-$, and IV^- were formed by condensation of a layer on $IIIb^-$.

Although, with bubbling, few carriers are found with mobilities less than 0.1, with spraying the greatest portion of the charge comes from the slow carriers of mobilities less than this value. These large heterogeneous carriers are unstable droplets formed by the spraying and are in the process of evaporating. In general it can be seen from the curves of the preceding article that the ratio of negative to positive electrification approaches unity for carriers of mobility less than 0.1. These carriers are so large (diameter greater than 20 molecules) that, although the outer component of the double layer is negative, one would expect little sign preference. These results are consistent with previous observations on visible droplets measured by the Millikan oil-drop method.[10]

Violence of Bubbling

When the bubbling is more "violent" than usual, there are two changes in bubbling mechanism: (1) More surface is brought into play because of the fact that more bubbles are formed, thus resulting in an increase in the charge produced (see Table I of the preceding article); (2) The bubble films are more extensively torn by the air blast. Consequently the number of large carriers of mobility less than about 0.1 is increased (see Fig. 10); and in addition, the positive charges residing in the body of the liquid[3] are more frequently exposed and torn

[9] Langevin, Ann. Chim. Phys. **8**, 238 (1905). Hassé, Phil. Mag. **1**, 139 (1926).

[10] Chapman, Physics **5**, 150 (1934).

off, so that the ratio of the number of positive carriers to the number of negative carriers is increased (see Table I of the preceding article).

When the bubbling is more gentle than usual, the above changes are reversed. The amount of charge produced is considerably reduced (as shown in Table I of the preceding article). The bubbles are larger than usual and are drawn out into thinner films before bursting. There is also less turbulence in the bubble stream. Hence the bubble film is not so extensively torn into thick fragments, and no large carriers are produced. Whether the electrification by bubbling arises from electron migration to the surface or from splitting of the polar structure of the water, or both, it would be expected that the relatively nonviolent breaking off of small droplets from the outer surface of the bubble film would produce no positively charged droplets. Experimentally none are observed.

Salt

In the bubbling of salt solutions, two prominent effects are noticed: the reduction of magnitude of groups I and II, and the appearance of large numbers of carriers of both signs with mobilities less than 0.1. Both effects may be attributed to the presence of electrolytic ions in the double layer. The concentration of electrolytic ions in the bubble film as it becomes thin just before bursting may differ by some orders of magnitude from the concentration in the body of the liquid. It appears as if the cations such as K^+, which are attracted to the negative outer surface of the double layer,[3] become associated with the electronic charges there, so that any small droplets which are formed are neutral, thereby accounting for the disappearance of groups I and II.

The concentration of electrolytic ions in the thin film is probably irregular (statistical fluctuations of small numbers). The ions disturb the normal cohesive forces in the film, thus affecting the mechanism of film-breaking so that uniform sizes of carriers are no longer produced. As a consequence one obtains a wide distribution of mobilities of carriers (as shown in Fig. 4 of the preceding paper, for instance).

The carriers of mobilities less than 0.1 probably contain electrolytic ions. The presence of these ions in the droplets reduces their vapor pressure, and tends to keep them from evaporating, so that they remain relatively large in size. The vapor pressure effect accounts for the decrease in mobility of the main maximum for solutions of 10^{-3} molal and greater.

In concentrated solutions (10^{-2} molal and greater) the ion densities in the surface layer become so great that it is increasingly unlikely that a droplet will be produced in which there is a numerical preponderance of one sign of ion over the other, because the association effects of ions in solution then tend to keep the positive and negative charges bound together. Hence at high concentrations the total amount of charge produced decreases with increasing concentration (see Table I of preceding paper).

The proportionally greater positive charge observed with $AlCl_3$ than with KCl is due to the fact that the Al^{+++} ion can still produce a charged droplet, even though there are as many as two Cl^- ions associated with it.

Sugar

The reduction in magnitude of the I^- and II^- groups with increasing concentration is much *less rapid* with sucrose solutions than with salt, because the sugar is electrically *inert* and cannot act to neutralize the electronic charge of the double layer. With increasing concentration of sugar, however, the sugar in the bubble film may increase the surface tension enough so that fewer small droplets are formed, thus finally reducing the magnitude of the I^- and II^- groups. [For the opposite effect see the section on "Soap," below.]

Even in weak sugar solutions, more carriers are formed than is the case with distilled water. Thus the presence of sugar in the thin bubble film seems to provide "nuclei" so that an increased number of large droplets can be formed from the bubble film (i.e., effectively there is an increase in the amount of surface that is torn apart). The amount of charge thus produced is greater than with distilled water (see Figs. 6–9 and Table I of the preceding paper). The breaking of the surface of the sugar solutions is fairly uniform, as is shown by the number of discrete groups in Fig. 7 of the preceding paper.

With increasing concentration the reduction of vapor pressure of the large carriers containing sugar molecules shifts the main maximum (labelled group V in Fig. 9 of the preceding paper) to lower mobilities, just as in the case of salt. Although in the case of salt, the electrolytic ions may have caused a more extensive breaking of the surface (as above suggested for sugar), they also tended to neutralize the double layer, so that only for very low concentrations was there an increase in the total amounts of electrification with increasing concentration.

At high concentration when many large droplets are produced, fragments of some of the large neutral droplets may break off. These secondary droplets, if charged, will be negative (since the outer component of the double layer is negative) leaving the large droplet positively charged. This mechanism can account for the facts that in Fig. 9 of the preceding paper there are more fast negative carriers than positive ones, and that there is an equivalent excess of slow positive carriers.

Humidity Effects

Under the usual conditions of operation the relative humidity of each of the three air blasts is about 35 percent. Hence it is possible for any of the large droplets formed in the bubbling of distilled water to evaporate. As a result, very few carriers of mobilities less than 0.1 are observed, since most of the larger carriers have evaporated down to the stable IV and IIIb configurations before entering the Erikson tube. [Compare Figs. 1 and 11 of the preceding paper.]

When the humidity of the blasts is just less than 100 percent, evaporation of the larger carriers is inhibited. Consequently more of the charge is concentrated in the groups of low mobility than is the case with dry air (see Fig. 11 of the preceding paper). Since the carriers are larger than with dry air, they diffuse less rapidly to the walls, and hence the measured total amounts of electrification are greater. The humidity of the auxiliary blast is ordinarily the determining factor in the humidity experiments, because if the electrode is 2.5 cm downstream, the carriers spend about thirty times as long in the auxiliary blast as they do in the Erikson tube.

In the experiment of Fig. 11 of the preceding paper, in which the humidity of the auxiliary blast was just less than 100 percent, it is seen that the high humidity has caused the negative group II to become well smeared into the background. In previous bubbling experiments[1] where there was no dry auxiliary blast connected to the bubbler, the negative group II was for the same reason smeared completely out, so that it was not observed.

It is to be noted that high humidity affects the spectrum of the negative carriers much more than it does the positive, a fact which might be in conformity with the well-known preferential condensation of supersaturated water vapor on negative ions.

When the auxiliary blast is slightly supersaturated, evaporation in the auxiliary blast is retarded to such an extent that carriers of all sizes are observed. It can be seen in Fig. 12 of the preceding paper that as the length of time spent in the dry blast in the Erikson tube is increased (by increasing the downstream distance and decreasing the volume of the blast) there is an increased amount of evaporation of large carriers, so that the average mobility of the carriers becomes greater.

It is seen in the bubbling experiments that high humidity causes a slight decrease in mobility of many of the peaks. In the case of spraying, the humidity in the chamber and in the inlet to the Erikson tube is always 100 percent, so that one would expect the spraying groups to be slightly lower in mobility than the bubbling groups, as in fact they are. The spraying groups at mobilities $+0.70$ and $+0.49$ are the groups that shift into the strong positive group observed when spraying salt solutions.[1] Apparently these two groups are peculiar to spraying; no bubbling analogues have been detected with certainty.

Soap

The results obtained with solutions of sodium stearate are *not unlike* the results on salt and sugar. Group I behaves as it does with salt solutions, and the slowest group behaves like the group V of sugar. The appearance of group II^- is almost exactly the same as that of group II^- of hot water, illustrated in Fig. 13 of the preceding paper. In both cases this effect is

probably due to the reduction of surface tension in the bubble film causing production of an increased number of small droplets. The increase in magnitude of the group II^- in the case of weak solutions of sodium stearate is not inconsistent with its alkaline nature (see discussion on "Group II," above). The increase in the total amounts of electrification with increasing concentration is similar to the case with sugar, and likewise may be due to the fact that an increasing amount of surface is brought into play.

Working with solutions of sodium oleate, Johonott[11] has observed films as thin as 6×10^{-7} cm. In fact, the films he observed were *stratified* so that as many as five different thicknesses of film could be observed at one time. A carrier having a diameter of 6×10^{-7} cm has a mobility of 0.08. The fact that carriers discussed in this paper have mobilities ranging about equally on both sides of this value, coupled with the fact that the results on soap are not unlike the other results, is corroborative evidence in favor of the bubble-film-breaking mechanism advanced as a basis for interpretation.

In conclusion, the writer takes pleasure in expressing his gratitude to Professor L. B. Loeb for his helpful guidance and assistance in interpreting the results.

[11] Johonott, Phil. Mag. **47**, 501 (1899); Phys. Rev. **20**, 388 (1905).

OCTOBER 1, 1938 PHYSICAL REVIEW VOLUME 54

The Magnetic Anisotropy of Copper Sulphate Pentahydrate, $CuSO_4\cdot5H_2O$, in Relation to its Crystal Structure. Part II

K. S. KRISHNAN AND A. MOOKHERJI
Indian Association for the Cultivation of Science, Calcutta, India

(Received July 5, 1938)

In Part I of this paper were reported some magnetic measurements on the crystal of $CuSO_4\cdot5H_2O$. The crystal, though triclinic, has nearly uniaxial magnetic symmetry, and the symmetry axis is the direction of minimum susceptibility for the crystal. This observed uniaxial symmetry and the negative sign of the anisotropy were shown to follow naturally from the known fine structure of the crystal, and the direction of the symmetry axis also is nearly that predicted from the structure. In the present paper are described further magnetic studies on the crystal, and a more detailed correlation with its structure. The magnetic data are also discussed in relation to the magnitude and the asymmetry of the internal electric fields acting on the Cu^{++} ions in the crystal. A general method is described for determining, for any triclinic crystal, the principal magnetic axes and susceptibilities, i.e., the constants of the magnetic ellipsoid.

1. Explanation of the Magnetic Anisotropy of Paramagnetic Crystals

In some recent papers[1, 2] we have discussed the magnetic anisotropy of several organic crystals in relation to the anisotropy of the constituent molecules and their relative orientations in the crystal lattice. When the molecular anisotropy is known, either from measurements on the magnetic double refraction of the substance in the liquid state or in state of solution in suitable solvents, or theoretically from considerations of the structure of the molecules, we can utilize the observed data for the anisotropy of the crystal to obtain much useful information regarding the orientations of the molecules in the unit cell of the crystal. On the other hand, if the molecular orientations in the crystal are already known from x-ray analysis, the magnetic measurements on the crystal may be used for calculating the molecular anisotropy, which is an important molecular constant.

[1] Krishnan and Mookherji, Phys. Rev. **50**, 860 (1936), which is Part I of this paper.
[2] Krishnan, Guha and Banerjee, Phil. Trans. Roy. Soc. **A231**, 235 (1932); Krishnan and Banerji, Phil. Trans. Roy. Soc. **232**, 99 (1935); Zeits. f. Krist. **A91**, 173 (1935).

In a paramagnetic crystal also the anisotropy of the crystal may be regarded as arising from that of certain paramagnetic units; the magnitude of the crystal anisotropy will depend on the anisotropy of these units and their orientations relative to one another. These anisotropic units, however, are not the molecules as in the organic crystals, but are constituted as follows: Each paramagnetic ion (or atom) in the crystal is under the influence of the strong, and generally asymmetric, electric fields of the neighboring electrically charged atoms. Under the influence of these fields the paramagnetic ion may exhibit, as was shown by Van Vleck,[3] Penney and Schlapp,[4] a magnetic anisotropy. The magnitude and the asymmetry of these fields will be determined practically by the positions of the atoms *immediately* surrounding the paramagnetic ion, those that are further away contributing relatively very little to the fields. Thus the paramagnetic ion and the charged atoms immediately surrounding it constitute a group which may be magnetically anisotropic; and such a group forms the anisotropic paramagnetic unit which we referred to previously. There will be in general more than one such group in the unit cell of the crystal, and the magnetic anisotropy of the crystal as a whole will therefore be determined by the anisotropy of these groups and their orientations relative to one another; in the same manner in which the anisotropy of an organic crystal is determined by the anisotropy, and the relative orientations, of the constituent molecules. The relative *positions* (or the density of packing) of the paramagnetic groups in the crystal lattice, as distinguished from the *orientations* of the groups relative to one another, will not appreciably affect the anisotropy, again as in the organic crystals, since the mutual influence of their magnetic moments will be very small.[5]

If we know the structure of the above paramagnetic groups, i.e., if we know the distributions of the charged atoms around the paramagnetic ions, it should be possible, at any rate theoretically, to calculate the magnitude and the asymmetry of the electric fields acting on the paramagnetic ions, and thence to calculate the principal magnetic susceptibilities of the groups. Further if we know the relative orientations of the different groups present in the unit cell of the crystal, it should be possible to predict the principal magnetic susceptibilities of the crystal. Conversely, from the observed principal susceptibilities of the crystal, and the known orientations of the different paramagnetic groups present in the unit cell, we can readily calculate the principal susceptibilities of these groups, i.e., the principal susceptibilities which the crystal would have if all the paramagnetic groups in it were identical and their orientations parallel.[6] We can then try to correlate these magnetic data deduced for the group with its structure. Thus a study of the magnetic properties of paramagnetic crystals can throw light on some aspects of their fine structure.

The crystal of copper sulphate pentahydrate is very suitable for illustrating some of these points.

2. Temperature Variation of the Susceptibility of $CuSO_4 \cdot 5H_2O$ Powder and the Structure of the Crystal

The crystal of $CuSO_4 \cdot 5H_2O$ is triclinic, in the space group C_i^1. Its unit cell has the dimensions[7]

$$a = 6.12\text{A} \qquad \alpha = 82°16'$$
$$b = 10.7 \qquad \beta = 107°26'$$
$$c = 5.97; \qquad \gamma = 102°40';$$

and it contains two molecules of $CuSO_4 \cdot 5H_2O$.

Jordahl[8] has discussed theoretically the magnetic susceptibility of $CuSO_4 \cdot 5H_2O$ powder at different temperatures, in relation to the splitting of the energy levels of the Cu^{++} ion under the action of the crystalline electric fields. In particular, he found that the observed deviation of the effective magnetic moment of the Cu^{++} ion in the crystal from the theoretical value for the free ion corresponds to a field of predominantly

[3] Van Vleck, *Theory of Electric and Magnetic Susceptibilities* (Oxford University Press, 1932), Chap. XI; Phys. Rev. **41**, 208 (1932).

[4] Penney and Schlapp, Phys. Rev. **41**, 194 (1932) and **42**, 666 (1932).

[5] We are considering here the simple magnetic interaction between the moments induced in neighboring groups, which will be of the order of the volume susceptibility of the crystal and negligible. The exchange interactions, in paramagnetic crystals, between neighboring spin-moments, even when appreciable, will not produce an anisotropy.

[6] Studies on the susceptibility of the crystal powder at different temperatures can also give us a rough estimate of the anisotropy of these paramagnetic groups.

[7] Beevers and Lipson, Proc. Roy. Soc. **A146**, 570 (1934).

[8] Jordahl, Phys. Rev. **45**, 87 (1934).

TABLE I. *Tetragonal angles of* Cu^{++} *ions in unit cells of crystal.*

	'a'	'b'	'c'
z_I	78°	130°	52°
z_{II}	70°	41°	69°
Normal to the $z_I - z_{II}$ plane	155°	68°	50°

cubic symmetry. We can state this result in a slightly different way thus. Taking the Cu^{++} ion under consideration as the origin of a suitably oriented system of rectangular coordinates, and denoting the potential of an electron placed at the point $x\ y\ z$, because of the electric field, by an expression of the type[8]

$$\Phi = D(x^4+y^4+z^4)+Ax^2+By^2-(A+B)z^2, \quad (1)$$

he found that the terms involving the fourth power, which are due to the cubic part of the field, are much greater than the square terms, which are due to the rhombic part. He further found that the direction of the deviation from the free ion value corresponds to a positive value of D; which shows that the cubic field should be due to an octahedral distribution of six equal negative charges round the Cu^{++} ion; since four negative charges at the corners of a tetrahedron, or eight at the corners of a cube, will give a negative value for D.[9]

This prediction has been verified experimentally by the recent x-ray analysis of the structure of this crystal by Beevers and Lipson.[7] It is actually found that each Cu^{++} ion in the crystal is surrounded by six negatively charged oxygen atoms which form an approximately regular octahedron. Four of them, which belong to four water molecules, form a square, of side equal to about 2.8A, with the Cu^{++} ion at the center; the other two oxygens, which are contributed by two SO_4 groups, lie nearly centrally above and below this square. The distance between either of these two oxygens and any of the water oxygens at the corners of the square is about 3.1A.

3. The Tetragonal Symmetry of the Internal Electric Fields Acting on the Cu^{++} Ions and the Magnetic Anisotropy of the Crystal

As we mentioned just now, the octahedron of oxygen atoms is only approximately regular; those belonging to the water molecules are closer to the central Cu^{++} ion than the other two. The octahedron will thus be drawn out along one of its diagonals, namely along the line joining the two sulphate oxygens. As a consequence, the field acting on the Cu^{++} ion should have approximately tetragonal symmetry, with the above long diagonal of the octahedron as the tetragonal axis. In other words the expression for the potential of the field should approximate to the form

$$\Phi = D(x^4+y^4+z^4)+A(x^2+y^2-2z^2), \quad (2)$$

and the susceptibility of the ion along the z axis (the tetragonal axis) should be greater than that along the other two axes.

Now there are two such Cu^{++} ions in the unit cell of the crystal, and their respective tetragonal axes z_I and z_{II} are found, from the parameters given by Beevers and Lipson, to make the angles with the 'a,' 'b,' 'c' crystallographic axes given in Table I. The angle between z_I and z_{II} is about 98°, *which is nearly a right angle.* We should therefore expect: (1) the normal to the plane containing the z_I and z_{II} axes to be one of the principal magnetic axes of the crystal; (2) the susceptibility of the crystal along this axis to be less than the other two principal susceptibilities, which should be nearly equal. In other words the crystal should be nearly uniaxial magnetically, and the symmetry axis should be the direction of minimum susceptibility for the crystal, and should lie along the normal to the plane containing the z_I and z_{II} axes, i.e., along the direction which makes angles of 155°, 68° and 50°, respectively, with the 'a,' 'b,' 'c' axes.

All these results deduced from the structure of the crystal are verified by the magnetic measurements described in Part I of this paper. Two of the principal susceptibilities of the crystal are nearly equal, and greater than the third (by about 300×10^{-6} per gram molecule of $CuSO_4 \cdot 5H_2O$, at room temperature), and the axis of minimum susceptibility makes with the 'a,' 'b,' 'c' axes angles of 156°, 65° and 52°, respectively, which are nearly the angles predicted from the structure.

The directions of the other two principal magnetic axes of the crystal, of nearly equal susceptibility, can also be predicted from the structure. They should lie along the two bisectors

[9] Gorter, Phys. Rev. **42**, 437 (1932).

of the angle between z_1 and z_2, the interior bisector (i.e., of the acute angle) corresponding to the larger susceptibility. We shall show presently that these two directions also, predicted from the structure, agree with observation.

4. Determination of the Magnetic Constants of a Triclinic Crystal

Before describing the magnetic studies on $CuSO_4 \cdot 5H_2O$, we may offer some preliminary remarks on the determination of the magnetic constants of a triclinic crystal, i.e., the directions of the three principal magnetic axes and the susceptibilities α, β, γ along them; $\alpha \leq \beta \leq \gamma$. Instead of measuring α, β and γ directly, it is more convenient experimentally to determine the anisotropies $\gamma-\beta$ and $\beta-\alpha$, and the susceptibility along any one convenient direction in the crystal, or the susceptibility of the powder, $(\alpha+\beta+\gamma)/3$.

Taking up first the determination of the magnetic axes, we may mention that if one of them is located, the other two may be obtained easily, by suspending the crystal at the end of a thin fiber in a uniform horizontal magnetic field, with the known principal magnetic axis vertical, and finding the directions in the horizontal plane which tend to lie along the field and perpendicular to it, respectively. It should be possible to locate the γ axis (the axis of maximum susceptibility for the crystal) by mounting it in a suitably designed light "universal" rotating stage in which the crystal can turn round freely in any direction, and by placing it in a uniform magnetic field; the γ axis will naturally place itself along the field. The rotating parts of the mount have to be of a material whose susceptibility is almost nothing, so that the rotating couple due to the field acting on them will be negligible.

The method however offers at present serious experimental difficulties.

5. The M Axes

Analogous to the two optic axes of a crystal, there are two magnetic directions, which we may call the M axes,[10] which are the normals to the two central circular sections of the magnetic ellipsoid. The two M axes will naturally lie in the $\alpha\gamma$ plane, i.e., the plane containing the directions of the minimum and the maximum susceptibilities of the crystal, and make with the γ axis angles of V and $-V$, respectively, where[11]

$$\tan^2 V = (\beta-\alpha)/(\gamma-\beta). \qquad (1)$$

Instead of determining the three principal magnetic axes, and the anisotropies $\gamma-\beta$ and $\beta-\alpha$, we may therefore alternatively determine the two M axes, and the anisotropy $\Delta\chi$ for any one selected plane in the crystal.

If the crystal is suspended with either of the M axes vertical in a uniform horizontal magnetic field, it will behave like an isotropic crystal, and it should be possible to utilize this property to determine directly the M axes. Here again the experimental difficulties are great, and are similar to the difficulties of determining the γ axis. We have therefore to depend on indirect methods for the determination of these directions.

6. Magnetic Data for $CuSO_4 \cdot 5H_2O$

Coming back to copper sulphate, we determined in Part I, by suspending the crystal in a uniform horizontal magnetic field with different known planes successively horizontal, the directions of maximum and minimum susceptibilities in each of these planes, and the anisotropy $\Delta\chi$ (i.e., the difference between the maximum and the minimum susceptibilities) in each plane. Since the number of crystal planes for which such measurements were made was large, (actually eight) the data obtained should be much more than sufficient to give the magnetic axes and the anisotropies. However, since two of the principal susceptibilities of $CuSO_4 \cdot 5H_2O$ are nearly equal, i.e., since $\gamma-\beta$ is very small in comparison with $\beta-\alpha$, in order to locate the γ and the β axes with certainty, it would be desirable to use more accurate data than those given in Part I. We have therefore repeated the magnetic measurements described there using the following more precise technique.

The crystal was kept immersed in a liquid medium having the same volume susceptibility

[10] The name "magnetic axes" would have been preferable, but it has come into general use to denote the principal axes of the magnetic ellipsoid.

[11] Analogous to the expression $\tan^2 V = (\gamma^2/\alpha^2)(\beta^2-\alpha^2)/(\gamma^2-\beta^2)$ defining the angle between the two optic axes.

as the mean volume susceptibility of the crystal. The medium was an aqueous solution of manganous sulphate of suitable concentration, which had been saturated with copper sulphate so as to prevent the crystal from going into solution. With this arrangement the small rotating couple which may act on the crystal in the magnetic field, because of the asymmetry of shape of the crystal and the imperfect homogeneity of the field, is eliminated. The rotating couple acting on the crystal under these conditions should be due to its anisotropy alone.

In calculating the anisotropy $\Delta\chi$ for any given plane in the crystal from the observed critical angle of rotation of the torsion-head, namely α_0, we used in Part I the simple formula (see Eq. (1), p. 861 of reference 1)

$$\lambda = \alpha_0 - \pi/4, \tag{2}$$

where λ denotes $\Delta\chi \cdot mH^2/(2Mc)$. It should be emphasized here that this formula is only approximate, though a sufficiently good one under the usual conditions of measurement of anistropy; it is correct to less than 0.5 percent when $\alpha_0 = 2\pi$ (i.e., one rotation), and in our measurements α_0 is always much greater than this angle. When, however, the observed critical angle α_0 is small, we have to use the more rigorous formula

$$\lambda = (\alpha_0 - \pi/4 - \sigma)/\cos 2\sigma, \tag{3}$$

where

$$\sin 2\sigma = 1/2\lambda. \tag{4}$$

σ is the extra angle in excess of $\pi/4$ (measured from the equilibrium position of the crystal in the field) over which the crystal turns before reaching the unstable position.

The experimental results are given in Table II. The $\Delta\chi$'s are expressed in the usual unit, 10^{-6} c.g.s. e.m.u., and refer to one gram molecule of $CuSO_4 \cdot 5H_2O$. The last three columns in the table will be explained later.

7. Location of the M Axes

From the data given in Table II the two M axes may be located in either of the following ways.

(1) We may utilize the observational data for the directions of maximum and minimum susceptibilities for the different crystal planes. For brevity we may call these two directions in a given plane the "setting-directions;" when the crystal is suspended in the magnetic field with the plane horizontal, it sets with the above directions along and perpendicular to the field, respectively. The setting-directions in a plane are thus analogous to the extinction-lines in crystal optics, and our present problem of determining the two M axes from observations on the setting-directions for the requisite number of planes, n (equal to 4 for a triclinic crystal, as we shall see presently), in the crystal is equivalent to the problem in crystal optics of determining the two optic axes of a biaxial crystal when the

Table II. *The magnetic data refer to 26°C.*

Serial Number	Mode of Suspension	Orientation in the Field	$\Delta\chi$	θ	θ'	$\Delta\chi/(\sin\theta \sin\theta')$
1	'c' ax. vert.	($\bar{1}00$) at 27°.2 to the field and ($\bar{1}\bar{1}0$) at 53°.3 to it.	183	49°	55°	296
2	'a' ax. vert.	(011) at 2°.7 to the field and (021) at 17°.6 to it.	60	24	31	286
3	($\bar{1}00$) and ($\bar{1}11$) vert.	($\bar{1}00$) at 45°.5 to the field and ($\bar{1}11$) at 14°.0 to it.	263	86	105	273
4	($\bar{1}\bar{1}0$) and ($\bar{1}11$) vert.	($\bar{1}\bar{1}0$) at 62°.6 to the field and ($\bar{1}11$) at 9°.5 to it.	264	92	108	278
5	(100) horiz.	'c' ax. at 58°.9 to the field and the intersection of ($\bar{1}00$) and ($\bar{1}11$) at 8°.0 to it.	146	43	51	276
6	(110) horiz.	'c' ax. at 43°.9 to the field and intersection of ($\bar{1}\bar{1}0$) and ($\bar{1}11$) at 12°.6 to it.	213	55	71	275
7	($\bar{1}10$) horiz.	'c' ax. at 90°.0 to the field and the intersection of ($\bar{1}10$) and ($\bar{1}11$) at 2°.5 to it.	117	44	36	286
8	($\bar{1}11$) horiz.	The intersection of ($\bar{1}11$) and ($\bar{1}00$) at 20°.2 to the field and the intersection of ($\bar{1}11$) and ($\bar{1}\bar{1}0$) at 45°.4 to it.	26	17	18	288
						Mean = 282

TABLE III. *Location of the M axes and of the principal magnetic axes.*

	'a'	'b'	'c'
M_1	156°	74°	49°
M_2	149°	53°	55°
α	154°	64°	51°
β	66°	85°	42°
γ	80°	27°	103°

TABLE IV. *Directions of principal magnetic axes as deduced from structure.*

	'a'	'b'	'c'
Normal to z_I and z_{II}: (α)	155°	68°	50°
Bisectors of the angle between z_I and z_{II}: exterior: (β)	66°	86°	42°
Bisectors of the angle between z_I and z_{II}: interior: (γ)	85°	22°	100°

extinction-lines on n different-faces have been observed. The optical problem has been discussed in detail by Weber,[12] Johnsen,[13] and Hilton.[14] It has been shown that a unique solution is possible when $n=1$, 2 or 4 according as the crystal is orthorhombic, monoclinic or triclinic. (It is, of course, assumed that all the n faces have general positions.) A further observation on one such face to find out which of the two extinction lines on the face corresponds to the larger refractive index will determine whether the γ axis is the acute bisectrix or the obtuse bisectrix of the angle between the two optic axes. Practical methods have been developed, both graphical and analytical, to determine the optic axes from the observed extinction-lines on the required number of faces.

Thus in the crystal of $CuSO_4 \cdot 5H_2O$, which is triclinic, observations on the setting directions for four faces are sufficient to determine uniquely the two M axes. Actually we have such data for eight faces, and from these data we have tried to locate the two M axes, both by the geometrical method of Hilton and by the trial and error method described by Johnsen. We find, however, that, because of the small angle between the two M axes, though its acute bisectrix is determined accurately in this manner, there is some uncertainty in the location of the M axes themselves. We have therefore adopted the following alternative method which utilizes the experimental data for the anisotropy for different crystal planes.

(2) For a given plane in the crystal whose normal makes angles θ and θ' with the two M axes, the magnetic anisotropy $\Delta\chi$ is given by the simple relation

$$\Delta\chi=(\gamma-\alpha)\sin\theta\cdot\sin\theta'. \qquad (5)$$

The location of the M axes reduces therefore to finding two directions such that $\Delta\chi/(\sin\theta\cdot\sin\theta')$ may have the same value for all the planes; θ and θ' are the angles which the two directions make with the normal to the plane for which the anisotropy is $\Delta\chi$.

This is conveniently done by the trial and error method, by using stereographic projection for the measurement of angles. The angular parameters for the two M axes given in Table III were obtained in this manner. The corresponding values of θ, θ' and $\Delta\chi/(\sin\theta\cdot\sin\theta')$ for the different crystal planes are given in the last three columns of Table II; as will be seen from the table, $\Delta\chi/(\sin\theta\cdot\sin\theta')$ has practically the same value for all the planes, namely about 280.

8. The Principal Magnetic Axes and the Anisotropy of the Crystal

Knowing the M axes, we can deduce readily the α, β and γ axes of the magnetic ellipsoid, since the α and the γ axes are the two bisectors (the interior and the exterior bisectors, respectively, in this crystal), of the angle between the two M axes. Their directions also are given in Table III.

Further, from the directions of the M axes given in Table III the magnetic axial angle $2V$ comes out as 159°. From this value, and the equation $\Delta\chi/(\sin\theta\cdot\sin\theta')=280$, we obtain

$$\gamma-\alpha=280, \quad \gamma-\beta=10.$$

9. The Magnetic Constants of the Crystal Deduced from its Structure

The directions of the principal magnetic axes of the crystal, deduced from its structure, are given in Table IV. On comparing these values with the corresponding values given in Table III, we find that they agree well. This is very gratifying, and may be taken to be a striking confirmation on the one hand of the structure proposed by Beevers and Lipson for the crystal from x-ray studies, and on the other of the theory

[12] Weber, Zeits. f. Krist. **56**, 1 and 96 (1921).
[13] Johnsen, Centralblatt Min. 1919, p. 321.
[14] Hilton, Mineral. Mag. **19**, 233 (1921).

of Van Vleck, Penney and Schlapp, which attributes the magnetic anisotropy of paramagnetic crystals to the asymmetry of the internal electric fields acting on the paramagnetic ions in the crystals.

10. The Asymmetry of the Internal Electric Fields Acting on the Cu^{++} Ions

Let us consider again the paramagnetic unit groups, each consisting of a Cu^{++} ion in the center, and six negatively charged oxygen atoms forming an octahedron about it, with one of its diagonals, the z axis, drawn out. Let us denote the gram molecular susceptibility of the group along the z axis, i.e., the axis of tetragonal symmetry, by $K_{\parallel}$, and that along directions perpendicular to the tetragonal axis by $K_{\perp}$. Let us further denote the obtuse angle between the z axes of the two paramagnetic groups in the unit cell, i.e., between z_I and z_{II}, by 2φ. (As we mentioned in an earlier section, the x-ray data of Beevers and Lipson give $2\varphi=98°$.) Then evidently

$$\left.\begin{aligned}\alpha&=K_{\perp}\\ \beta&=K_{\perp}\sin^2\varphi+K_{\parallel}\cos^2\varphi\\ \gamma&=K_{\perp}\cos^2\varphi+K_{\parallel}\sin^2\varphi\end{aligned}\right\}, \tag{6}$$

$$\therefore\quad \left.\begin{aligned}\gamma-\alpha&=(K_{\parallel}-K_{\perp})\sin^2\varphi\\ \beta-\alpha&=(K_{\parallel}-K_{\perp})\cos^2\varphi\end{aligned}\right\}. \tag{7}$$

From these relations we obtain

$$\tan^2\varphi=(\gamma-\alpha)/(\beta-\alpha), \tag{8}$$

which, in view of relation (1) for the tangent of the half-angle between the two M axes, *viz.*, $\tan^2 V=(\beta-\alpha)/(\gamma-\beta)$, gives

$$\tan\varphi=\operatorname{cosec} V. \tag{9}$$

Substituting for V the value $\frac{1}{2}\times 159°$, obtained from our magnetic measurements, we get

$$2\varphi=91°,$$

as compared with 98° obtained from the x-ray data. The difference is small, and is not unexpected, since the tetragonal symmetry which we have assumed for the paramagnetic groups is only approximate; the line joining the two sulphate oxygens, which we have taken to be an axis of tetragonal symmetry, is not exactly perpendicular to the square of water oxygens, but deviates from that direction by a small angle.

Coming back to Eqs. (7), we further obtain

$$K_{\parallel}-K_{\perp}=(\gamma-\alpha)+(\beta-\alpha), \tag{10}$$

i.e., $$K_{\parallel}-K_{\perp}=550.$$

In other words, if all the octahedra in the crystal were identical and were oriented in the same way (i.e., with their tetragonal axes along the same direction), two of the principal susceptibilities of the crystal would be equal and *less* than the third by about 550×10^{-6} per gram molecule of $CuSO_4\cdot5H_2O$, at 26°C; the third susceptibility is along the common direction of the tetragonal axes of all the paramagnetic groups. This anisotropy characteristic of the paramagnetic unit group, as distinguished from the observed anisotropy for the crystal as a whole, is the proper measure of the asymmetry of the electric fields acting on the Cu^{++} ions in the crystal.

We should mention here that the mean susceptibility of the crystal, equal to $(\alpha+\beta+\gamma)/3$, or $(K_{\parallel}+2K_{\perp})/3$, is about 1420×10^{-6} per gram molecule, at 26°C. The magnetic anisotropy of the paramagnetic group, *viz.*, $K_{\parallel}-K_{\perp}=550\times10^{-6}$, is thus about 40 percent of the mean susceptibility, and is very large.

LETTERS TO THE EDITOR

Prompt publication of brief reports of important discoveries in physics may be secured by addressing them to this department. Closing dates for this department are, for the first issue of the month, the eighteenth of the preceding month, for the second issue, the third of the month. Because of the late closing dates for the section no proof can be shown to authors. The Board of Editors does not hold itself responsible for the opinions expressed by the correspondents.

Communications should not in general exceed 600 words in length.

On the Stability of Stellar Neutron Cores

The quite regular variation of stellar energy generation with stellar mass has seemed to justify the hope that neither the structure nor the mechanism of energy generation would differ essentially from star to star. With increased knowledge of the rates of nuclear reactions, it has grown clear that such reactions must take place in stellar interiors, and that, on the basis of a standard Eddington model, reactions must occur which can account in order of magnitude for the radiation of the lighter stars. In particular it would seem that the formation of deuterons by proton collision, and at the least partially regenerative capture of protons by elements between carbon and oxygen could be made to account successfully for the main sequence stars.[1] Nevertheless it has been clear that these reactions could in no way account for the enormously greater radiation of such stars as Capella, and that for these either one would have to invoke other and readier nuclear reactions, with a correspondingly reduced time scale, or one would here be led, as in the earlier arguments of Milne, to expect serious deviations from the Eddington model.

It is in this connection that the suggestion[2] of a condensed neutron core, which would make essential deviations from the Eddington model possible even for stars so light that without a core a highly degenerate central zone could not be stable, still seems of some interest. Essential for a discussion of the role of such a core, is the estimate of the minimum mass for which it will be stable. An estimate of Landau, based apparently on the requirement that the sum of the gravitational and kinetic energies per particle of core should be lower than the energy per particle in stable nuclei (Landau chose oxygen), led to the value 0.001 solar masses for the limiting mass. This figure appears to be wrong; if one takes only gravitational attraction into account, the binding energy of a neutron in the core does not become equal to nuclear binding energies until the core mass is about $\frac{1}{3}$ that of the sun. It is true that Landau's requirement is unnecessarily severe: In order that the core be stable with respect to the most firmly bound nuclei (say calcium) it is only necessary that the neutron's free energy in the core be less than that in the nucleus. Since the total core energy is proportional to the 7/3 power of the number of particles, the magnitude of the free energy in the core is 7/3 the mean binding energy. One thus gets a limiting core mass of $\frac{1}{6}$ that of the sun. It seems that these results can be obtained without serious error by assuming a uniform density for the core: The actual polytrope gives only a slightly greater stability (roughly ten percent).

A core of this high mass, even in a star considerably more massive than the sun, would involve a complete breakdown in the Eddington model, since so heavy a core would be surrounded by a degenerate zone which would use up the star's total mass. The question of the actual stability of core models thus involves a consideration of the contribution of nuclear forces to the core-binding. The forces which must be known are those acting between a pair of neutrons; and no existing nuclear experiment or theory gives a complete answer to this question. If, however, we assume that the forces between neutrons are of the spin exchange saturating type ($\sigma\cdot\sigma'$), they help to reduce the lower limiting mass for core stability only to about $\frac{1}{10}$ that of the sun; the degenerate zone surrounding such a core must have nearly the sun's mass; and thus if such a core existed, the Eddington model would be completely wrong except perhaps for very massive stars.

If, on the other hand, one gives up the requirement of saturating two body forces and accepts an explanation of saturation along the lines of the suggestion of Critchfield and Teller,[3] he will be led to suppose that the forces between all pairs of nuclear particles are, except for Coulomb forces, the same, and that the only important factor making the binding energy of a neutron in the core smaller than in say a Ca nucleus is the increased kinetic energy which the promotion required by the exclusion principle involves. With this assumption the minimum core mass is very much reduced, and a mass of a few percent of that of the sun would insure its stability. For core masses under 0.03 that of the sun, the mass of the degenerate zone will be less than that of the core.

It seems clear that even in the heaviest stars no core will be formed until practically all sources of nuclear energy have been, at least for the central material of the star, exhausted. The arguments given above cannot, therefore, be regarded as showing that, even with the most favorable assumption about nuclear forces, actual stars have cores; but they do show that forces of the often assumed spin exchange type preclude the existence of a core for stars with masses comparable to that of the sun.

J. R. OPPENHEIMER
ROBERT SERBER

Department of Physics,
University of California,
Berkeley, California,
September 1, 1938.

[1] Bethe and Critchfield, Phys. Rev. **54**, 248 (1938). We are indebted to Dr. Bethe for an interesting discussion of these questions.
[2] Gamov, *Atomic Nuclei and Nuclear Transformations*, second edition (Oxford, 1936), p. 234. Landau, Nature **141**, 333 (1938).
[3] Critchfield and Teller, Phys. Rev. **53**, 812 (1938).

The Interaction of Slow Neutrons with Gases

The slow neutron-proton interaction has heretofore been investigated through the use of solid or liquid hydrogenous materials in which the proton binding within the molecular structure has been important in determining the effective cross section values.[1–6] Theoretical calculations by Fermi,[7] Bethe,[8] Arley[9] and others have shown that, with the Born approximation, the cross section for zero energy neutrons should be proportional to the square of the reduced mass of the system, and the cross section dependence on energy level spacing and neutron energy for thermal neutrons has been indicated. The detailed calculations of Schwinger and Teller[10] on the scattering by *ortho*- and *para*- H_2 have shown the manner in which the spin dependence, the nature of the energy level system, and the range of the neutron-proton interaction enter into the problem.

As a further step in this development, an investigation has been made of the variation in cross section of a series of hydrogenous substances containing increasing numbers of protons—hydrogen (H_2), methane (CH_4), ethane (C_2H_6), propane (C_3H_8), butane (C_4H_{10}), and paraffin ($\sim C_{22}H_{46}$). Since the design of the apparatus lends itself well to the measurement of other gases, the cross sections of He, Ne, and A have been measured, and in addition, the values for N_2 and O_2 have been re-determined by this direct method.

The experimental arrangement utilized two duplicate steel cylinders 30 cm in length, fitted with duraluminum end caps designed to withstand ~3000 lb./in.^{2} pressure. One cylinder was connected to a gas introduction apparatus, and the gas pressures measured either by a two-meter mercury manometer, or by calibrated Bourdon gauges. The other cylinder was evacuated and used as a calibrated comparison "dummy," in order to correct for the absorption by the cell itself. Alternate runs were taken with the gas cylinder and dummy cylinder interposed in the beam. The neutron beam (about 1 meter long) was accurately defined by shields and diaphragms of both boron carbide and cadmium. The cylinders were lined with Cd to prevent detection of scattered neutrons. The results are summarized in Tables I and II.

The increase in cross section per proton from liquid H_2 to H_2 gas is probably due to the additional transitions arising from the appreciable population of higher levels above $J=0$ and $J=1$ in the case of the gaseous H_2 at room temperature. It is interesting to note that in the series from methane to paraffin, the variations in cross section are quite closely proportional to the square of the reduced mass, even if considerations of energy level spacing are neglected.

TABLE I. *Interaction of ~300°K neutrons with bound protons.*

SUBSTANCE	STATE	CROSS SECTION PER PROTON ($\times 10^{-24}$ cm^2)*
Hydrogen (H_2) normal	liquid	24.0[11]
Hydrogen (H_2)	gas	32.0
Methane (CH_4)	gas	45.5
Ethane (C_2H_6)	gas	46.6
Propane (C_3H_8)	gas	47.1
Butane (C_4H_{10})	gas	50.0
Paraffin ($\sim C_{22}H_{46}$)	solid	50.7

* Weighted averages obtained from a series of measurements at several different pressures. The probable errors are approximately ±1.5 percent.

TABLE II. *Interaction of slow neutrons with the nuclei of gases.*

SUBSTANCE	STATE	CROSS SECTION PER NUCLEUS ($\times 10^{-24}$ cm^2)
Helium	Gas	1.51
Neon	Gas	2.94
Argon	Gas	2.51
Nitrogen	Gas	12.0
Nitrogen	Liquid	12.8[11]
Oxygen	Gas	4.1
Oxygen	Liquid	4.05

The 300°K neutron-proton cross section for paraffin has been increased over previous values to 50.7×10^{-24} cm^2. This cross section has been shown to increase[4] by a factor of 1.31 for ~120°K neutrons, corresponding to $\theta=65.9\times10^{-24}$ cm^2. Since the zero-energy neutron-proton cross section should be four times larger than that for the free proton (for such a large molecule), the free proton-neutron cross section must therefore be revised upwards to a minimum of about 16.5×10^{-24} cm^2. The energy of the virtual singlet level of the deuteron must thus be correspondingly reduced, and the various theoretical calculations based on this value readjusted.

All the rare gases measured have very small cross sections. The cooperation of Dr. F. R. Balcar and the Air Reduction Company is much appreciated.

HENRY CARROLL
J. R. DUNNING

Columbia University,
New York, N. Y.,
September 1, 1938.

[1] Dunning, Pegram, Fink and Mitchell, Phys. Rev. **48**, 277 (1935).
[2] Amaldi and Fermi, Phys. Rev. **50**, 899 (1936).
[3] Fink, Phys. Rev. **50**, 738 (1936).
[4] Powers, Goldsmith, Beyer and Dunning, Phys. Rev. **53**, 947 (1938).
[5] Goldhaber and Briggs, Proc. Roy. Soc. **162**, 127 (1937).
[6] Frisch, von Halban and Koch, Kgl. Danske Vidensk. Selsk. Mat.-fys. Med. **XV**, No. 10 (1938).
[7] Fermi, Ric. Scient. **8**, II, 13 (1936).
[8] Bethe, Rev. Mod. Phys. **9**, 124 (1937).
[9] Arley, Kgl. Danske Vidensk. Selsk. Mat.-fys. Med. **XVI**, 1 (1938).
[10] Schwinger and Teller, Phys. Rev. **52**, 286 (1937).
[11] Dunning, Manley, Hoge and Brickwedde, Phys. Rev. **52**, 1076 (1937); Brickwedde, Dunning, Hoge and Manley, Phys. Rev. **54**, 266 (1938); Comparison values from this paper are indicated.

Wave-Length of the New Nitrogen Line

The new nitrogen line ^4S–^2P, which was recently reported by me with a tentative wave-length of 3471A, has been observed with an instrument of higher dispersion than the one used in its discovery and with a narrower slit. A neon comparison spectrum was used and there is now no question as to an upper limit for the wave-length of the line since it lies a fraction of an angstrom unit on the short wave-length side of the strong neon line at 3466.578. A series of measurements indicates an average wave-length of 3466.3. A new series of exposures with narrower slit and larger dispersion will soon be made and a better wave-length obtained.

JOSEPH KAPLAN

University of California at Los Angeles,
Los Angeles, California,
September 14, 1938.

Nuclear Isomerism and Internal Conversion

According to Weizsäcker,[1] one may explain nuclear isomerism by assuming that the lowest excited state of the nucleus has an angular momentum differing by several units from that of the ground state. Selection rules may then be invoked to increase the lifetime of time of the excited level, against gamma-ray transitions to the ground state, to such a large value that the normally slower beta-processes may compete effectively in destroying the upper state. The γ-ray—β-ray branching ratio will depend on the relative lifetimes for the two modes of decay, but when the latter are of the same order of magnitude, the γ-ray transitions should be observable. Hebb and Uhlenbeck[2] have suggested that the failure of attempts to observe these gamma-rays is probably due to the high probability of internal conversion. (The internal conversion coefficient increases rapidly as the spin change increases, and as the energy difference decreases).[3]

We have therefore looked for a line spectrum of conversion electrons from one of the isomeric forms of Rh^{105}, formed from Rh by slow neutron capture. To decrease the absorption of slow electrons in the rhodium target as well as in the detector walls, the target was electrolytically deposited inside a Ni cylinder, and the counter walls were constructed of 0.005 mm Al. An absorption curve of the radiation from the 4.2 min. isomer showed the presence of two components; the harder one was identified through its absorption coefficient, with the well-known primary beta-rays of this period. The softer component, which accounted for about 30 percent of the total counts, had an energy of 35–60 kev. That this soft component was not instrumental could be demonstrated by the fact that no such soft group was observed to follow the 44 sec. Rh period under identical geometrical conditions.

From these data, we may draw the following conclusions regarding the 4.2 min. isomer:

(1) The radiation does not consist of *one* simple continuous beta-ray spectrum.

(2) The radiation does not consist of two simple beta-ray spectra superposed, since no hard γ-ray is observed. Also, the partial decay constant for the hypothetical soft beta-rays is too great for their energy.

(3) The soft component is therefore composed of conversion electrons from a γ-ray of about 80 kev. To prove that this gamma-ray transition precedes the beta-ray emission, it will be necessary to show that the characteristic x-rays which must follow the internal conversion are Rh $K\alpha$ and not Pd $K\alpha$. This will be attempted in the future. For the present, it should suffice to show that all the experimental results may be explained by assuming that *the soft radiation is an "electron line" emitted by internal conversion in the transition from the metastable state to the ground state of the* Rh^{105} *nucleus.*

On this assumption, the 44 sec. penetrating component arises in beta-transitions from the ground state of Rh^{105} to the ground state of Pd^{105}. This same transition gives the hard component of the longer period, but it proceeds at a slower rate, as the Rh^{105} ground state (44 sec.) is now formed by γ-ray decay from the 4.2 min. level. This assumption could be tested by examining the early part of the 4.2 minute decay curve, i.e., before the 44 sec. period was in equilibrium with the longer one. Unfortunately the high initial intensity of the 44 sec. period makes this test impossible. This simple picture requires that the beta-ray spectra of the two isomers be identical. The experimentally observed difference might be accounted for by assuming the existence of direct beta-transformations from the excited state of Rh^{105} to the ground state of Pd^{105}.

A detailed account of this work will appear in the *Journal de Physique.*

BRUNO PONTECORVO

Laboratoire de Chimie Nucléaire,
Collège de France, Paris,
July 24, 1938.

[1] Weizsäcker, Naturwiss. **24**, 813 (1936).
[2] Hebb and Uhlenbeck, Physica **5**, 605 (1938).
[3] Pontecorvo, *Travaux du Congrès du Palais de la Decouverte* (Paris, 1937).

Preliminary Report on the Radioactivity Produced in Y, Zr, and Mo

A study of the radioactivity produced in Y, Zr, Cb and Mo started at the Radiation Laboratory, University of California, Berkeley, by one of the authors, has been continued by making chiefly neutron bombardments on these elements from the cyclotron in the Institute of Physical and Chemical Research, Tokyo. Both lithium and beryllium targets were bombarded by 20 to 100 μa of 5.5 to 7.6 Mev deuteron beam at Berkeley and 20 to 40 μa of about 3 Mev in Tokyo to produce fast and slow neutrons. The results obtained on yttrium are given in Table I.

A further careful chemical test and a study of β-rays must be done for the assignment of the shorter periods. The 2.3 hr. period is expected to be due to Dy contamination. The results obtained on zirconium are given in Table II.

The 34 d period might be due to Hf contamination. The 70 hr. period assigned to be Y^{92} here seems likely to

TABLE I. *Radioactivity induced in yttrium by neutron bombardment.*

Bombardments	Observed Periods			
Slow neutrons	—	2.3 hr.	66 hr.	—
Fast neutrons	60 min.	—	66 hr.	55 days
Sign	e^-	e^-	e^-	e^-
Chemical test	—	—	Y	Sr
Assignment	?	Dy^{165}?	Y^{90}	Sr^{89}
Upper limit derived from K–U plot	—	—	2.1±0.1 Mev	—

TABLE II. *Radioactivity induced in zirconium by neutron and deuteron bombardment.*

Bombardments	Observed Periods						
Slow neutrons	—	—	17 hr.	—	—	—	63 d
Fast neutrons	—	3 weak hr.	—	70 hr.	70 hr.	—	63 d
Deuterons (8 Mev)	90 min.	2.5 hr.	—	—	3 d	weak 34 d	63 d
Sign	e^-	e^-	e^-	e^+	e^-	e^-	e^-
Chemical test	—	—	Zr	Zr	Y	Cb	Zr
Assignment	—	Y^{91}?	Zr^{95}	Zr^{89}	Y^{92}	Cb^{95}?	Zr^{93}
Upper limit derived from K–U plot	—	—	1.25 ±0.1 Mev	1.03 ±0.1 Mev	1.3 ±0.1 Mev	—	0.25 ±0.3 Mev

TABLE III. *Radioactivity induced in molybdenum by neutron bombardment.*

BOMBARDMENTS	OBSERVED PERIODS			
Slow neutrons	—	24 min.	64 hr.	—
Fast neutrons	17 min.	—	64 hr.	several days
Sign	ϵ^+	ϵ^-	ϵ^-	—
Chemical test	Mo	Mo	Mo	—
Assignment	Mo^{91}	Mo^{101}	Mo^{99}	?
Upper limit derived from K–U plot	1.8 ±0.4 Mev	1.3 ±0.1 Mev	1.0 ±0.1 Mev	—

belong to Y^{90}, but the discrepancy between the upper limits obtained is far beyond the experimental error. With fast neutrons one more short period of about 30 min. has been observed. The results obtained so far on columbium are still too ambiguous for publication, because the activity is usually very weak and moreover the chemistry of it is very difficult.

The results obtained when molybdenum samples were bombarded by neutrons are given in Table III.

No trace of the 36 hr. period reported by Fermi and his collaborators was found.

It is a pleasure to express our thanks to Professor E. O. Lawrence for the privilege of using his cyclotron. Thanks are also due to Dr. Y. Nishina and Professor K. Kimura for their valuable help and encouragement. We wish to acknowledge the assistance given to us by Mr. K. Shinma, Mr. F. Yamasaki and Mr. N. Mori. The experiment has been aided by grants from the Research Corporation, the Chemical Foundation, the Josiah Macy, Jr., Foundation, the Japan Society for the Promotion of Scientific Research, the Oji Paper Manufacturing Company, Mitsui Ho-Onkwai Foundation, Tokyo Electric Light Company and the Japan Wireless Telegraph Company.

R. SAGANE
S. KOJIMA
G. MIYAMOTO
M. IKAWA

Department of Physics,
Department of Chemistry (M.I.),
Tokyo Imperial University,
Tokyo, Japan,
August 22, 1938.

Internal Conversion of γ-Rays in Element 43

Radioactive element 43 has been examined in a magnetic spectrograph, and is found to have three internally converted γ-rays. Segrè and Seaborg,[1] in studying the radioactivity of element 43, discovered a new six-hour period, and noticed that the electrons emitted by it gave an absorption curve characteristic of a single energy group rather than of a continuous distribution as in a normal β-ray spectrum. They kindly prepared a sample of this material for the magnetic spectrograph and the accompanying photograph was obtained (Fig. 1). The two lines

FIG. 1. Magnetic spectrogram of electrons emitted by radioactive element 43.

are due to internal conversion in the K and L shells of element 43 and have the proper separation for an element in this neighborhood. (The fine scratch is a fiducial mark.) The γ-ray energy is 129 kev. This isotope is formed by the β-decay of radioactive molybdenum

The long-lived isotopes of element 43 formed directly by deuteron bombardment of Mo were also tried in the spectrograph and gave lines corresponding to γ-rays of 87 kev and 184 kev. They are chemically element 43, but it is not yet known with what periods they are associated.

Other cases of internal conversion which have been reported are Ga[2] and Cd[3]. Ga has been photographed in the spectrograph, but Cd has not yet been tried. The author has also found internal conversion of a 230 kev γ-ray in a new 30-hour Ba isotope by absorption measurements, but at present, the activity is too weak to photograph. The electrons, x-rays and γ-rays have all been observed for this Ba, and there are no natural β-rays associated with it. A theoretical discussion of internal conversion has been given by Dancoff and Morrison.[4]

It is a pleasure to thank Drs. Seaborg and Segrè for preparing the radioactive samples and Professor E. O. Lawrence for encouragement in the work. This research has been aided by grants from the Research Corporation.

D. C. KALBFELL

Radiation Laboratory, Physics Department,
University of California,
Berkeley, California,
September 6, 1938.

[1] Complete explanation to appear soon in *The Physical Review*.
[2] L. Alvarez, Phys. Rev. **53**, 606 (1938).
[3] Ridenour, Delsasso, White, and Sherr, Phys. Rev. **53**, 770 (1938).
[4] S. M. Dancoff and P. Morrison, Phys. Rev. **54**, 149 (1938).

Location of Resonances in Boron Plus Proton Reactions

Gentner[1] has found the gamma-ray resonance in the reaction

$$_5B^{11}+{}_1H^1\rightarrow{}_6C^{12}+\gamma$$

to be at 180 kev. Allen, Haxby and Williams[2] place the alpha-particle resonance in the reaction

$$_5B^{11}+{}_1H^1\rightarrow{}_4Be^8+{}_2He^4$$

at 159 kev and the gamma-ray resonance at about the same voltage. A recent paper by Oppenheimer and Serber[3] has prompted new measurements of these resonances.

The alpha-particle and gamma-ray yields from the above reactions have been measured simultaneously with protons of energies up to 200 kev and thick boron targets. These measurements show that the two resonances coincide to within 1 kev and occur at 165±4 kev.

B. WALDMAN
R. C. WADDEL
D. CALLIHAN
W. A. SCHNEIDER

College of the City of New York,
New York University,
Washington Square College,
September 9, 1938.

[1] Gentner, Zeits. f. Physik **107**, 354 (1937).
[2] Allen, Haxby and Williams, Phys. Rev. **53**, 325 (1938).
[3] Oppenheimer and Serber, Phys. Rev. **53**, 636 (1938).

On the Electrical Properties of Multilayers

Multilayers of various stearates deposited on ebonite rods were suspended in a "Faraday cage" connected to an electrometer in order to detect and measure electrostatic charges in these multilayers. It was found that "*X*-type" multilayers were always positively charged whereas "*Y*-type" multilayers were uncharged. Furthermore, this charge was found to be proportional to the area of the multilayer and to increase regularly with the number of layers deposited. Simple tests showed that this was not a simple charge on the exterior of the multilayer but a summation of charges distributed more or less uniformly throughout the volume.

The technique of constructing these multilayers is a modification of that described by Blodgett.[1] A monomolecular layer of stearic acid was spread on various substrates and compressed by a castor oil piston. The substrate consisted of distilled water with a salt of one of the following divalent elements Mg, Ca, Ba or Pb at a concentration of 10^{-4} molal, and was adjusted to certain *p*H values; *p*H 6.3 was obtained with 10^{-3} molal $KHCO_3$ and *p*H 9.0 by adding KOH.

A magnesium substrate produced only *Y*-multilayers, barium produced *Y*-multilayers at *p*H 6.3 but *X*-multilayers at *p*H 9.0. Lead produced *X*-multilayers at *p*H 5.5. Calcium produced *X*-layers at *p*H 9.0 and *X*-layers, after about 10 dips, at *p*H 6.3 if the speed of dipping was less than 0.25 cm/sec. but *Y*-layers if the dipping rate was in excess of this value. Under no circumstance did high dipping speeds produce a large net negative charge in the multilayers; the high speed merely prevented the accumulation of positive charges.

A charged multilayer may be neutralized by dipping it rapidly, e.g. about 15 cycles per minute for a 2.5 cm dip, through a monolayer on a calcium substrate at *p*H 6.3. If, however, the rate of dipping be slow, e.g. less than 4 cycles per minute, an increase in charge will be obtained consistent with that obtained from the addition of the several *X*-layers added. High dipping speeds through the substrate create negative frictional charges; normally these charges are promptly dissipated by conduction into the substrate but if the multilayer is charged some of these negative frictional charges are bound by the electric attraction, resulting in the formation of a double layer, the excess frictional charge dissipating into the solution as usual. Variation of dipping speed had no appreciable effect with *p*H 9.0 substrates.

We have been able also to demonstrate experimentally that the positive charges in the *X*-multilayer are due to charged atoms or ions adsorbed on the floating stearate monolayer from the salts in the substrate and picked up with the monolayer in the plating process.

The *X*-layers produced from a calcium substrate at *p*H 6.3 exhibited a rate of charging per dip which accelerated almost exponentially in the course of the first 10 dips; simultaneously the contact angle between multilayer and monolayer increased, from about 45° in the first few dips, to 90° before the 10th dip; also, the type of barrier motion changed from that characteristic of *Y*-type deposits to that characteristic of *X*-type deposits. These related phenomena have their origin, we believe, in the increase in concentration of substrate OH ions in the immediate vicinity of the immersed ebonite cylinder, this local rise in *p*H being due to the electrostatic field of the accumulating charge in the multilayer. Accompanying this increased *p*H will be, provided the dipping rate be slow, an increase in the percent of stearic acid molecules transformed into stearate and accompanying adsorbed ions.

After 400 or more *X*-layers have been deposited on the ebonite it has a silvery sheen and depressed meniscus during its withdrawal from the substrate. The monolayer which had apparently deposited on the cylinder going down slid off completely on withdrawal, presumably because of the electrical repulsion between the positively charged multilayer and monolayer. The silvery sheen is caused by an included layer of air.

Finally, numerous hitherto puzzling observations[2] on the electrical properties of multilayers can be explained and correlated by our findings. A more detailed publication is in preparation.

ROY W. GORANSON
W. A. ZISMAN

Geophysical Laboratory,
Carnegie Institution of Washington,
Washington, D. C.
September 16, 1938.

[1] K. Blodgett, J. Am. Chem. Soc. **57**, 1007 (1935).
[2] E. Porter and J. Wyman, Jr., J. Am. Chem. Soc. **59**, 2746 (1937); **60**, 1083 (1938). R. W. Goranson and W. Zisman, Phys. Rev. **53**, 668 (1938). I. Langmuir and F. Norton, J. Am. Chem. Soc. **60**, 1513 (1938). W. D. Harkins, Phys. Rev. **53**, 908 (1938). J. Bikerman, Trans. Faraday Soc. **34**, 800 (1938).